uOttawa

L'Université canadienne
Canada's university

FACULTÉ DES ÉTUDES SUPÉRIEURES ET POSTOCTORALES

uOttawa

L'Université canadienne
Canada's university

FACULTY OF GRADUATE AND POSDOCTORAL STUDIES

Elmira Ahmady
AUTEUR DE LA THÈSE / AUTHOR OF THESIS

M.Sc. (Biochemistry)
GRADE / DEGREE

Department of Biochemistry, Microbiology and Immunology
FACULTÉ, ÉCOLE, DÉPARTEMENT / FACULTY, SCHOOL, DEPARTMENT

The Functional Role of A-type Lamin Interacting Transcription Factor (LITF) During Skeletal Myogenesis

TITRE DE LA THÈSE / TITLE OF THESIS

Patrick Burgon
DIRECTEUR (DIRECTRICE) DE LA THÈSE / THESIS SUPERVISOR

CO-DIRECTEUR (CO-DIRECTRICE) DE LA THÈSE / THESIS CO-SUPERVISOR

Bernard Jasmin

Robin Parks

Gary W. Slater
Le Doyen de la Faculté des études supérieures et postdoctorales / Dean of the Faculty of Graduate and Postdoctoral Studies

The Functional Role of A-type Lamin Interacting Transcription Factor (LITF) during Skeletal Myogenesis

Elmira Ahmady, BSc.

Thesis submitted to the Faculty of Graduate and Postdoctoral Studies, in partial fulfillment of the requirements for the M.Sc. degree in Biochemistry

Department of Biochemistry, Microbiology and Immunology
Faculty of Medicine
University of Ottawa

Your file Votre référence
ISBN: 978-0-494-65551-1
Our file Notre référence
ISBN: 978-0-494-65551-1

ABSTRACT

Lamin A/C (LMNA) is ubiquitously expressed in tissues, however specific missense mutations in LMNA result in discrete tissue specific phenotypes such as muscular dystrophy. Using a yeast-two-hybrid assay against a human heart cDNA library, a previously uncharacterized cDNA clone, A-type lamin interacting transcription factor (LITF), was identified. ***In this thesis the major objective was to determine the function of LITF using C2C12 mouse myoblast cell line. It is hypothesized that LITF is a myogenic factor that is required for myogenesis.*** Initiation of C2C12 differentiation led to an increase in LITF protein expression by 6 hours and peaking at 18 hours. LITF mediated chromatin immunoprecipitation from C2C12 nuclei with array analysis revealed a significant enrichment ($p<0.00001$) of promoter regions of developmentally important muscle transcription factors (Six1, Six4, Mef2c, Myogenin) and several other genes implicated in cell cycle and differentiation. Electrophoretic mobility shift assays and co-transactivation experiments revealed that LITF is capable of binding specific DNA sequences and activating transcription. Specific knockdown of LITF in C2C12 led to a reduction in the expression of Myogenin, MyoD and myosin heavy chain with a significant reduction in myotube formation. Collectively this data suggests that LITF may be a myogenic transcription factor/regulator.

ACKNOWLEDGEMENTS

I am exceptionally grateful to Dr. Patrick G. Burgon, my thesis supervisor for his continued guidance and support throughout the last two years at the University of Ottawa Heart Institute. I would have not been able to obtain the valuable skills in molecular and cellular biology and biochemistry without the acceptance to his laboratory and his helpful feedback and support throughout my studies. His continuous encouragement motivated me to be a productive graduate student and enjoy taking part in the exciting research of characterizing the function of a novel transcription factor and sharing my findings with the scientific community.

I also appreciate the helpful recommendations of my committee members, Dr. Ilona Skerjanc and Dr. Rashmi Kothary. Also, I would like to express my gratitude to Dr. Alex Blais and Yubing Liu for all their help with the ChIP-on-chip studies and their valuable time. In addition, I would like to express my gratitude to Dr. Alex Stewart and Allen Teng for their valuable advice in my project and experimental designs.

I would also like to express my appreciation to my past and present lab family: Anne-Marie Burgon, Darwin Burgon, Shelley Deeke, Ruxandra Gheorge, Laura Kenney, Lara Kouri, Stanimira Krotneva, Seham Rabaa, Adam Turner, Branka Vulesevic and Kitty Wu with whom all this would not have been possible. You made my time in the lab very enjoyable and the last two years will be unforgettable. Thank you for all the support and helpful advice in all aspects of my life. Thank you for helping me practice presentations, editing my work and answering all my questions. Incubation times would not have been the same without you guys!

Also, a big thanks to my neighbouring lab members Dr. Adolfo de Bold, Dr. Mercedes de Bold, Linda Connor, Shahreen Amin, Asna Choudury, Monica Forero and Amy Martinuk for their support and guidance throughout my studies. I can always count on you guys for that last micro-liter of restriction enzyme that I always seem to be low on right before the next step in my reaction!

Furthermore, thank you to all my colleagues and friends at the Heart Institute and Arjeta Gusinjac and Karen Soueidan for making my graduate experience a productive and enjoyable one. My time spent as VP-social with the Biochemistry, Microbiology, Immunology Graduate Student Association (BMIGSA) was greatly enjoyed and unforgettable friendships made.

Lastly, to my family, thank you for all the support, love and encouragement and listening to me all those times when experiments wouldn't work or sharing the happiness of a PCR reaction that worked! Thank you for believing in me and encouraging me to pursue my Masters when at times I thought it was impossible. Thank you for listening to me practice presentations and pretending you understood what I was talking about! Thank you for all the rides late at night for time-course experiments and accompanying me weekends in the lab when I said I only have 20 minutes of work but managed to keep you in the lab for the next 5 hours. Mac photo booth can be pretty entertaining and useful at times. To everyone who I forgot to mention all your support is greatly appreciated.

TABLE OF CONTENTS

Abstract ..... **ii**
Acknowledgement ..... **iii**
Table of Contents ..... **v**
List of Abbreviations ..... **vii**
List of Figures and Tables ..... **ix**
List of Figures Copyrighted with Permission ..... **x**

Chapter 1- General Introduction **1**

1.1 Nuclear Lamins 2
1.1.1 Physiological significance of nuclear lamins 2
1.1.2 Classes of lamins and structure 3
1.1.3 Lamin expression patterns 7
1.1.4 Lamins and diseases 8
1.1.5 Mouse models of laminopathies 9
1.1.6 A-type lamins as markers of stem cell differentiation and ageing 10
1.1.7 Molecular models of laminopathies 11

1.2 Identification and initial characterization of a novel A-type lamin interacting transcription factor 16

1.3 Hypothesis, Rationale, and Objective of proposed study 29

Chapter 2- Experimental Procedures **30**

2.1 Cell culture techniques 31
2.1.1 Growth conditions 31
2.1.2 Generation of stable cell lines 31

2.2 Whole cell extract preparation and western blotting 32
2.2.1 LITF expression during normal C2C12 cell differentiation 32
2.2.2 Determination of the efficacy of LITF knockdown 33
2.2.3 Analysis of the expression of Myogenin, MyoD, Six1 and Six4 in LITF-KD1 and LITF-KD2 cell lines 34

2.3 RNA isolation, semiquantitiatve RT-PCR and quantitative real-time PCR 35

2.4 Immunofluorescence microscopy 36
2.4.1 LITF localization during normal C2C12 cell differentiation 36
2.4.2 Myosin heavy chain expression in LITF-KD1 and LITF-KD2 37

2.5 Chromatin Immunoprecipitation and ChIP-on-chip studies 37
2.5.1 Electrophoretic mobility shift assay of ChIP-on-chip targets 42

2.6 LITF-shRNAmir transfection of C2C12 myoblasts.....43

2.7 Sequencing.....44

2.8 PCR primers.....45

2.9 Statistical Analysis.....45

Chapter 3- LITF expression during normal C2C12 cell differentiation.....46

3.1 C2C12 cells: Model system for studying the role of LITF in skeletal myogenesis.....47
3.2 Skeletal myogenesis.....47

3.3 Results.....52
3.3.1 LITF mRNA and protein expression during normal C2C12 cell differentiation.....52
3.3.2 LITF localization changes during normal C2C12 cell differentiation.....53

Chapter 4- LITF interacts with chromatin.....63

4.1 LITF co-localization with LMNA and PML nuclear bodies.....64

4.2 Results.....65
4.2.1 ChIP assay confirm LITF interaction with chromatin.....65
4.2.2 LITF enriches for genes that are important in commitment, development, differentiation, apoptosis and growth.....66
4.2.3 LITF binds to DNA directly and is able to activate Transcription.....72

Chapter 5- LITF is required for myotube formation.....77

5.1 shRNAmir technology to study stable LITF down-regulation.....78

5.2 Results.....81
5.2.1 LITFshRNAmir downregulate LITF expression.....81
5.2.2 LITF is required for myotube formation during skeletal myogenesis in C2C12 cells.....84

Chapter 6- General Discussion and Conclusions.....93

Appendix.....108

References.....117

Curriculum Vitae.....123

LIST OF ABBREVIATIONS

AD- EDMD- Autosomal dominant Emery-Dreifuss Muscular Dystrophy
bHLH- Basic-helix-loop-helix
bp- Base pairs
BSA – Bovine serum albumin
cDNA- Complementary DNA
ChIP- Chromatin Immunoprecipitation
CMT2B- Charcot-marie-tooth neuropathy type 2B
DAPI- 4', 6-diamidino-2-phenylindole
DCM-CD- Dilated cardiomyopathy with conduction defect
DH5-alpha- *E.coli* cells
DM- Differentiation Medium
DMD- Duchenne muscular dystrophy
DMEM – Dulbecco's modified Eagle's medium
DMSO – Dimethyl sulfoxide
dsDNA- Double stranded DNA
DTT- Dithiothreitol
E. Coli – Escherichia Coli
EDTA- Ethylenediaminetetraacetic acid
EMSA- Electrophoretic mobility shift assays
ERK – Extracellular signal-regulated kinase 1/2
ES- Embryonic stem cells
EST- Expression sequence tags
FBS – Fetal bovine serum
FPLD- Dunnigan type familial partial dystrophy
GAPDH- Glyceraldehye-3-phosphate dehydrogenase
GM- Growth Medium
HEK293- human embryonic kidney cells
HGF- Hepatocyte growth factor
HGPS- Hutchinson-gilford progeria syndrome
HRP- Horseradish peroxidase
IF- Intermediate filaments
IGF- Insulin-like growth factors
IgG- Immunoglobulin G
INM- Inner nuclear membrane
IP- immunoprecipitation
JAK- Janus Kinases
JNK- c-Jun N-terminal kinases
Kbp- Kilo base pairs
KD- Knockdown
kDa- KiloDalton
KO- Knockout
LB - Luria-Bertani
LITF- A-type lamin interacting transcription factor
LMG1B- Limb girdle muscular dystrophy type 1B

LMNA- Lamin A/C gene
LMNB1- Lamin B1 gene
LMNB2- Lamin B2 gene
MAPK – Mitogen-activated protein kinase
MEF2- Myocyte enhancer factor 2
MHC- Myosin heavy chain
MRF- Myogenic regulatory factors
NE- Nuclear extract
NLS- Nuclear localization signal
PBS – Phosphate-buffered saline
PI3K- Phosphatidylinositol-3-kinase
PML- Promyelocytic leukemia
PMSF- Phenylmethylsulphonyl fluoride
pRB- Phosphorylated retinoblastoma protein
PVDF- Polyvinylidene Fluoride
PVDF- Polyvinylidene Fluoride
RARα- Retinoic acid receptor alpha
RT- Room temperature
SDS-PAGE - Sodium dodecyl sulfate Polyacrylamide gel electrophoresis
shRNA- Short hairpin RNA
shRNAmir- Short-hairpin mircroRNA
SRF- Serum response factor
TBE- Tris Borate EDTA
TBST- Tris-Base tween-20
TGFβ – Transforming growth factor beta
X-EDMD- X-linked Emery Dreifuss Muscular Dystrophy
Y2H- Yeast-two-hybrid

LIST OF FIGURES

Figure 1.1: Lamin A/C (LMNA) gene structure and associated mutations 5
Figure 1.2: Laminopathies and Age-related diseases 14
Figure 1.3: Sequence alignment of LITF and analysis of homology 18
Figure 1.4: LITF binds Lamin A/C *in vitro* 20
Figure 1.5: LITF expression profile analysis 23
Figure 1.6: LITF and LMNA localization in HL-1 cells and C2C12 myoblasts 25
Figure 1.7: LITF localization in C2C12 cells. 27
Figure 2.1: Schematic diagram of chromatin immunoprecipitation (ChIP) assay 38
Figure 3.1: Stages of skeletal myogenesis and key regulatory factors involved 50
Figure 3.2: LITF mRNA expression pattern during C2C12 cell differentiation 55
Figure 3.3: LITF expression pattern during normal C2C12 cell differentiation 57
Figure 3.4: LITF localization during the time-course of C2C12 cell differentiation 59
Figure 4.1: LITF interacts with chromatin 69
Figure 4.2: LITF, a novel transcription factor 75
Figure 5.1: LITF shRNAmir processing and formation 80
Figure 5.2: shRNAmir knockdown of LITF protein expression in C2C12 cells 83
Figure 5.3: Western blot analysis of LITF expression in stably knockdown cell lines 88
Figure 5.4: LITF is required for myogenesis and myotube formation 90
Figure 5.5: Percent of nuclei in myotubes compared to total number of nuclei 92
Figure 6.1: Expression profile analysis of mouse LITF in miRNA-1-2 knockout mice 103
Figure 6.2: Expression profile analysis of human LITF in patients with DMD 105
Figure 6.3: Schematic diagram of LITF's role in skeletal myogenesis and putative targets 107
Figure S1: LITF peptide neutralization 116

LIST OF TABLES

Table 1.1: Diseases related to mutations of LMNA gene encoding lamins A and C. Chromosome location 1q21.3. 13
Table 2.1: PCR primer sequences used in experiments 45
Table 4.1: Biological process ontologies enriched by putative LITF gene targets 71
Table S1: Pooled replicated independent experiments of putative LITF targets identified by ChIP-on-chip analysis 109
Table S2: ChIP sequencing BLAT results 115

FIGURES IN THESIS COPYRIGHTED WITH PERMISSION FROM PUBLISHERS

FIGURE 1.1

This figure is reprinted by permission from Macmillan Publishers Ltd: *Nature Review Genetics*, Capell BC & Collins FS, Human laminopathies: Nuclei gone genetically awry, Figure 2, pg 942, Volume 7, Issue 12, copyright (2006). (11)

FIGURE 1.2

This figure is reprinted by permission from Blackwell Publishing Limited: *Journal of Anatomy*, Pekovic V & Hutchison CJ, Adult stem cell maintenance and tissue regeneration in the ageing context: the role for A-type lamins as intrinsic modulators of ageing in adult stem cells and their niches, Figure 1, pg 8, Volume 213, Issue 1, copyright (2008).(59)

FIGURE 3.1

This figure is reprinted from *Trends in Cell Biology*, Volume 16, Issue 1, Lluís F, Perdiguero E, Nebreda AR, & Muñoz-Cánoves P, Regulation of skeletal muscle gene expression by p38 MAP kinases, Figure 1, pg 37, Copyright (2005), with permission from Elsevier. (38)

Chapter 1:

General Introduction: Identification and Characterization of a Novel A-type Lamin Interacting Transcription Factor (LITF)

GENERAL INTRODUCTION

Skeletal myogenesis is a complex multi-step pathway involving a spectrum of transcription factors and signaling molecules such as MyoD, Myogenin, Pax7 and many more. Although many of the myogenic regulatory factors have been identified they do not alone explain the process of skeletal myogenesis. The exact mechanisms and all players involved are not known. The identification of novel targets in this process can shed light into the exact cascade of events and modifications in the pathway that are occurring. The recognition of a novel A-type lamin interacting transcription factor (LITF) and its characterization is important in providing new insight into the events involved in skeletal myogenesis and conceivably the development of lamin-associated diseases including muscular dystrophy or cardiomyopathies.

1.1 Nuclear Lamins

1.1.1 Physiological Significance of Nuclear Lamins

Nuclear lamins are type V intermediate filament (IF) proteins found in the nuclei of all multi-cellular eukaryotes and are major components of the nuclear lamina (15, 19, 26, 60, 75). The nuclear lamina is a stable structure that is part of the nuclear envelope lying between the inner nuclear membrane (INM) and peripheral chromatin (4, 19). Located within the nuclear lamina are many lamin-associated proteins such as chromatin modifying proteins, transcriptional repressors (36) and structural proteins (19, 26, 60, 67, 70, 91). Lamins are essential scaffolding components of the nuclear envelope and provide strength and stability to cells, making them critical for normal nuclear function (6, 42, 70). Furthermore, lamins contain chromatin-binding sites and are believed to be involved in DNA replication, meiosis, mitosis, connecting the nucleus to cytoskeletal networks, apoptosis and gene transcription

(19, 26, 60, 75, 70) Lamins can bind directly or indirectly through histones to nucleic acids and chromatin. Lamin-chromatin interactions are conserved throughout evolution. Lamins can affect chromatin organization and can regulate the epigenetic state of chromatin (18, 19, 24, 46, 69).

1.1.2 Classes of Lamins and Structure

Lamins have been classified into A/C, B1 and B2 sub-types on the basis of their amino acid sequences as well as their biochemical properties. A-type lamins and lamin C are the result of alternative splicing of the Lamin A/C gene (LMNA). Lamin B1 and B2 proteins are encoded by the lamin B1 (LMNB1) and lamin B2 (LMNB2) genes, respectively (11, 26, 60).

The structure of lamin proteins consists of a central α-helical rod domain containing four coiled- coil repeats (coil 1A, 1B, 2A, and 2B) flanked by two terminal globular domains. These globular domains include an amino terminal head (N-terminus) and carboxy terminal tail (C-terminus) (Figure 1.1) (11). Lamin proteins form coiled-coil dimers and therefore are capable of undergoing dimerization. The lamin tail domain contains a ~120 amino acid immunoglobulin (Ig)-fold which is a common site for many LMNA associated mutations and is involved in interactions with DNA, lipids and other proteins, such as the structural protein titin. Lamins contain within their C-terminal tail a nuclear localization signal (NLS), which is essential for the transport of lamins into the nucleus (11, 26, 60, 74). Moreover, lamins A, B1 and B2 (excluding lamin C) contain a specific 98-amino acid carboxy tail and lamin C has a unique 6–amino acid carboxy tail. Lamins A, B1 and B2 (excluding lamin C) contain a unique motif in their C-terminus known as a –CAAX

(Cysteine-Aliphatic-Aliphatic-any amino acid) motif which is important for undergoing post-translational modifications and processing of pre-mature forms of lamin A, B1 and B2 to mature forms. Inhibition of farnesylation by farnesyltransferase (FT) inhibitors results in the loss of processing (19). All lamins (A, B1 and B2) except lamin C undergo post-translational modifications. These post-translational modifications include: farnesylation, methylation, sumoylation and phosphorylation (26, 60, 70, 75). Farnesylation is the addition of farnesyl isoprenoid group (15 carbons) to C-terminus cysteine residue by farnesyltransferase (FT) (63). Farnesylation is a lipid modification and anchors the protein to the membrane (63). Methylation is also performed on the cysteine residue by the enzyme isoprenylcysteine methyltransferase (ICMT). Farnesylation and methylation of the C-terminus tail are important for the nuclear lamina association of lamins A, B1 and B2 and protein-protein interactions (19). Furthermore lamins can undergo sumoylation and phosphorylation (26, 60, 70, 75) at their –CAAX motif. Phosphorylation is important for the disassembly of A and B type lamins or the breakdown of the nuclear lamina during interphase and at the start of mitosis (19). Zhang et al. have shown that lamin A is a target of sumoylation at lysine 201 (93) where there exists the presence of a sumoylation consensus sequence ΨKXE (where Ψ is a hydrophobic residue, K= lysine, X= any amino acid and E= glutamic acid). Sumoylation is a post-translational modification that involves the covalent addition of small ubiquitin-like modifier (SUMO) polypeptide to a target protein. Sumoylation is thought to be important for normal lamin A function and subcellular localization since in dilated cardiomyopathy (DCM) models caused by mutations in lamin A decreased sumoylation of lamin A is evident (93).

Figure 1.1 Lamin A/C (LMNA) gene structure and associated mutations.
The Lamin A/C (LMNA) gene (57.6kb) structure is composed of a central alpha-helical rod domain flanked by two terminal globular domains. The globular domains include an N-terminal globular domain and C- terminal globular domain. Present at the C-terminal domain of lamin A but not lamin C is a CAAX motif. The LMNA gene is composed of 12 exons. Lamin C is encoded by exons 1-9 and a portion of exon 10. Lamin A is the results of alternative splicing of the LMNA gene which results in the addition of exons 11 and 12 and removal of the portion of exon 10 that is lamin C specific. Outlined in this figure are examples of various mutations of the LMNA gene that result in several diseases collectively termed laminopathies. This figure is reprinted by permission from Macmillan Publishers Ltd: Nature Review Genetics, Capell BC & Collins FS, Human laminopathies: Nuclei gone genetically awry, Figure 2, pg 942, Volume 7, Issue 12, copyright (2006). (11)

Figure 1.1

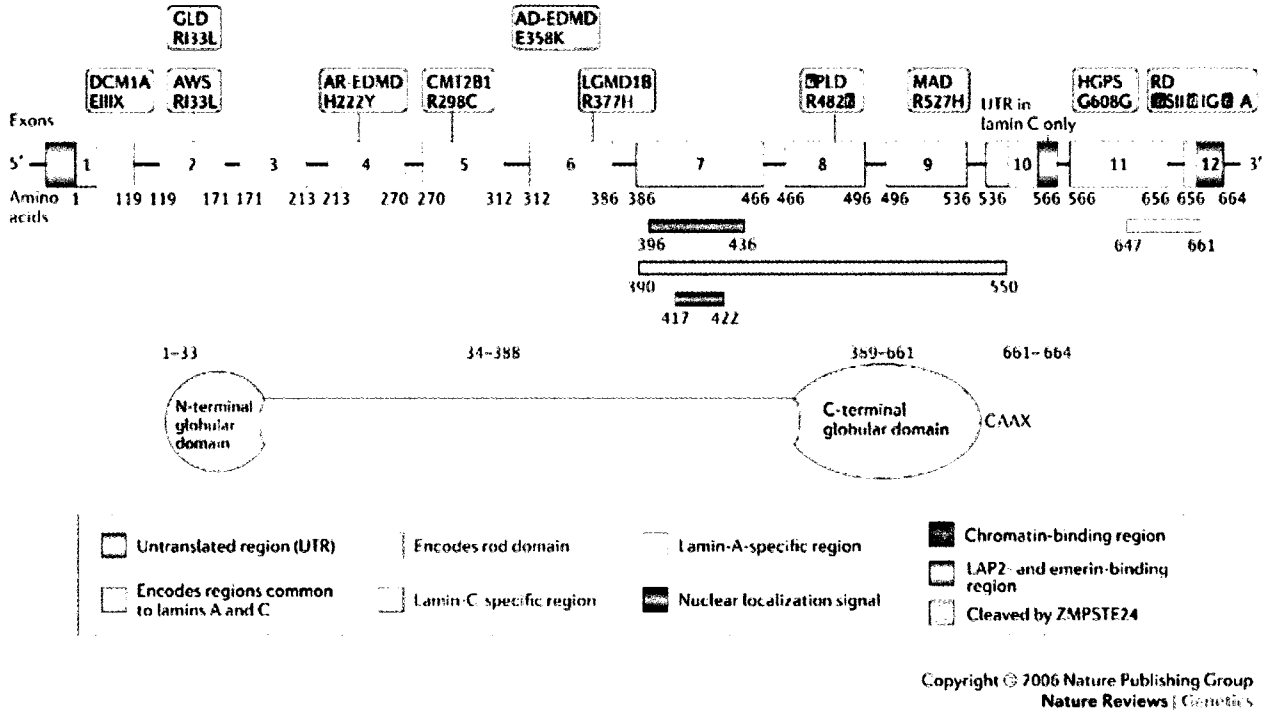

This figure is reprinted by permission from Macmillan Publishers Ltd: Nature Review Genetics, Capell BC & Collins FS, Human laminopathies: Nuclei gone genetically awry, Figure 2, pg 942, Volume 7, Issue 12, copyright (2006). (11)

1.1.3 Lamin expression patterns

All vertebrate cells express at least one B-type lamin, however, A-type lamins are primarily expressed in differentiated cells of higher organisms (26, 60, 75). In mice, B-type lamins are expressed throughout early development, while Lamin A/C are first detected in the trophoblast on embryonic day 9 (E9), in the embryoblast on day 10, and in myoblasts and other mesenchymal tissue by day 11 (81). Animal studies have demonstrated that mice deficient in Lamin A/C develop normally until birth but later show a progression of skeletal muscle wasting and growth retardation associated with muscular dystrophy and cardiomyopathy. Differentiation into myotubes is impaired in immortalized $lmna^{-/-}$ myoblasts cultures as observed by delayed myotube formation and down-regulation of important myogenic transcription factors MyoD and pRb as well as a reduced desmin expression (23). However, $lmna^{-/-}$ primary cells are still capable of forming myotubes (23, 73). This observation between immortalized $lmna^{-/-}$ myoblasts and $lmna^{-/-}$ primary cells confirms the importance of a proper nuclear lamina for differentiation to proceed (73). Fibroblasts from $lmna^{-/-}$ mice have defects in nuclear mechanics and mechanotransduction and overall defective "nucleo-cytoskeletal" integrity (7, 30, 49, 73). Homozygous mice lacking LMNB1 survive embryonic development but die at birth with defects in bone and lung. Analysis of embryonic fibroblasts from LMNB1 deleted mice shows abnormalities in nuclear structure and clustering of nuclear pore complexes (73, 88). Mice that are null for lamin A but express both B and C type lamins appear to be healthy (6, 73, 77, 88).

1.1.4 Lamins and Diseases

Mutations in the Lamin A/C (LMNA) gene lead to a spectrum of degenerative diseases in humans with more than 10 different clinical syndromes collectively termed laminopathies (Table 1.1) (5, 10-11,13, 26, 32, 41, 44, 48, 51, 58, 60, 77, 83, 86). To date, approximately 200 mutations have been found in LMNA according to the database of "nuclear envelopathies" (http://www.umd.be). Mutations in the LMNA gene can be classified into four groups of disorders with overlapping phenotypes: **1)** diseases of striated muscle (Autosomal Dominant form of Emery-Dreifuss Muscular Dystrophy (AD-EDMD) (22, 40, 47, 50, 84-85), Dilated cardiomyopathy (DCM) (48, 78, 84), and limb-girdle muscular dystrophy type 1B (LMG1B)), **2)** lypodystrophy syndromes affecting adipose tissue deposition (Dunnigan-type familial partial lipodystrophy (FPLD) and mandibuloacral dysplasia (MAD)) **3)** a peripheral neuropathy (Charcot-Marie-Tooth neuropathy type 2B (CMT2B)) and **4)** accelerated aging disorders (Hutchinson-Gilford progeria syndrome (HGPS) and Werner's syndrome) (60, 73, 88) . There are only two mutations in lamins B1 and B2: **1)** autosomal-dominant leukodystrophy, (56) which is caused by a duplication of LMNB1 and **2)** acquired partial lipodystrophy (29) which is caused by LMNB2 mutations.

The striated muscle diseases caused by LMNA mutations are characterized by muscle wasting, as muscle fibers do not function properly overtime, and subsequently leading to progressive muscular weakness. Individuals with AD-EDMD undergo dystrophy specific for certain muscle groups as well as conduction defects. DCM-CD patients experience dilation of heart chambers, hypertrophy, arrhythmic conduction defects and cardiac arrest (48, 88). Mutations in lamins can also affect nuclear function and nuclear integrity leading to changes

in downstream elements and nuclear targets. The molecular mechanism behind the development of these diseases and lamin-interacting targets roles have yet to be discovered.

1.1.5 Mouse Models of Laminopathies

Currently four mouse models exist for studying diseases caused by LMNA mutations such as muscular dystrophy, cardiomyopathy and progeria (73). In the first mouse model lamin A or C proteins are not expressed ($lmna^{-/-}$). Lamin A/C null mice ($lmna^{-/-}$) have shown to rapidly develop muscle wasting and cardiomyopathy indicative of human EDMD and die about 6-8 weeks of age (73). In humans, heterozygous LMNA mutations cause disease but are asymptomatic in mice (73, 88). A number of signaling pathways are altered in response to deletion of LMNA expression. Some of these signaling pathways include: MAPK (map kinase), p38, pRb (phosphorylated retinoblastoma protein), Wnt, MyoD, and TGF beta (transforming growth factor β). Initiation of MAPK signaling leads to sequential activation of several kinases: JNK (c-Jun N-terminal kinases) and ERKs (extracellular-signal-regulated kinases). Upon activation, p38, JNK, and ERKs phosphorylate a number of transcription factors including GATA4 and MEF2. In addition, pRb-MyoD abnormalities have been observed in mouse models of EDMD and human models of AD-EDMD and X-EDMD. In skeletal muscle, pRb (a binding partner of Lamin A/C) coupled to the myogenic basic-helix-loop-helix transcription factor, MyoD, induces myogenic gene expression and cell cycle arrest. In cells lacking Lamin A/C expression, inactivation of pRb is disturbed leading to a delay in cell differentiation (73, 88).

The second mouse line established carries a missense mutation (histidine-to-proline substitution at amino acid 222 (H222P)) (1, 73). This model represents a good model for

studying laminopathies that result in muscular dystrophy similar to the human disease. Adult mice that are homozygous for this mutation show reduced locomotion and abnormal walking posture. In addition, by 9 months of age mice with H222P mutation demonstrate cardiac fibrosis, heart chamber dilation and conduction defects resulting in death. The female homozygote shows these phenotypes at a later stage and survives for a longer period of time (73, 88).

The third mouse model was designed to study dilated cardiomyopathy with conduction defects (DCM-CD) and involves a missense mutation in the LMNA gene (asparagine-to-lysine substitution at amino acid 195-N195K). The last model involves the production of transgenic mice in which a mutant form of lamin A, M371K which causes EDMD was expressed in the heart. Analysis revealed that mice expressing the M371K mutant have disrupted cardiomyocytes and abnormal nuclei and had an early death by 2-3 weeks of age (73,88).

1.1.6 A-Type Lamins as markers of stem cell differentiation and ageing

A-type lamins have also been shown to be markers of stem cell differentiation (14, 59) and ageing (8, 43, 45, 52, 71, 82). Adult stem cells have been identified in most mammalian tissues and are essential for the repair and regeneration of tissues. A reduction in the number of adult stem cells results in many of the age-related disease pathologies and a decrease in tissue-regenerative responses (8). In particular, the phenotypes observed in LMNA mutations are similar to those seen in age-related disorders. Several mesenchymal tissues affected by LMNA mutations are also similarly affected in age-related diseases (Figure 1.2) (59). *Pekovic and Hutchison,* (59) recently have proposed that A-type lamins

may act like receptors that receive signals from the cytosol, and that these signals may be associated with lamins emerging role in stem cell differentiation and cellular ageing (59). In support of this new concept the loss of A-type lamins in both humans and mice results in a rapid ageing syndrome, progeria (8,45).

Lamin A/C expression has been shown to be a marker of human and mouse embryonic stem (ES) cell differentiation. ES cells are obtained from the inner cell mass blastocyst-stage embryos. ES cells have unlimited proliferative capacity and hence are said to be pluripotent. Undifferentiated mouse and human ES cells express lamins B1 and B2 but not Lamin A/C. It is only during human/mouse ES cell differentiation (before the down-regulation of the pluripotency marker Oct-3/4) that Lamin A/C expression is activated. This data further elaborates the important roles of nuclear lamins in cell maintenance and differentiation (14, 59).

1.1.7 Molecular models of laminopathies

The reasons why mutations in the LMNA gene lead to a spectrum of diseases still remains contradictory (60, 89). Nevertheless, four models have attempted to explain the mechanisms that lead to lamin-associated diseases. The first model states that the development of laminopathies is due to changes in nuclear mechanics and mechano-transduction responses. This is evident through studies demonstrating deformations in the nucleus and distortions in nuclear activity due to the lack of lamins A or C (60).

The second model asserts that it is lamins A and C, which are involved in regulating cell type-specific gene expression. It is mutations in the lamin A and C gene that lead to mis-regulation of tissue specific genes (60).

The third model further states, that lamins A and C are involved in regulating cell type-specific gene expression affecting adult stem cell differentiation. This model is supported by evidence that shows lack of lamins A and C are markers of undifferentiated embryonic stem (ES) cells (60).

Lastly, the fourth model is based on the premise that mutations in LMNA cause permanent farnesylation of cysteine residues in lamin A which is toxic to cells. As a result, this affects many aspects of nuclear activity including chromatin organization, gene expression and nucleus morphology (60).

Table 1.1. Diseases related to mutations of LMNA gene encoding lamins A and C. Chromosome location 1q21.3 (5, 10-11, 13, 26, 32, 41, 44, 48, 51, 58, 60, 77, 83, 86).

Disease	Major Phenotype	Representation of mutations
	Diseases of striated muscles	
Autosomal dominant Emery-Dreifuss muscular dystrophy (AD-EDMD)	Slow progressing muscle weakness and wasting; conduction defects in heart	Throughout coding sequence, includes amino acid substitutions, frameshift and premature stop codons
Autosomal recessive Emery-Dreifuss muscular dystrophy (AR-EDMD)	Slow progressing muscle weakness and wasting, conduction defects in heart	Single homozygous mutation at C664T giving rise to amino acid substitution H222Y
Limb girdle muscular dystrophy type 1B (LMG1B)	Progressive muscle weakness of hip girdle and proximal arm and leg muscle	Amino acid substitution, codon deletion, and splice donor mutations reported
Dilated cardiomyopathy with conduction system defect (DCM-CD)	Impaired systolic function and dilation of the left or both ventricles. Variable skeletal muscle involvement	Throughout coding sequence, includes amino acid substitutions, frameshift and premature stop codons
	Peripheral Neuropathy	
Autosomal recessive Charcot-Marie-Tooth neuropathy type 2B (CMT2B)	Demyelination of motor nerves, motor deficits, absent deep-tendon reflexes	Single autosomal recessive change in the rod domain of A-type lamins
	Lypodystrophy syndromes	
Autosomal dominant Dunnigan-type familial partial lipodystrophy (AD-FPLD)	Loss of subcutaneous white adipose tissue from the limbs, gluteal regions and regions of the trunk; concomitant accumulation of white adipose tissue in neck, face and abdominal regions	Amino acid substitutions on the surface of an Ig like fold in the tails of lamin A and C
	Accelerated aging disorders	
Autosomal dominant Hutchinson-Gilford progeria syndrome (HGPS)	Premature ageing, cardiovascular diseases, growth retardation, loss of subcutaneous fats, poor muscle development	Abnormal splice donor site in exon 11 of LMNA

Figure 1.2. Laminopathies and Age-related diseases. Schematic diagram showing the similarities between mesenchymal tissues (brain, bone, skin, adipose, heart, skeletal muscle and vasculature) that are affected in age-related diseases (pink) and human diseases that are caused by specific mutations in the Lamin A/C gene (blue). This figure is reprinted by permission from Blackwell Publishing Limited: *Journal of Anatomy*, Pekovic V & Hutchison CJ, Adult stem cell maintenance and tissue regeneration in the ageing context: the role for A-type lamins as intrinsic modulators of ageing in adult stem cells and their niches, Figure 1, Pg 8, Volume 213, Issue 1, copyright (2008). (59).

Figure 1.2

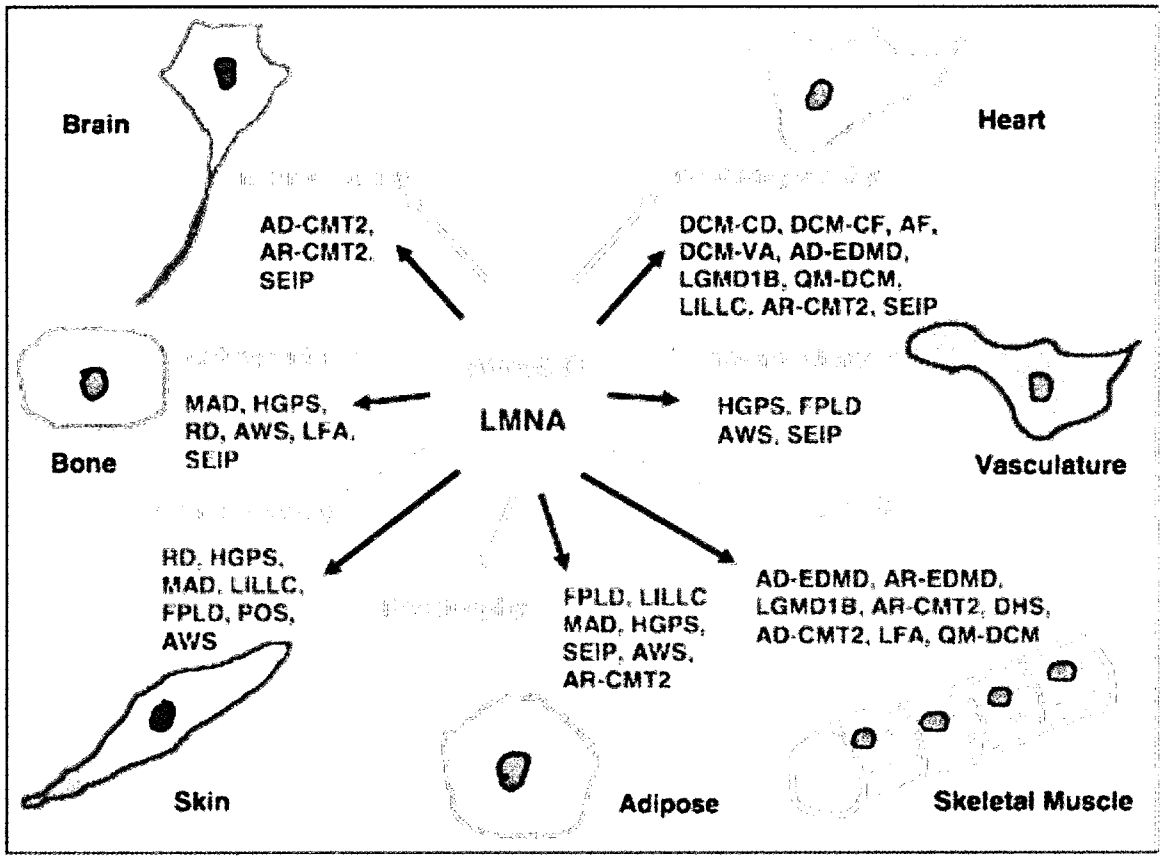

This figure is reprinted by permission from Blackwell Publishing Limited: *Journal of Anatomy*, Pekovic V & Hutchison CJ, Adult stem cell maintenance and tissue regeneration in the ageing context: the role for A-type lamins as intrinsic modulators of ageing in adult stem cells and their niches, Figure 1, Pg 8, Volume 213, Issue 1, copyright (2008). (59).

1.2 Identification and Initial Characterization of a Novel A-type lamin interacting transcription factor (LITF)

Mutations in the rod-1 domain of Lamin A/C (LMNA) gene leading to AD- EDMD and DCM-CD are associated with both skeletal and cardiac phenotypes, respectively. This suggests that there is a muscle-specific or heart-specific protein(s) that interact with the rod-1 domain of Lamin A/C. Thus, alteration of Lamin A/C interaction(s) with a tissue specific protein(s) may be responsible for the pathogenesis of tissue-specific laminopathies. To identify the proteins that interact with the rod-1 domain of LMNA a yeast-two-hybrid (Y2H) interaction screen was employed using the N-terminal globular and rod-1 domain as bait (amino acids 1-230). Proteins encoded by a pooled human heart complementary DNA library (Clonetech) were screened for their ability to interact with the rod-1 domain of LMNA. A previously uncharacterized cDNA clone, the A-type lamin interacting transcription factor (LITF) clone (C6orf142) was identified by Dr. Patrick Burgon.

LITF was mapped to human chromosome 6p12.1 and subsequently identified as a putative open reading frame (C6orf142, GenBank number: NM_138569). The human LITF gene consists of 13 exons and spans over 247 kilobases (kb). It is predicted to translate a 458 amino acid protein (Figure 1.3). The mouse homologue of LITF is mapped to chromosome 9E and consists of at least seven known isoforms and 12 putative exons. The protein encoded by the human heart-derived cDNA clone is approximately 69% identical to the mouse sequence (2310046A06Rik).

To confirm that the LITF-Lamin A/C interaction identified in the yeast transcriptional assay was direct, *in vitro* co-precipitation assays were performed. Two major splice variants of LITF were initially cloned from mouse hearts and fused in frame with a hexa-histidine epitope tag. Various combinations of purified His_6-LITF and GST-Lamin recombinant

proteins were incubated together at room temperature. LITF was co-precipitated with Lamin A/C as detected by immunoblotting for the GST-tag fused to lamin (Figure 1.4). Lamin did not pellet in the absence of LITF. The presence of exon 3 of LITF resulted in a marked reduction in lamin binding which suggests that exon 3 of LITF disrupts or inhibits binding to LITF and that it may play a regulatory function in LITF function.

LITF is a unique vertebrate gene and does not portray similarities to any other known human proteins. Structural or functional domains within the primary amino acid sequence or the nucleic acid sequence of LITF remain unknown. Comparisons of the deduced 458 amino acid protein, or the nucleic acid sequence against the GenBank database revealed no significant similarities with any other human gene. Homologous forms of LITF in non-human vertebrate genomes or EST databases were identified. However, no significant homologous forms of LITF were observed in invertebrates. This data suggested that LITF plays an important regulatory or functional role in Lamin A/C biology. Hence, LITF like Lamin A/C may be involved in biological processes such as cell differentiation, fate determination or commitment, regeneration and ageing.

Figure 1.3. A) Sequence alignment of deduced amino acid sequence of mouse LITF and other species for analysis of homology. A conserved LITF core domain is revealed. LITF-specific polyclonal antibodies were raised against the two highlighted (yellow) mouse LITF peptides. B) Alignment of the deduced amino acid sequence of the largest LITF isoform between species. Asterisks (*) indicate identical amino acids, double points (:) are conserved exchanges, single points (.) are homologous amino acids. Numbers indicate the position of the last amino acid for each line. This figure is courtesy of Dr. P. Burgon.

Figure 1.3

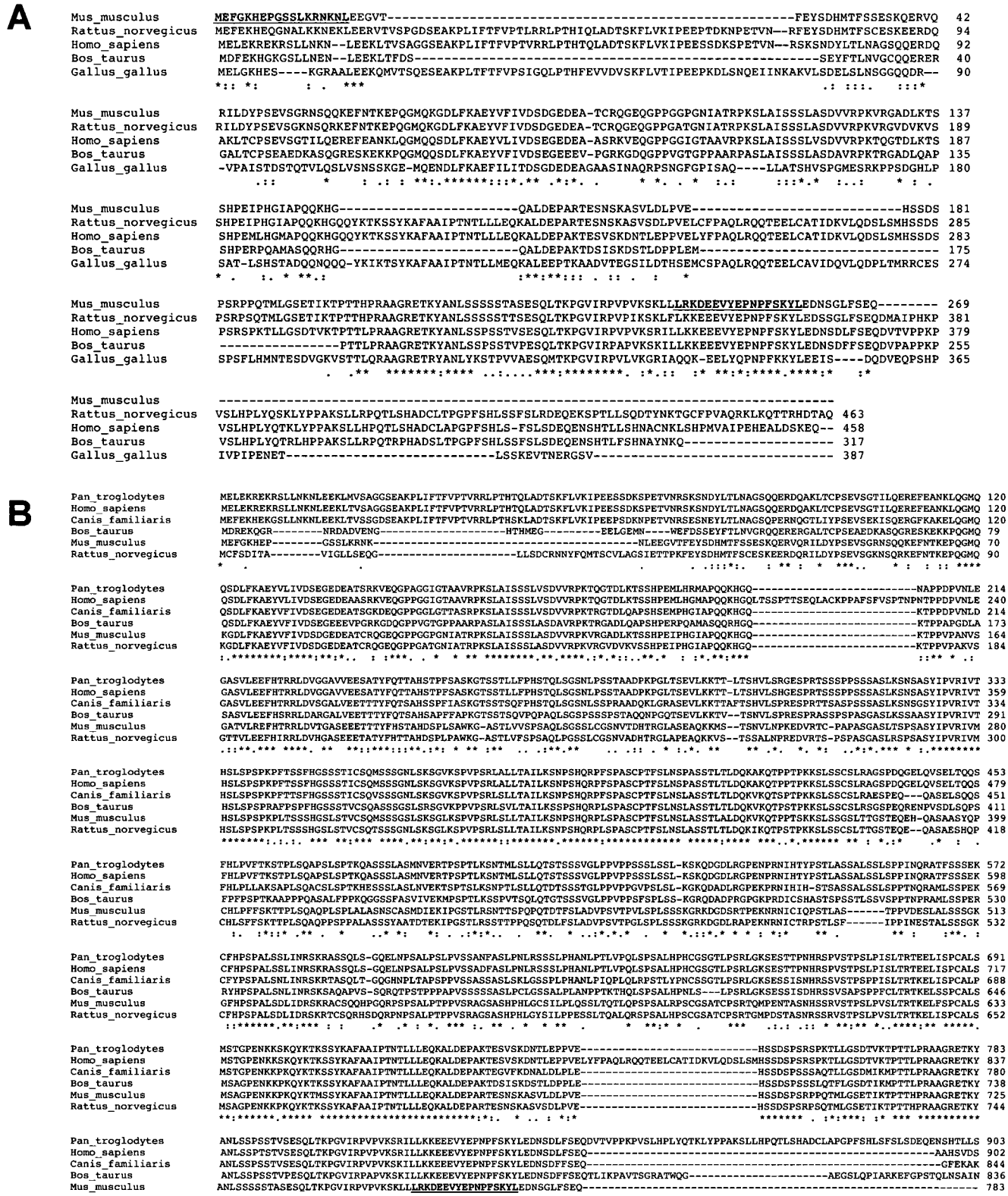
A
Mus_musculus
Rattus_norvegicus
Homo_sapiens
Bos_taurus
Gallus_gallus
B
Pan_troglodytes
Homo_sapiens
Canis_familiaris
Bos_taurus
Mus_musculus
Rattus_norvegicus

Figure 1.4. LITF binds Lamin A/C *in vitro*. Purified recombinant LITF binds recombinant rod 1 domain of Lamin A/C directly in Immunoprecipitation assay. Both the full length LITF and the short form of LITF (LITF(ΔExon3)) were sub-cloned in frame with an N-terminal hexa-histidine tag of a pET100 vector and recombinant His_6-LITF and GST-Lamin were subsequently expressed in *E.coli.* Western analysis was performed using anti-GST (Cell Signaling) and anti-LITF polyclonal antibodies. A 1:10 dilution of the total starting material was run on the same gel (left panel). Assay was repeated two additional times with similar results. Figure was obtained with permission from Dr. P. Burgon.

Figure 1.4

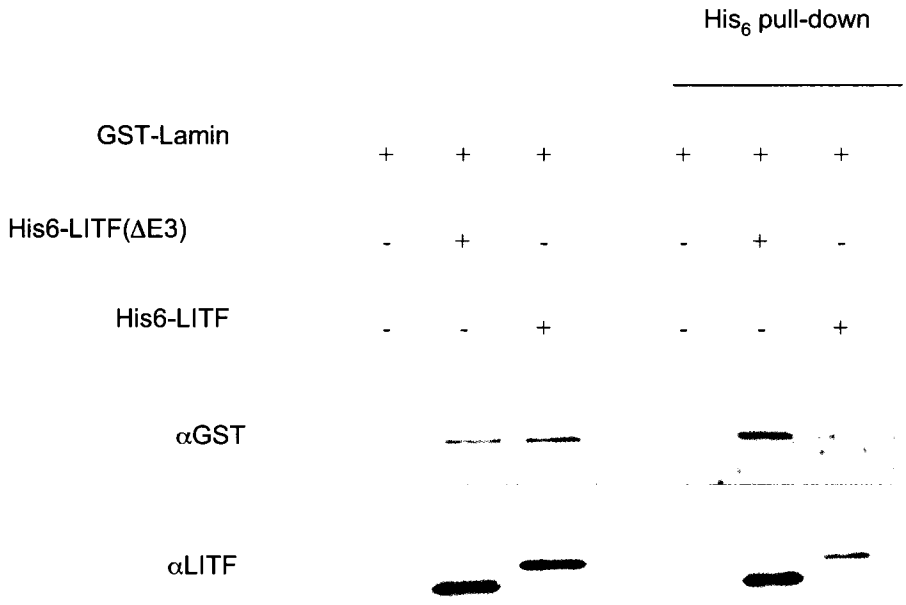

Courtesy of Dr. Patrick Burgon

In mice, LITF mRNA is primarily associated with the heart and brain, whereas in humans it is mostly associated with the heart and skeletal muscle as demonstrated by Northern profile analysis (Figure 1.5A). Real-time PCR of LITF mRNA from various mouse tissues showed a similar distribution of LITF expression as the Northern profile analysis, with smooth muscle > skeletal muscle > heart > brain (Figure 1.5B). According to the Allen Brain Atlas, LITF staining in the brain mainly corresponds to the hippocampus and olfactory bulb regions (16, 37). Western blot analysis was performed to assess LITF protein expression in different mouse tissues: brain, heart, skeletal muscle, liver and lung. LITF is present within all mouse tissues tested and seven different LITF isoforms are observed. The functional role of these different isoforms is currently being investigated within our laboratory. In addition, LITF expression was assessed in three transformed mouse cell lines C2C12 (mouse myoblast), HL-1 (cardiac muscle cell line, from the AT-1 mouse atrial cardiomyocyte tumor lineage) and C3H10T1/2 (multi-potent mesenchymal cells) (Figure 1.5C). It is interesting to note that the pattern of distribution of the LITF isoforms in the transformed cell lines is similar to those of the tissue they were derived from (Figure 1.5C).

LITF is expressed endogenously within C2C12 cells (adult mouse myoblasts) and HL-1 (heart derived) cells. The specificity of the LITF antibody has been confirmed using peptide neutralization experiments (Appendix, Figure S1). In HL-1 (Figure 1.6) and C2C12 cells there is a very clear punctate staining of LITF within the nucleus and a diffuse cytosolic staining is evident (Figure 1.7A-E). Furthermore, LITF co-localizes with Lamin A/C in the nuclear envelope as well as the nucleus. LITF localization is also seen within promyelocytic leukemia (PML) nuclear bodies of C2C12 myoblasts (Figure 1.7F).

Figure 1.5 LITF expression profile analysis. A) Specific expression of LITF in mouse. Distribution of LITF expression by Northern analysis in mouse and human tissues revealed two major LITF RNA transcripts. 10μg of poly-A enriched RNA was loaded per lane. LITF is primarily associated with the heart and brain in mouse (left panel) and skeletal muscle and brain in human (right panel). Loading control used was B-Actin. **B)** Normalized tissue distribution of LITF expression in adult mice (n=3) tissues as determined by real-time PCR. **C)** Western blot analysis of LITF protein expression in mouse tissues (brain, heart, skeletal muscle, liver and lung) and transformed mouse cell lines (C2C12 mouse myoblast, HL-1-heart derived cells, C3H10T1/2-mesenchymal cells). Figures are obtained with permission from Dr. P. Burgon (Principal Investigator), Laura Kenney (Previous Laboratory Technician) and Shelley Deeke (MSc. Candidate, Dr. Burgon's Lab).

Figure 1.5

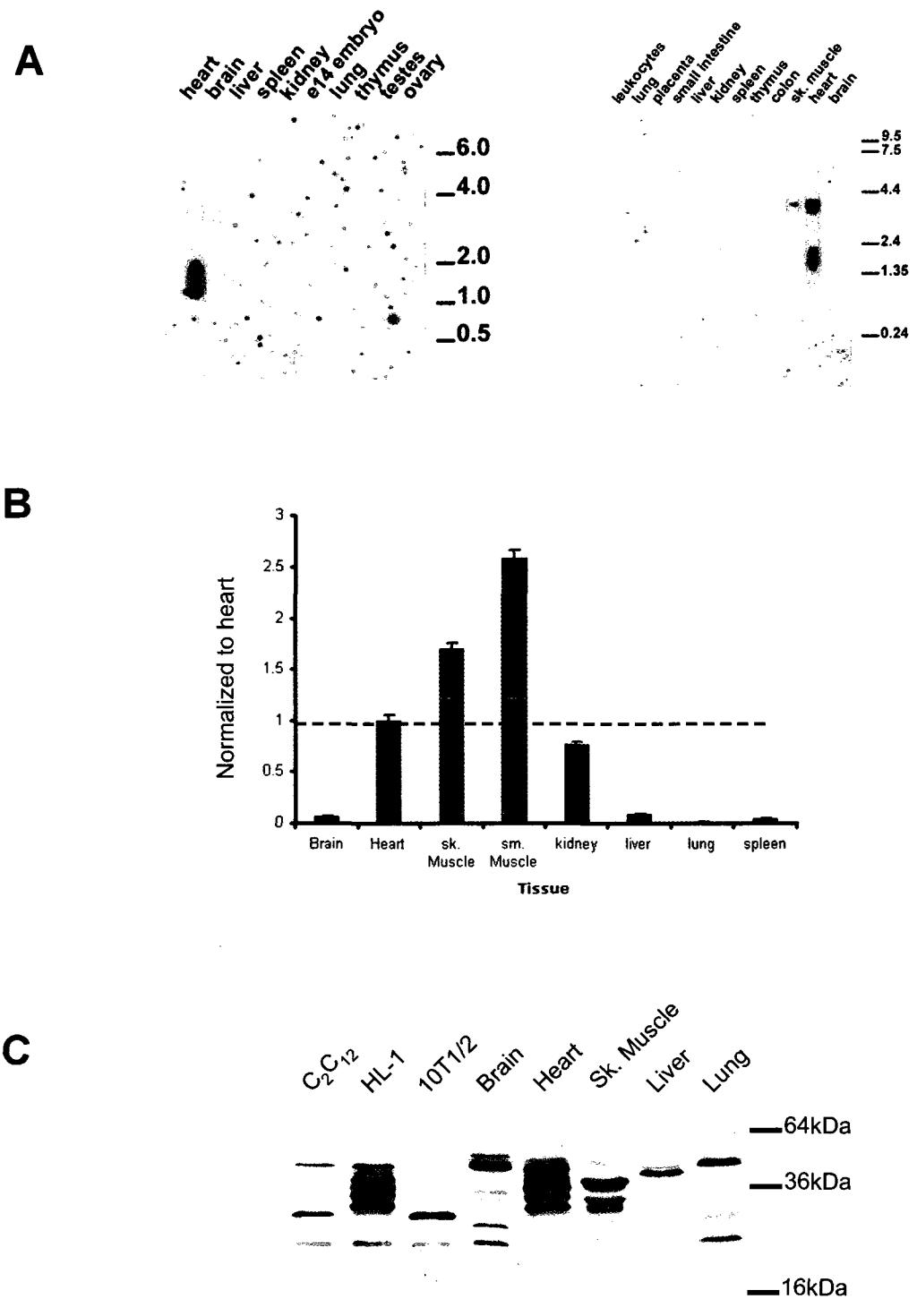

Courtesy of : Dr. Patrick Burgon, Laura Kenney, Shelley Deeke

Figure 1.6 LITF and LMNA localization in HL-1 (heart-derived cells) and C2C12 (mouse myoblast) cell line. LITF localizes with Lamin A/C (LMNA) in the nucleus of HL-1 cells and C2C12. A) HL-1 cells were stained with a specific LITF antibody (C-LITF):green, Lamin A/C antibody :red and DAPI staining of nuclei : Blue. White arrows indicate where there is co-localization (yellow) between LITF and LMNA within the nucleus and at the nuclear envelope. B) Mouse C2C12 myoblast cells were stained with a specific LITF antibody (C-LITF): green and Lamin A/C red, DAPI: blue. Co-localization (yellow) of LMNA and LITF is indicated in yellow and by the white arrows. This figure was obtained with permission from Lara Kouri (MSc. Candidate) and Dr. P. Burgon.

Figure 1.6

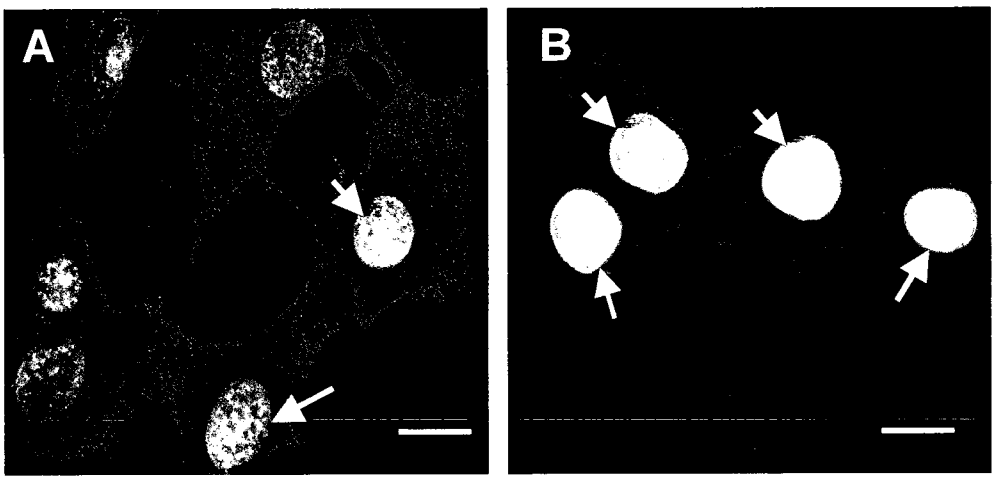

Figure 1.7 LITF localizes in C2C12 cells. A-D) LITF localizes to the nucleus of C2C12 myoblast cells in a punctate staining manner as well as a diffuse cytosolic staining. DAPI: blue, C-LITF: green. E) LITF localizes to C2C12 differentiated myotubes as shown by myosin heavy chain (MHC) staining. DAPI: blue, LITF: green, MHC: red. F) Punctate staining of LITF with PML bodies of the nucleus in C2C2 cells. LITF: green, PML: red, Co-localization (yellow).

Figure 1.7

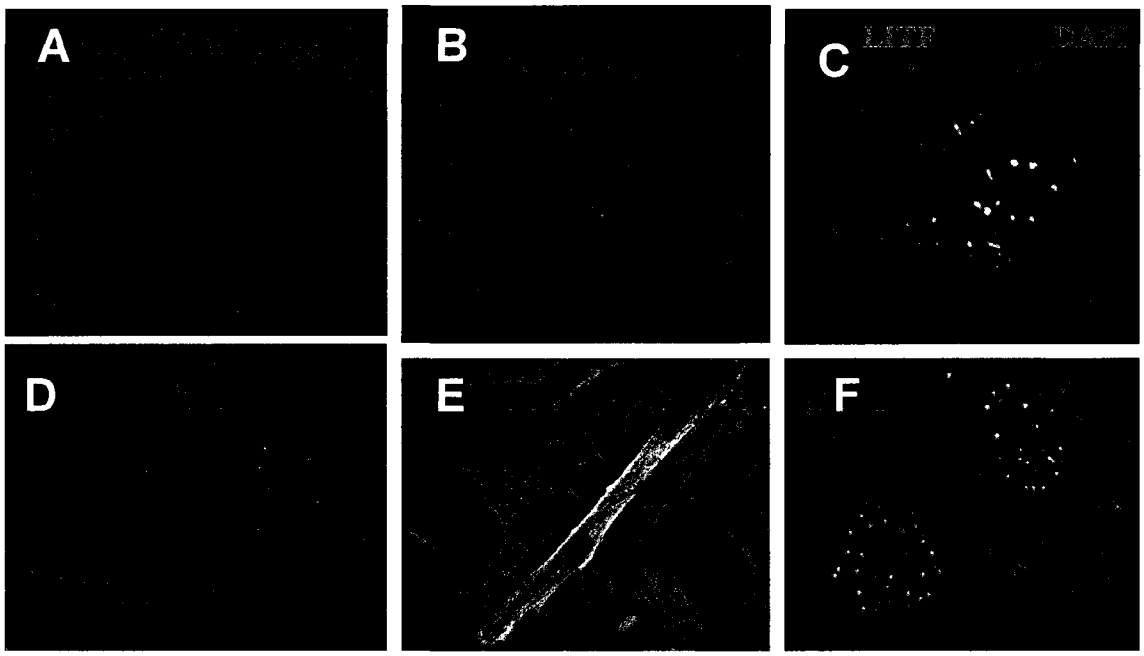

1.3Hypothesis, Rationale and Objective of proposed study

The presence of specific missense mutations in the rod-1 domain of Lamin A/C gene from amino acids 190-230, which result in EDMD and DCM-CD suggested the presence of a muscle or cardiac-specific factor(s) that interact with this domain of Lamin A/C. This led to the discovery of LITF through a yeast-two-hybrid screen (described in section 1.2) and the postulation that LITF must be involved in the process of skeletal myogenesis. My primary aim was to determine the function of LITF using a well characterized and established mouse myoblast cell line C2C12. The endogenous expression of LITF in C2C12 cell line and its potential role in skeletal myogenesis started the foundation of my project.

OVERALL AIM: To determine the function of A-type lamin interacting transcription factor (LITF) using C2C12 cells as a model system.

HYPOTHESIS: LITF is necessary for the progression of skeletal myogenesis and for proper myotube formation.

SPECIFIC AIMS:

1) To define LITF expression pattern during normal C2C12 cell differentiation into myotubes. (Chapter 3)

   Methods employed: Western Blot analysis, Semi-quantitative RT-PCR and Immunofluorescence microscopy.

2) To determine the potential functional targets of LITF. (Chapter 4)

   Methods employed: Chromatin Immunoprecipitation (ChIP), ChIP-on-chip, electrophoretic mobility shift assays (EMSA) and Bioinformatic analysis.

3) To examine the effects of shRNAmir-mediated down-regulation of LITF on myogenic differentiation through generation and characterization of LITF stably knockdown C2C12 cells. (Chapter 5)

   Methods employed: Generation of stable cell lines using shRNAmir, Western Blot analysis, and Immunofluorescence microscopy.

Chapter 2:

Experimental Procedures

2.1 Cell Culture Techniques

2.1.1 Growth conditions

Mouse C2C12 myoblast cell line were obtained from the American Type Culture Collection (ATCC no.CRL-1772) and were cultured at 37°C in an atmosphere of 10% CO_2 in growth medium (GM) which consists of Dulbecco's Modified Eagle's Medium supplemented with 20% fetal bovine serum (FBS) (Fisher Scientific), 1% vol/vol penicillin-streptomycin (Invitrogen) and 2mM L-glutamine (Invitrogen). To induce myogenic differentiation, confluent cells were subjected to differentiation by switching growth media to differentiation medium (DM). Differentiation medium (DM) consisted of DMEM complemented with 2% horse serum (Fisher Scientific) and 1% vol/vol penicillin-streptomycin. Cell culture dishes used were all cell culture treated and were purchased from Fisher Scientific.

2.1.2 Generation of stable cell lines

C2C12 cells were transfected with four different shRNAmir constructs (three targeting LITF and an pGIPZ empty vector control) purchased from OpenBiosystems using ArrestIn transfection reagent (OpenBiosystems) in 60mm cell culture plates were selected in growth medium containing 1.5μg/mL of dihydrochloride puromycin (Sigma). Media was changed daily for four weeks until clones were selected. These clones were further cultures and expanded and subjected to genotyping to confirm identity.

2.2 Whole cell extract preparation and Western Blotting

2.2.1 LITF expression during normal C2C12 cell differentiation

To determine LITF, Myogenin and α-Tubulin protein expression during normal C2C12 cell differentiation C2C12 myoblasts were plated in growth medium at a dilution of 1:20 in 60mm cell culture treated plates (Corning). Differentiation was induced at about 60% confluency by switching to DMEM supplemented with 2% horse serum (DM). GM was removed from plates and cells were washed with DM then incubated with fresh DM. Differentiation medium was changed daily.

Whole cell extracts were harvested at 0, 6, 9, 18, 24, 30, 48 and 72 hours post-differentiation (n=3). Proteins were extracted using 300µl of lysis buffer containing: 50mM Tris-HCl [pH= 8.0], 200mM NaCl, 20mM NaF, 20mM β-glycerolphosphate, 0.5% NP-40, 0.1mM Na_3Vo_4, 1mM dithiothreitol (DTT), 1xProtease inhibitor cocktail (Roche, 1 tablet/7.0mL), and phosphatase inhibitor cocktails (Sigma, 0.1mL/7.0 mL). Cells were scraped from dishes and lysates pipetted into 1.5mL centrifuge tubes. Lysates were incubated on ice for 20 minutes and then cleared by centrifugation at 10,000xg for 10 minutes at 4°C. Supernatants collected and protein concentrations were determined using Bio-Rad protein assay dye reagent concentrate kit (Biorad) and values read using the Bio-Rad Model 3550-UV Microplate Reader (O'Brien Lab, Heart Institute). Proteins were resolved on a 15% 0.75mm thick SDS-TrisGlycine polyacrylamide gel at 100V (Biorad Gel Apparatus) and transferred to PVDF membranes (Millipore) for 1 hour at 100V at 4°C. Transfer buffer is composed of 190mM glycine, 25mM tris base and 20% cold methanol. Upon transferring, membranes were blocked in 5% nonfat milk (Nestle) dissolved in Tris base-Tween-20 (TBS-T, 10%TBS (500mM Tris, 1.5M NaCl), 0.1% Tween-20) for 1 hour after which they were

incubated with appropriate primary antibody in 5% nonfat milk overnight with gentle shaking at 4°C.

For Western blot analysis, the following primary antibody concentrations were used: LITF antibodies were raised in rabbits against two synthetic peptides N-MEFGKHEPGSSLKRNKNL-C and N-LRKDEEVYEPNPFSKYL-C (21st Century Biochemicals). The LITF antibody designed to the c-terminus entitled C-LITF was used for western blot analysis, 1:50 000 of rabbit antibody (generated in house); Myogenin mouse monoclonal IgG 1:1000 (Clone F5D sc12732; Santa Cruz Biotechnology) and anti-α Tubulin mouse monoclonal 1:5000 (T9026, Sigma).

Membranes were then incubated with HRP-conjugated anti-rabbit and anti-mouse IgG secondary antibody (Santa Cruz Biotechnology) for 1 hour at room temperature with gentle shaking. Immunoblot signals were detected with a SuperSignal West Pico Chemiluminescent Kit as per manufacturers protocol (Thermo Scientific) and were developed on an X-ray film (Sigma).

2.2.2 Determination of the efficacy of LITF knockdown

To determine the efficacy of LITF knockdown in C2C12 cells, cells were transiently transfected with three LITFshRNAmirs (n=3). Transfected cells were grown to confluency and lysed using lysis buffer to collect protein lysates. LITF and Myogenin expressions were detected in protein lysates using immunoblotting (1:50 000 of C-LITF of rabbit polyclonal antibody and 1:1000 of Myogenin mouse monoclonal IgG (Clone F5D sc12732; Santa Cruz Biotechnology)). Protein bands were normalized to α Tubulin using anti α- Tubulin mouse monoclonal antibody (1:5000 dilution (T9026, Sigma)).

2.2.3 Analysis of the expression of Myogenin, MyoD, Six1 and Six4 in LITF-KD1 and LITF-KD2 cell lines

To determine levels of LITF, Myogenin, MyoD, Six1, Six4 and Tubulin protein expression in normal C2C12 cells as well as KD cell lines (KD1 and KD2), C2C12 myoblasts were plated in growth medium at a confluence of 10% in 60mm cell culture treated plates (Corning, Fisher Scientific). Differentiation was induced at about 60% confluency by switching to DM. Plates were washed with DM then incubated with fresh DM.

Protein lysates were harvested at 0, 24, 48, 72, 96 and 120 hours post differentiation and Western Blot analysis was performed as described above (n=3). For Western blot analysis, the following primary antibody concentrations were used: mixed (N/C) polyclonal LITF antibody 1:50 000; Myogenin mouse monoclonal IgG 1:1000 (Clone F5D sc12732; Santa Cruz Biotechnology); MyoD mouse monoclonal IgG 1:500 (Clone 5.8A, sc32758; Santa Cruz Biotechnology), anti-α Tubulin mouse monoclonal 1:5000 (T9026, Sigma). Six1 and Six4 rabbit polyclonal antibodies (1:1000 dilutions) were a generous donation from Dr.Alex Blais laboratory (University of Ottawa).

Membranes were then incubated with HRP-conjugated anti-rabbit and anti-mouse IgG secondary antibody (Santa Cruz Biotechnology) in 5% nonfat milk (Nestle) dissolved in Tris base-Tween-20 (TBS-T, 10%TBS (500mM Tris, 1.5M NaCl), 0.1% Tween-20) for 1 hour at room temperature with gentle shaking, and immunoblot signals were detected with a SuperSignal West Pico Chemiluminescent Kit (Thermo Scientific) followed by development on X-ray film (Sigma).

2.3 RNA isolation, Semiquantitative RT-PCR, quantitative Real-time PCR (qPCR)

For establishing a time course of LITF RNA expression, during normal C2C12 cell differentiation, total RNA was extracted at 0, 6, 9, 18, 24, 30, 48 and 72 hours post differentiation (n =3) for semiquantitative RT-PCR and times 0, 9, 12, 24, 30, 48, 72 for quantitative real-time PCR (n=3). Appropriate RNAse-free laboratory equipment was used (including RNAase free microfuge tubes and pipettes) and a sterile work area was maintained at all times. RNA was extracted from two different sets of C2C12 cells grown in 60mm plates using TRIzol Reagent (Invitrogen) according to manufacturer's protocol. RNA samples were DNase-treated prior to reverse transcriptase PCR (RT-PCR) according to manufacturers protocol (Promega). RNA samples were assessed for purity using the Bioanalyzer, RNA 6000 Nano Kit (Agilent Technologies, cat #5067-1511) and a QC (quality control) file was generated. 1.0μg of RNA was reverse transcribed using AffinityScript Multiple Temperature Reverse Transcriptase (Stratagene). cDNA was amplified with primers for Myogenin, Myod, LITF and GAPDH for semiquantitative RT-PCR. Primer sequences are shown in Table 2.1. Gene amplification was carried out as follows: 95 °C for 5 min, followed by 34 cycles in 3 steps: 95 °C for 30s, 60 °C for 30s, and 72 °C for 30s and 72 °C for 5min using Taq DNA polymerase (NEB). Melting curves were determined for all primers prior to use. The size of the PCR products was confirmed by analysis on a 2% agarose gel stained with ethidium bromide. For quantitative real-time PCR (qPCR) 1.0μg of RNA was reverse transcribed using AffinityScript Multiple Temperature Reverse Transcriptase (Stratagene). cDNA was amplified with primers for LITF. QPCR was performed using LightCycler® 480 SYBR Green I master and ran on LightCycler® 480 system (Roche).

2.4 Immunofluorescence Microscopy

2.4.1 LITF localization during normal C2C12 cell differentiation

C2C12 cells were grown on gelatin-coated coverslips in 12-well cell culture treated plates (Fisher Scientific). C2C12 cells were differentiated using differentiation medium and fixed at appropriate time points using pre-cooled methanol for 20 minutes on ice, and were washed carefully twice with phosphate-buffered saline (PBS). To reduce nonspecific binding, cells were blocked with PBS supplemented with 5% fetal bovine serum and 0.1% NP-40 in PBS for 30 minutes at room temperature with gentle shaking. Coverslips were then incubated with anti-C-LITF (1:10 000), anti-MHC (1:20) antibody (Developmental studies hybridoma bank) dissolved in 1.5% FBS/PBS for 1 hour at room temperature. After three washes with PBS, cells were incubated with fluorescent-conjugated secondary antibody 1:1000 (Alexa Fluor 568 goat anti-rabbit IgG (molecular probes), Regulus Red 594 anti-mouse IgG (LP Bio) in the dark for one hour. Next, the coverslips were washed three times in PBS and cell nuclei were counter-stained with DAPI (1μg/ml) (Invitrogen) for 3 minutes in the dark. Lastly, the coverslips were washed three times in PBS and mounted with fluorescent mounting medium (Dako) and images were then visualized using fluorescent microscopy (Zeiss Microscope, Dr. Alex Stewarts Laboratory, Heart Institute) (n=3).

2.4.2 Myosin heavy chain expression in LITF-KD1 and LITF-KD2

Normal C2C12 cells, pGIPZ encoding scrambled control, KD1 and KD2 cell lines were grown on gelatin-coated coverslips in 12-well cell culture dishes. Cells were differentiated for 0, 24, 72 and 120 hours in DM media (n=3). Coverslips were fixed and stained as described previously. Myosin heavy chain was detected using anti-MHC anti-mouse antibody 1:20 (Developmental studies hybridoma bank).

2.5 Chromatin Immunoprecipitation and ChIP-on-chip Studies

Chromatin was isolated from C2C12 cells using the SimpleChIP Enzymatic Chromatin IP kit using ChIP grade Protein G magnetic beads (Cell Signaling Technology) (Figure 2.1). Protein G magnetic beads were blocked with BSA to prevent non-specific binding. C2C12 myoblast cells were grown in 5x150 mm cell culture dishes (50 x 10^6 cells) and subjected to chromatin immunoprecipitation according to manufacturers protocol (Cell Signaling). Chromatin was sheared into approximately 5 nucleosomes using 2.5µl of micrococcal nuclease incubation for 20 minutes at 37°C with frequent inversions followed by 20 times dounce homogenization.

250µg of chromatin was immunoprecipitated with a specific LITF antibody and appropriate controls: positive control Histone H3 and negative control normal rabbit IgG. Chromatin was eluted from antibody/Protein G beads using 2x ChIP elution buffer (Cell Signalling) and magnetic beads pelleted using a Magnetic Separation Rack (n=4).

Figure 2.1 Schematic diagram of chromatin immunoprecipitation (ChIP) assay. C2C12 cells are fixed with formaldehyde to cross-link histone and non-histone proteins to DNA. Chromatin is digested with micrococcal nuclease followed by sonication to obtain 150-900bp DNA/protein fragments or nucleosomes. Immunoprecipitation is performed with a specific LITF antibody and the protein/DNA complex is captured by Protein G magnetic beads. Cross-links are reversed, and DNA is purified in DNA purification columns and analyzed by PCR, ChIP-on-chip and TOPO-TA cloning (n=4).

Figure 2.1

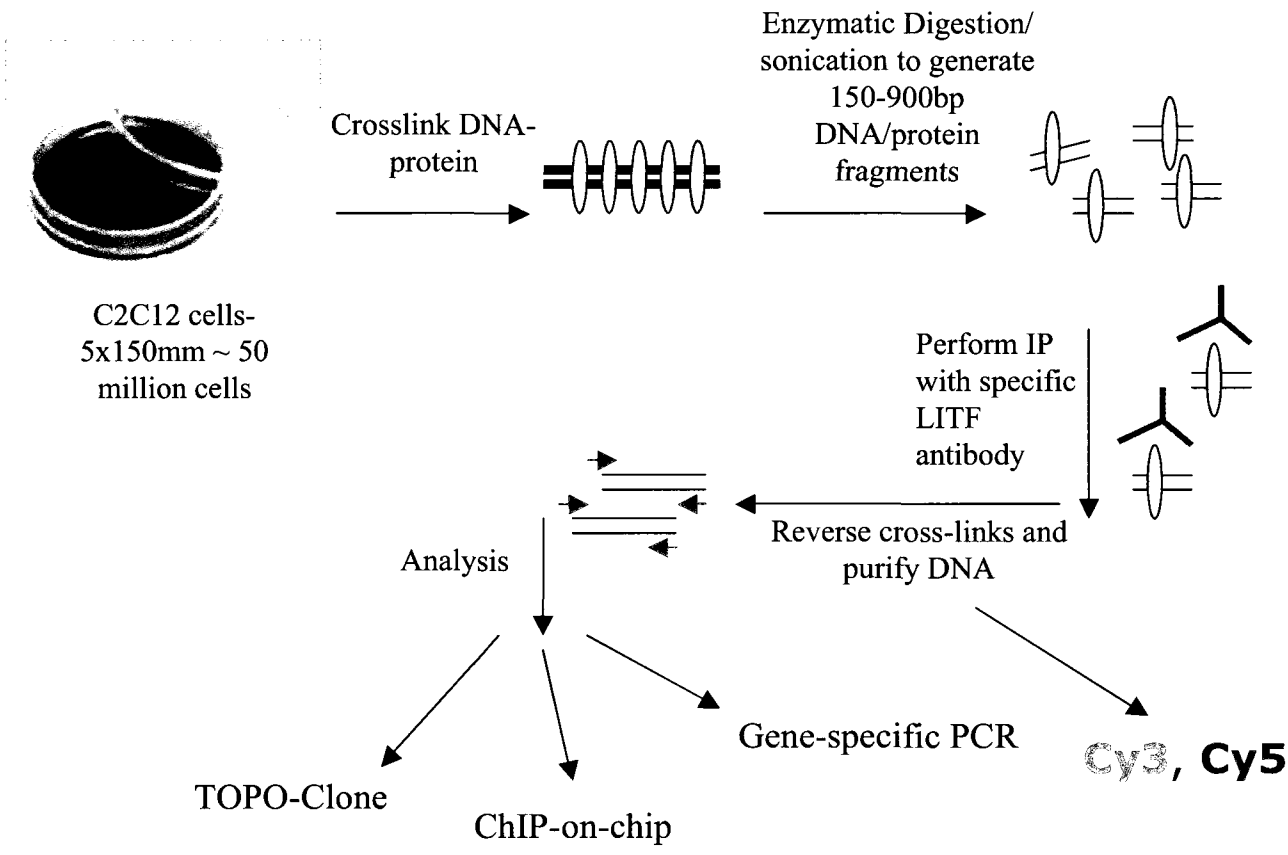
Crosslink DNA-protein
Enzymatic Digestion/ sonication to generate 150-900bp DNA/protein fragments
C2C12 cells- 5x150mm ~ 50 million cells
Perform IP with specific LITF antibody
Reverse cross-links and purify DNA
Analysis
Gene-specific PCR
Cy3, Cy5
TOPO-Clone
ChIP-on-chip

Following elution, 6ul 5M NaCl and 2.0ul of Proteinase K was added to eluted chromatin and incubated for 2 hours at 65°C to reverse protein-DNA cross-links. Following cross-linking DNA purification was performed using spin columns supplied within the kit. PCR was performed using regular Taq DNA Polymerase to add 5' and 3' linkers: oJW102: GCGGTGACCCGGGAGATCTGAATTC and oJW103: GAATTCAGATC to LITF immunoprecipitated ChIP DNA according to the method described by Agilent Mammalian ChIP-on-chip protocol (Agilent). Positive and negative control DNA was amplified with primers supplied in the kit to confirm that the ChIP experiment was performed successfully. Positive control included Histone H3 antibody, which recognizes many different species of the highly conserved Histone H3 protein (n=4). The purified positive control and negative DNA were amplified with primers specific for the mouse transcriptionally active ribosomal protein L3 (RPL30) gene locus which binds to Histone H3. DNA amplification was carried out as follows: 95°C for 5min, followed by 34 cycles in 3 steps: 95°C for 30s, 60°C for 30s, and 72°C for 30s and 72°C for 5min using Taq DNA polymerase (NEB). PCR products were isolated using QIAquick PCR purification kit columns (Qiagen). LITF PCR product (4.0μl) was TOPO-TA cloned into pCRII.1-TOPO (Invitrogen) and transformed into bacteria, *E.coli* (DH5-α cells (Invitrogen)) and plated onto ampicillin agar plates containing 50mg/ml ampicillin. Approximately 100 colonies were picked and direct PCR was performed using the following primers to pCRII.1-TOPO vector (Invitrogen) Forward: 5'-TCCGGCTCGTATGTTGTGTGGAAT-3' and Reverse: 5'-TGTGCTGCAAGGCGATTAAGTTGG-3' and sequenced using the BigDye Terminator v3.1 cycle sequencing kit (Applied Biosystems) to identify putative LITF targets. Several targets were obtained and analysis revealed they shared ontologies of commitment,

differentiation, growth, and apoptosis (BLAT, DAVID Bioinformatics Resources) (20, 31). Based on ChIP sequencing and in collaboration with Dr.Alex Blais it was determined that chromosome 11 (122Mbp) and chromosome 2 (182Mbp) have the most number of genes with ontologies similar to those in which putative LITF targets enrich for. Chromosome 11 (122Mbp) was chosen to be tiled out because it is smaller and allows for finer mapping. DNA arrays were designed to tile out mouse chromosome 11 and as well as 1600 promoter regions of genes with similar ontologies. LITF Immunoprecipitated DNA and Input (control) DNA were fluorescently labelled using Cy-3 and Cy-5 and hybridized using the SureHyb Hybridization chamber (Agilent) onto Agilent ChIP-on-chip microarray slides (n=2). Slides were scanned (Agilent scanner) and data extracted using the Agilent Feature Extraction Software. ChIP-on-chip was performed twice according to Agilent Mammalian ChIP-on-chip protocol. Putative LITF targets were analyzed using the USCS Cis-Genome Browser database and DAVID (Database for Annotation, Visualization and Integrated Discovery, 2008) bioinformatics tool for analysis of molecular function ontologies (20, 31).

In addition gene-specific PCR was performed on input and immunoprecipitated DNA using primers for Myogenin, Six1/4 and retinoic acid receptor alpha (RARα). Primer sequences used are shown in Table 2.1. DNA amplification was carried out as follow: 95°C for 5min, followed by 34 cycles in 3 steps: 95°C for 30s, 60°C for 30s, and 72°C for 30s and 72°C for 5min using Taq DNA polymerase (NEB).

2.5.1 Electrophoretic Mobility Shift Assays (EMSA) of ChIP-on-chip targets

DNA-protein binding was assayed with double-stranded DNA oligonucleotide probes that had been biotin 3'end DNA labeled according to manufacturer's protocol (Pierce). DNA oligonucleotides to Six1, Six3, Six4 and Retinoic acid receptor alpha (RARα), were designed (Table 2.1) (n=3). Reactions were performed in binding buffer [20mM HEPES (pH 7.9), 10% glycerol, 50mM KCl, 0.05% NP-40, 0.5mM EDTA, 0.5mM DTT, and 1mM PMSF] in the presence of 0.5μg of Poly(dI-dC), a nonspecific competitor, *in vitro* transcribed LITF protein using the T_NT Coupled T7/Sp6 Wheat Germ extract system according to manufacturer's instructions (Promega) or LITF antibody for 20 minutes at room temperature. Using the T_NT Coupled T7/Sp6 Wheat Germ extract system LITF in the pET100 vector was *in vitro* translated using T7 RNA polymerase. Products of the binding reactions were separated by polyacrylamide gel electrophoresis (PAGE) on a 6% gel in 0.5X TBE (Tris-Borate EDTA) for 1 hour at 100V. Binding reactions were transferred to nylon membrane (Millipore) and biotin-labelled DNA was detected using the LightShift Chemiluminescent EMSA kit as per manufacturers protocol (Promega, cat#20148) (n=3).

2.6 LITF-shRNAmir transfections of C2C12 myoblasts

Three mouse LITF-shRNAmir sequences based on the design of mir-30 in the pGIPZ vector targeting exon 2 and two targeting 3'UTR were purchased from OpenBiosystems. In addition, a non-silencing-GIPZ lentiviral shRNAmir control was purchased.

Sequences included

V2LMM_214053 (LITF-shRNAmir-1)
TGCTGTTGACAGTGAGCGAGCCAACTACTTGCTAATTATAGTGAAGCCACAGAT
GTATAGTTTAGCAGTAGTTGGCCTGCTACTGCCTCGA (3'UTR).

V2LMM_211301 (LITF-shRNAmir-3)
TGCTGTTGACAGTGAGCGCGCCTATAATGCCTTCTATTAATAGTGAAGCCACAGA
TGTATTAATAGAAGGCATTATAGGCTTGCCTACTGCCTCGGA (3'UTR).

V2LMM_130664 (LITF-shRNAmir-4)
TGCTGTTGACAGTGAGCGCCCAACTGATAAGAGTCCAGAATAGTGAAGCCACAG
ATGTATTCTGGACTCTTATCAGTTGGTTGCCTACTGCCTCGGA (Exon2).

The pGIPZ vector allows for assessment of transfection efficiency using turbo GFP marker and generation of stable cell lines using puromycin resistance selection. Bacterial cultures were spread onto ampicillin plates, colonies picked and grown for 16 hours in 37°C shaker/incubator in Luria-Bertani (LB) supplemented with 50 mg/ml ampicillin. Miniprep DNA was prepared using a standard phenol-chloroform alkaline lysis plasmid DNA miniprep protocol. DNA concentrations were determined using NanoDrop Spectrophotometer ND-1000. C2C12 cells in 60mm plates were transfected with 4.0μg of LITFshRNAmir plasmid DNA or control vector (pGIPZ) using Arrest-In transfection reagent (OpenBiosystems) in serum free, antibiotic free media according to manufacturer's protocol (n=3). A plate of untransfected C2C12 cells was also maintained as a control. Media of cells was changed 6 hours after transfection to DMEM + 20% FBS. 24 hours later cells were split

using 0.25% Trypsin-EDTA (Gibco) into 6-well plates and 48 hours from time of transfection protein was isolated as described previously. The protein lysates were made and analyzed by Western blotting for LITF, Myogenin and α -tubulin protein expression. The two LITF shRNAmir constructs LITFshRNAmir-1 and LITFshRNAmir-3 targeting 3'UTR of LITF were most successful at reducing LITF expression and were used to generate stable cell lines KD1 and KD2, respectively using 1.5μg/mL puromycin dihydrochloride (Sigma) selection for four weeks. Media was changed daily. Stable cell lines where studied for LITF expression by Western blot analysis and characterized by genotyping.

2.7 Sequencing

Plasmids were sequenced using BigDye Terminator v3.1 cycle sequencing kit (Applied Biosystems). 300ng of template DNA was added in the presence of appropriate buffers, BigDye and sequencing primers at a concentration of 3.2pmol. The reaction was placed in a thermal cycler and the following sequencing program was used: 95°C for 30sec, 50°C for 15sec, 60°C for 4 min, repeated for 25 cycles. After sequencing, the reaction was cleaned and purified using Millipore plates. Following the clean-up, sequencing reactions were placed in sequencing plates, denatured at 95°C for 5 minutes and then cooled down to 4°C before being placed in the sequencer.

2.8 PCR primers

Table 2.1 PCR primers used in experiments.

Gene	Primer Sequence
LITF expression during normal C2C12 cell differentiation	
Myogenin	F:5'-GCGGACTGAGCTCAGCTTAAG-3' R:5'-GCTGTCCACGATGGACGTAAG-3'
MyoD	F:5'-GAGCAAAGTGAATGAGGCCTT-3' R:5'-CACTGTAGTAGGCGGTGTCGT-3'
LITF	F:5'-CCAGGAAGCTCACTAAAGAGG-3' R:5'-ACAGGCCACTGTTGTCTTCAAGGT-3'
GAPDH	F: 5'-GTGAAGGTCGGTGTGAACG-3' R: 5'-ATTTGATGTTAGTGGGGTCTCG-3'
ChIP studies	
ChIP linkers	oJW102: GCGGTGACCCGGGAGATCTGAATTC oJW103: GAATTCAGATC
pCRII.I TOPO vector	F: 5'-TCCGGCTCGTATGTTGTGTGGAAT-3' R: 5'-TGTGCTGCAAGGCGATTAAGTTGG-3'
Gene specific ChIP-PCR	
Myogenin	F: 5'-GCGCAGGCTCAAGAAAGTGAATGA-3' R:5'-TGCTTTGCACCTGTTCTAGCTCTG-3'
Six1/4	F:5'-TGCCTCCGGTTCTTAAACCAGTTG-3' R: 5'-AAACTGCAGCAGCTGTGGCTGAAA-3'
RARα	F: 5'-CTTTGCTCTCAGTTCTGCCCTTGA-3' R:5'-TCCATACAAAGCCCTGGAGGAGTA-3'
Oligonucleotides used for EMSA	
Six1	F: 5'-CTCCCTCGGTGAGGGGTAGGGGTTGTGCGCGTAC-3' R: 5'-GTACGCGCACAACCCCTACCCCTCACCGAGGGAG-3'
Six3	F: 5'-GCAGGATCCCTACCCCAACCCCAGCAAGAAACGC-3' R: 5'-GCGTTTCTTGCTGGGGTTGGGGTAGGGATCCTG C-3'
Six4	F: 5'-CTGCCCACCTCTCCCCGCCCCCCACCTCGC TTCC-3' R: 5'-GGAAGCGAGGTGGGGGGCGGGGAGAGGTGGGCG-3'
RARα	F: 5'-GCTGGCATAACTGGGGGTGGGGTACTAGCTTGTC-3' R: 5'-GACAAGCTAGTACCCCACCCCCAG TTATGCCAGC-3'

2.9 Statistical Analysis

Results were analyzed with student t-test and a P-value of < 0.05 was considered significant with SYS STAT.

Chapter 3:

LITF expression during normal C2C12 cell differentiation

INTRODUCTION

3.1 C2C12 cells: Model system for studying the role of LITF in skeletal myogenesis

LITF is expressed endogenously within C2C12 cells (adult mouse myoblasts) and HL-1 (heart derived) cells (Figure 1.5, 1.6). C2C12 cells are a mouse myoblast cell line that was subcloned in Helen Blau's laboratory (Stranford University) from the C2 line of David Yaffe and Saxel (2, 90). The C2C12 cell line is very well established and characterized, and has been used for several myogenesis studies. C2C12 myoblasts can undergo differentiation in culture to form myotubes through the process of myogenesis. Differentiation can occur in one of two ways: 1) contact inhibition achieved through confluency or 2) starvation induced by serum withdrawal. The differentiation of C2C12 myoblasts *in vitro* mimics many of the gene expression patterns seen in the embryo. As a result, C2C12 cells represent an excellent model system to study myogenic gene regulation and in particular the role of LITF during this process. Thus, the aim of this chapter was to determine LITF expression during normal C2C12 cell differentiation into myotubes.

3.2 Skeletal Myogenesis

Skeletal muscle differentiation (myogenesis) is a highly regulated multi-step process, which results in muscle fibers being formed from existing muscle cells through sequential activation of several muscle specific transcription factors. Myogenesis involves the initial determination of mesodermal cells towards a myogenic lineage (Figure 3.1). Once committed to a myogenic fate the mononucleated proliferating muscle precursor cells (myoblasts) irreversibly withdraw from the cell cycle and undergo fusion, elongation and differentiation into striated multinucleated myotubes (9, 21, 34, 39, 53-54, 57, 65-66, 79).

Myotubes then form bundles of mature muscle called muscle fibers, which mark terminal differentiation. During each stage, the expression of specific muscle transcription factors are activated and lead to a cascade of reactions leading to the fusion of myoblasts into elongated myotubes (Figure 3.1) (38).

Myogenesis is primarily regulated by two families of transcription factors the myogenic regulatory factor (MRF) family and the myocyte enhancer factor 2 (MEF2) family. The MRF families of proteins are basic helix-loop-helix transcription factors (bHLH) and include: Myf5, Myogenin, MyoD and MRF4. Members of the MRF transcription factor family form heterodimers with E-proteins such as E12 or E47 and bind to specific DNA sequences, E-boxes, within the promoters of muscle specific genes. An E-box consensus sequence is defined by the following nucleotide bases CANNTG (64). The MEF2 family of transcription factors consists of four members: MEF2A, MEF2B, MEF2C and MEF2D, and interact as either homodimers or heterodimers with the MRF family of transcription factors to DNA sequences within the promoters of muscle genes that are AT-rich (64). This synergistic interaction between MEF2 and MRFs is required for the specific functional role of the bHLH MRF proteins during myogenic differentiation (64), leading to the subsequent expression of muscle-specific transcription factors, including those involved in terminal differentiation such as myosin heavy chain (MHC) and α-actin.

The bHLH families of transcription factors are involved in either the commitment of precursor muscle cells towards a myogenic lineage or the differentiation of the precursor muscle cells into myotubes. Myf5 and MyoD in particular are important in commitment whereas Myogenin and Mrf4 are important and required for the normal differentiation process. Myf5 is the first of the transcription factors to be expressed in the mouse myotome,

where it plays a key role in committing the precursor proliferating muscle cells to a myogenic faith. This task is later carried on by the transcription factors MyoD and MRF4. The expression of Myf5 and MyoD is thought to be the commitment step of skeletal myogenesis and their expression is detected in proliferating undifferentiated myoblasts. If both Myf5 and MyoD are absent than there is an absence of precursor myoblast populations and subsequent formation of skeletal muscle (64). However, normal muscle development occurs even in the absence of either Myf5 or MyoD suggesting "redundant roles" for each of these myogenic transcription factors (64).

The MRF member Myogenin functions downstream of both MyoD and Myf5 in the myogenic pathway and is required for progression of the myogenic program and differentiation of myocytes into terminally differentiated myotubes (9, 21, 53-54, 64, 79). Proliferating myoblasts do not express Myogenin until early differentiation. MyoD and MEF2 are involved in the induction of Myogenin expression during early differentiation. When Myogenin expression is detected this indicates that proliferating myoblasts have irreversibly withdrawn from the cell cycle and have initiated the differentiation program into myotubes (Figure 3.1). A lack of Myogenin causes inadequate muscle fiber formation hence skeletal muscle differentiation defects (57, 64, 65, 79).

In this chapter the aim was ***to determine LITF expression during normal differentiation into myotubes in order to deduce whether LITF participates in the process of skeletal myogenesis.*** LITF expression was compared to known myogenic regulatory factors Myogenin and myoD which are essential for skeletal myogenesis to proceed. Several methods including Western blot analysis, semi-quantitative RT-PCR and immunofluorescence microscopy were employed.

Figure 3.1. Stages of skeletal myogenesis and key regulatory factors involved. Myoblasts proceed to undergo fusion of nuclei resulting in formation of elongated myotubes upon activation of muscle specific transcription factors. Myf5 and MyoD promote myoblasts to a myogenic fate and Myogenin and MEF2 support myotube formation. Alpha-actin and myosin heavy chain are common markers of terminal differentiation and myotube formation. This figure is reprinted from Trends in Cell Biology, Volume 16, Issue 1, Lluís F, Perdiguero E, Nebreda AR, & Muñoz-Cánoves P , Regulation of skeletal muscle gene expression by p38 MAP kinases, Figure 1, pg 37, Copyright (2005), with permission from Elsevier.

Figure 3.1

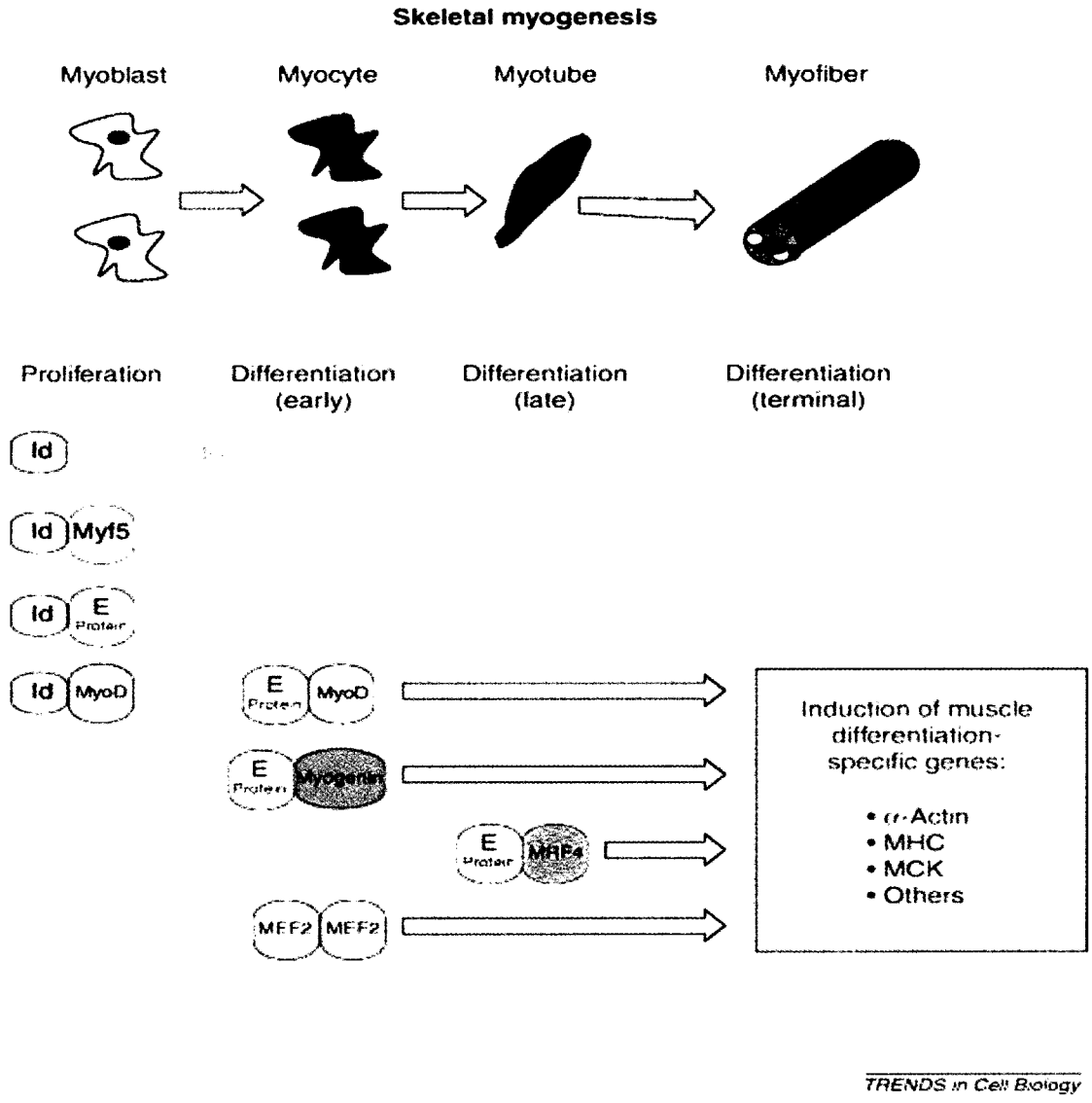

This figure is reprinted from Trends in Cell Biology, Volume 16, Issue 1, Lluis F, Perdiguero E, Nebreda AR, & Munoz-Canoves P , Regulation of skeletal muscle gene expression by p38 MAP kinases, Figure 1, pg 37, Copyright (2005), with permission from Elsevier. (38)

3.3 RESULTS

3.3.1 *LITF mRNA and protein expression changes during C2C12 cell differentiation*

To investigate the expression profiles of LITF protein and mRNA during the course of C2C12 cell differentiation from a myoblast into a myotube, Real-time PCR, semi-quantitative RT-PCR and Western blot analysis methods were employed. In the real-time PCR analysis RNA was isolated at time 0, 6, 12, 18, 24, 30, 48 and 72 hours post-differentiation (n=3) (Figure 3.2). For semi-quantitative RT-PCR and Western blot analysis RNA and protein were isolated from C2C12 cells at 0, 6, 9, 18, 24, 30, 48, 72 and 96 hours post-differentiation (n=3) (Figure 3.3 A-C). The established expression patterns of myogenic transcription factors MyoD and Myogenin were used as reference points to confirm that the process of C2C12 cell differentiation into striated myotubes was occurring as expected. Based on previously reported studies it was expected that MyoD expression appear early during commitment and proliferative stages of skeletal myogenesis in C2C12 cells. However, Myogenin expression is detectable during early differentiation and continues through terminal differentiation and is observed in differentiated myotubes. The above patterns were confirmed in the Western blot and semi-quantitative RT-PCR experiments performed (Figure 3.3 A-C).

Real-time PCR analysis revealed that LITF mRNA expression increased as early as 6 hours post-differentiation (~ 3-fold increase) compared to the undifferentiated myoblasts. Furthermore levels peaked at around 18 hours post-differentiation (0 versus 18 hour differentiated $p<0.0035$), significantly decreasing at 24 hours (18 versus 24 hours $p=0.001$) then going back up and staying high in differentiated myotubes (Figure 3.2).

Western blot analysis revealed that LITF protein expression changes with a similar trend as seen in mRNA levels during the tested time-course of C2C12 cell differentiation into myotubes (Figure 3.3A). LITF protein expression was evident in undifferentiated C2C12 cells as expected through the endogenous production of LITF by C2C12 cells. At 6 hours post-differentiation LITF protein levels were higher compared to undifferentiated C2C12 cells. Further, LITF protein levels peaked at about 18 hours post-differentiation decreased at around 24 hours and then elevated at 30 hours and continued to be detected in 96 hours differentiated C2C12 myotubes (Figure 3.3A). LITF protein expression was assessed using a specific LITF antibody designed to the c-terminus of LITF. As a result one band is evident with this C-LITF antibody.

Semi-quantitative RT-PCR on LITF mRNA also revealed that LITF mRNA expression fluctuates during the time course of C2C12 cell differentiation into myotubes, supporting both the quantitative RT-PCR and Western blot analysis data. Prior to RT-PCR RNA quality was analyzed using the Bioanalyzer RNA 6000 Nano Kit (Agilent) and a QC file generated (Figure 3.3B). RT-PCR analysis confirmed the expected presence of LITF mRNA in undifferentiated C2C12 cells. LITF mRNA expression peaked at about 18 hours post-differentiation in C2C12 cells, followed by a decrease in expression between 18 and 24 hours, and then levels returned up at 48 hours post differentiation (Figure 3.3C) (n=3).

3.3.2 *LITF localization changes during normal C2C12 cell differentiation*

We examined the localization of LITF in 0, 24, 48, 72, 96 and 120 hours differentiated C2C12 cells by immunofluorescence microscopy (Figure 3.4A-F) (n=3). Staining of 24 hour differentiated C2C12 cells with a specific C-LITF antibody (green) and

counter nuclei staining with DAPI (blue) demonstrated a predominate clear punctate localization of LITF within the nuclei of C2C12 cells (Figure 1.7 A-C).

To assess whether LITF localization changes during the time course of myoblast differentiation into myotubes C2C12 cells grown on gelatin-coated coverslips were also stained with myosin heavy chain (MHC) a marker of terminal differentiation and myotube formation. Staining of C2C12 cells with a LITF antibody (green) revealed mainly LITF nuclear localization in undifferentiated C2C12 cells (Figure 3.4A). However, upon initiation of differentiation a progressively increasing cytosolic LITF staining was observed. LITF localization was also seen within the formed myotubes (yellow) (Figure 3.4 E-F). Cytosolic staining of LITF is diffuse and may be associated with a cytosolic organelle.

Summary of findings

Based on the above experiments it was established that during skeletal muscle differentiation in C2C12 cells LITF protein and mRNA expression fluctuates. Therefore, suggesting that maybe LITF is regulated during myogenic differentiation of C2C12 myoblasts into myotubes. Also, that LITF may be important in the regulation of the expression of other myogenic transcription factors. Hence, we will use the C2C12 model system to determine the functional role of LITF during the process of myogenic differentiation. As a result the next step was to determine putative LITF targets (Chapter 4) and the biological significance (Chapter 5) of LITF interaction with the determined targets and their effects on the process of skeletal myogenesis.

Figure 3.2. LITF mRNA expression pattern during C2C12 cell differentiation into myotubes. Quantitative real-time PCR (qPCR) was performed to assess LITF mRNA expression during the time course of C2C12 cell differentiation. LITF mRNA levels were studied at 0, 6, 12, 18, 24, 30, 48 and 72 hours post-differentiation (n=3). A 3-fold increase in LITF mRNA level was observed at 6 hours post-differentiation and levels peaked significantly at around 18 hours (0 versus 18 hours differentiated $p<0.01$) and significantly decreased at around 24 hours (18 versus 24 hours $p<0.01$) with levels coming back up and remaining up in differentiated myotubes. Values shown are expression levels normalized to the 12 hour time point ± SEM, (n=3).

Figure 3.2

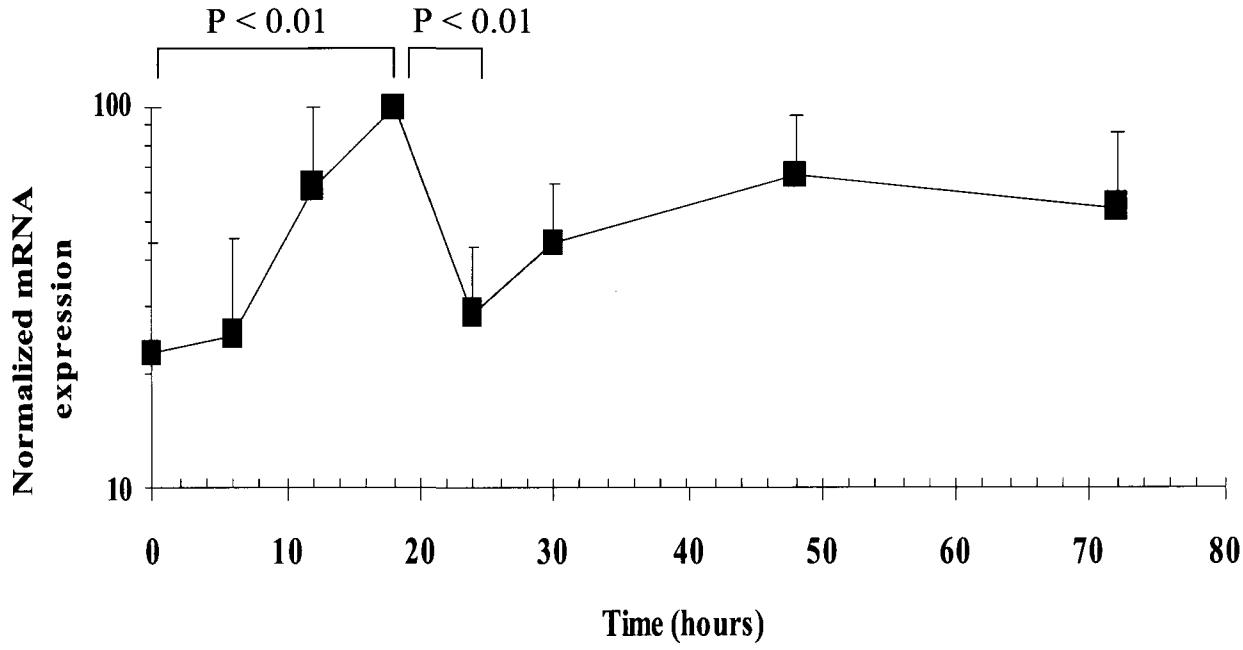
P < 0.01
P < 0.01
100
10
Normalized mRNA expression
0
10
20
30
40
50
60
70
80
Time (hours)

Figure 3.3. LITF expression pattern during C2C12 cell differentiation into myotubes. **A)** Western blot analysis of C-LITF, Myogenin and α-tubulin protein expression in differentiated C2C12 cells (0-96 hours) (n=3) **B)** Gel electrophoresis run summary of C2C12 differentiated RNA for RT-PCR. 18S and 28S ribosomes are shown as a QC file generated by bioanalyzer (Agilent Technologies). **C)** Semi-quantitative RT-PCR analysis of LITF, Myogenin, MyoD, and GAPDH expression in undifferentiated and 6, 9, 18, 24, 30, 48 and 72 hours post-differentiation C2C12 cells (n=3).

Figure 3.3

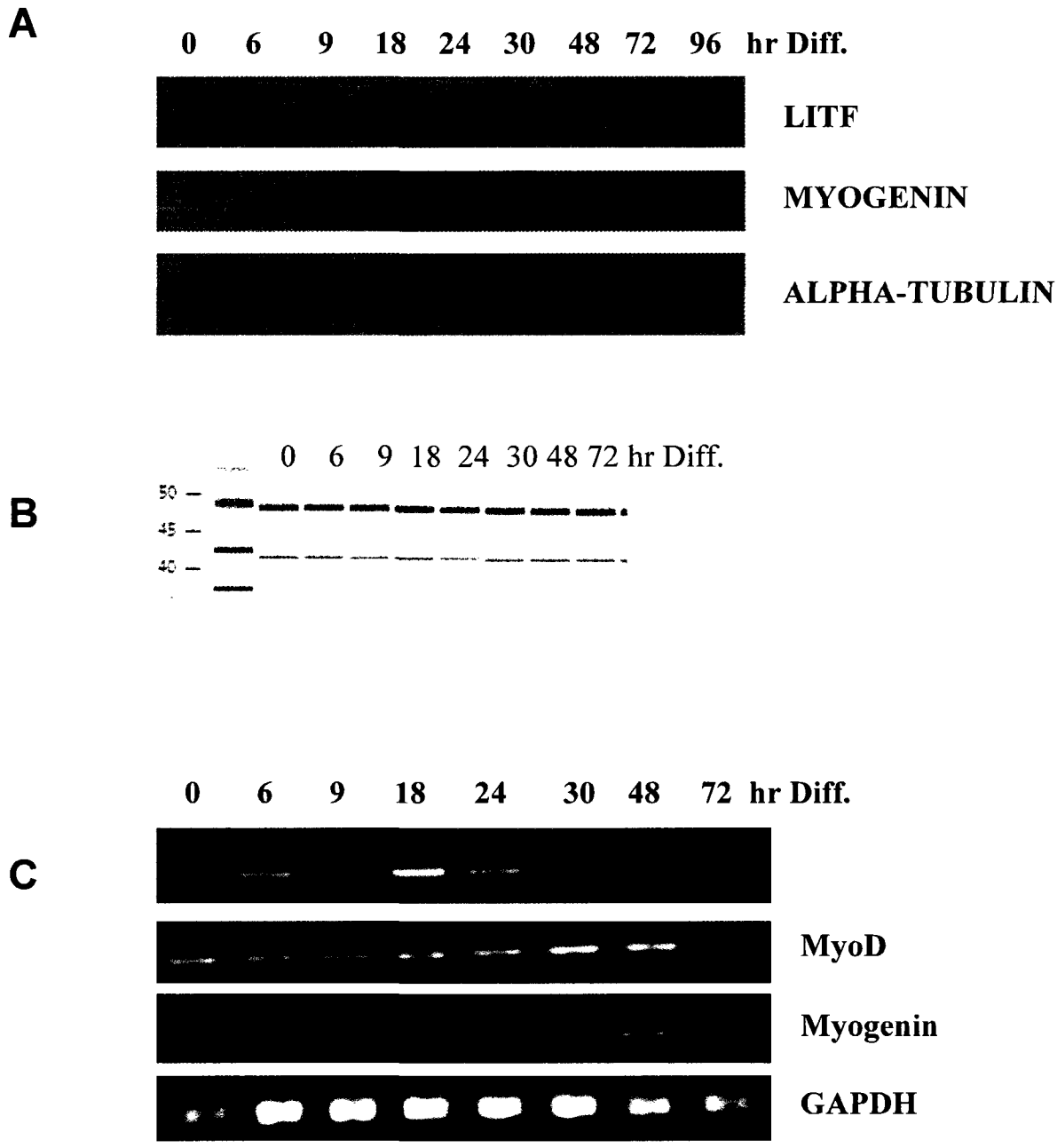
A
0 6 9 18 24 30 48 72 96 hr Diff.
LITF
MYOGENIN
ALPHA-TUBULIN
B
0 6 9 18 24 30 48 72 hr Diff.
50
45
40
C
0 6 9 18 24 30 48 72 hr Diff.
MyoD
Myogenin
GAPDH

Figure 3.4 LITF localization during the time-course of C2C12 differentiation into myotubes. Immunofluorescence staining of differentiated C2C12 cells. DAPI staining, LITF staining, MHC staining and merge images. DAPI: blue, C-LITF: green, Myosin heavy chain (MHC): red. A) Undifferentiated C2C12 myoblasts B) 24hr differentiated C) 48hr differentiated D) 72 hr differentiated E) 96hr differentiated F) 120hr differentiated Objective magnification of 63X using the Zeiss Microscope. —20μm

Figure 3.4

A

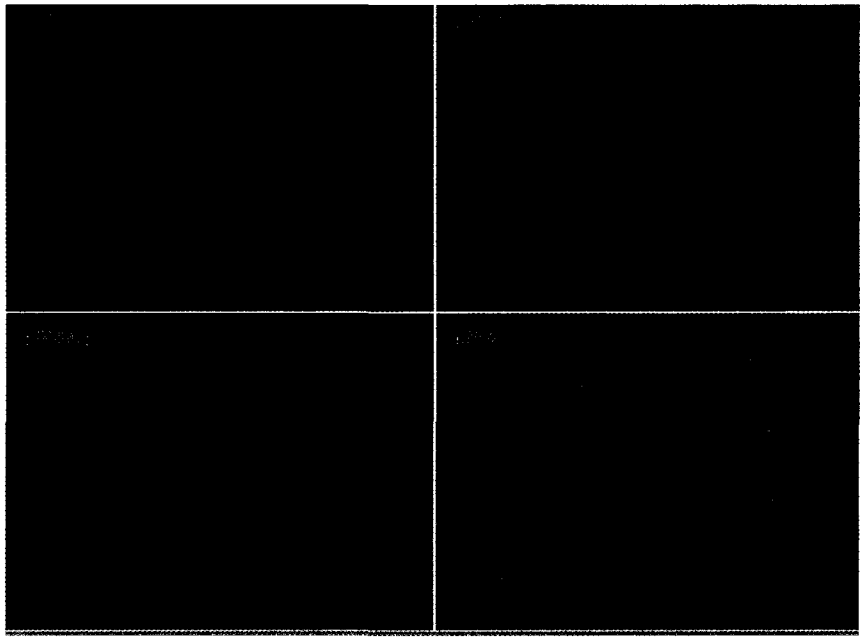

B

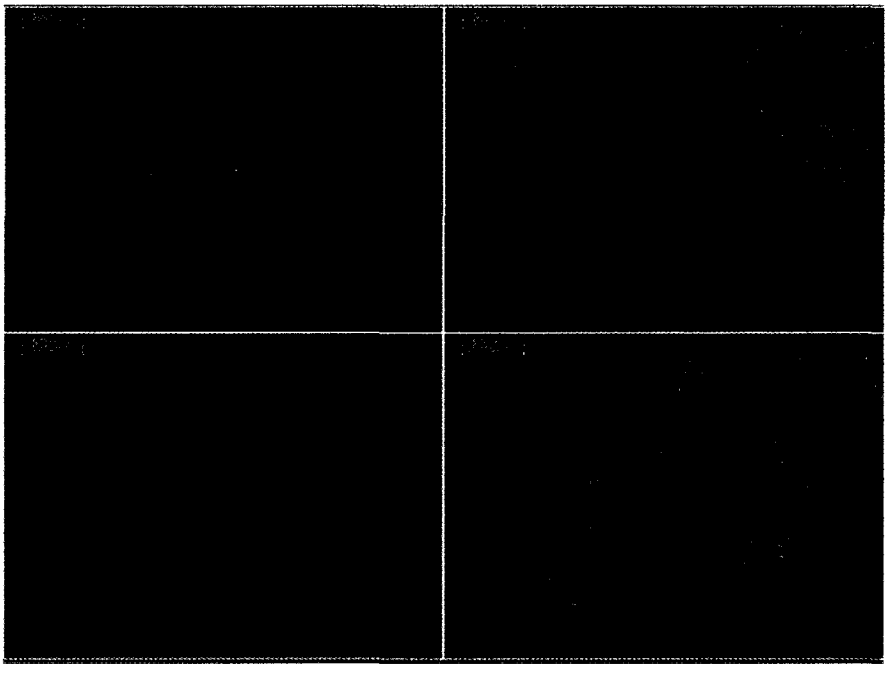

Figure 3.4

C

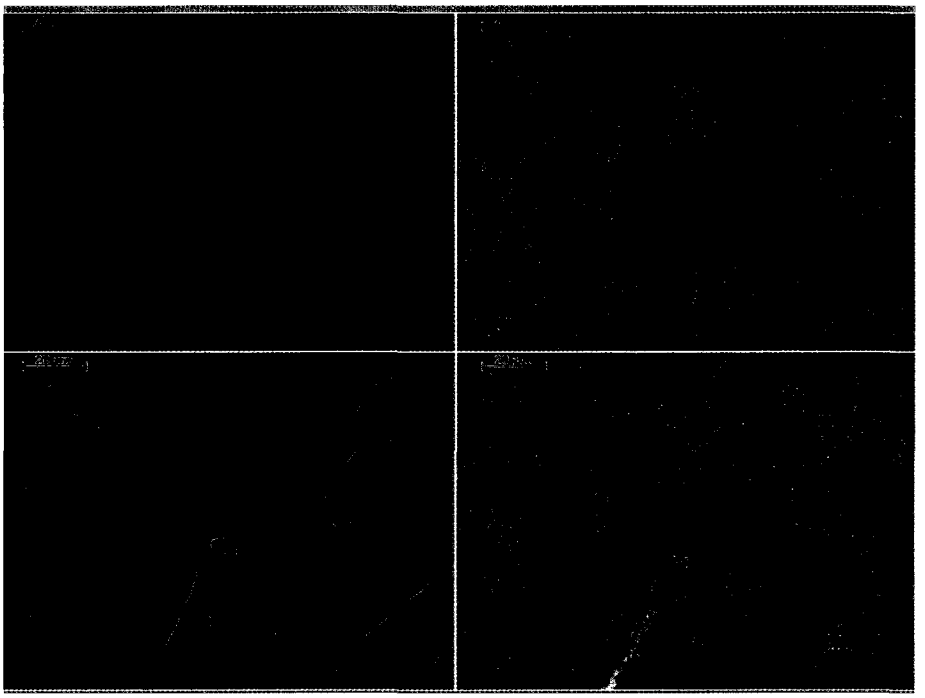

D

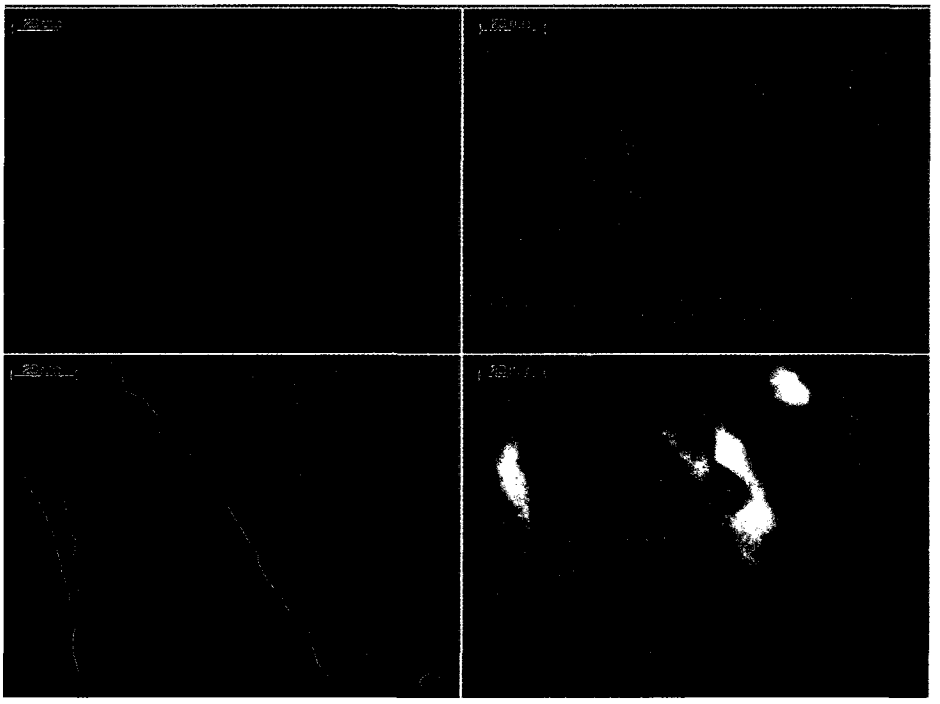

Figure 3.4

E

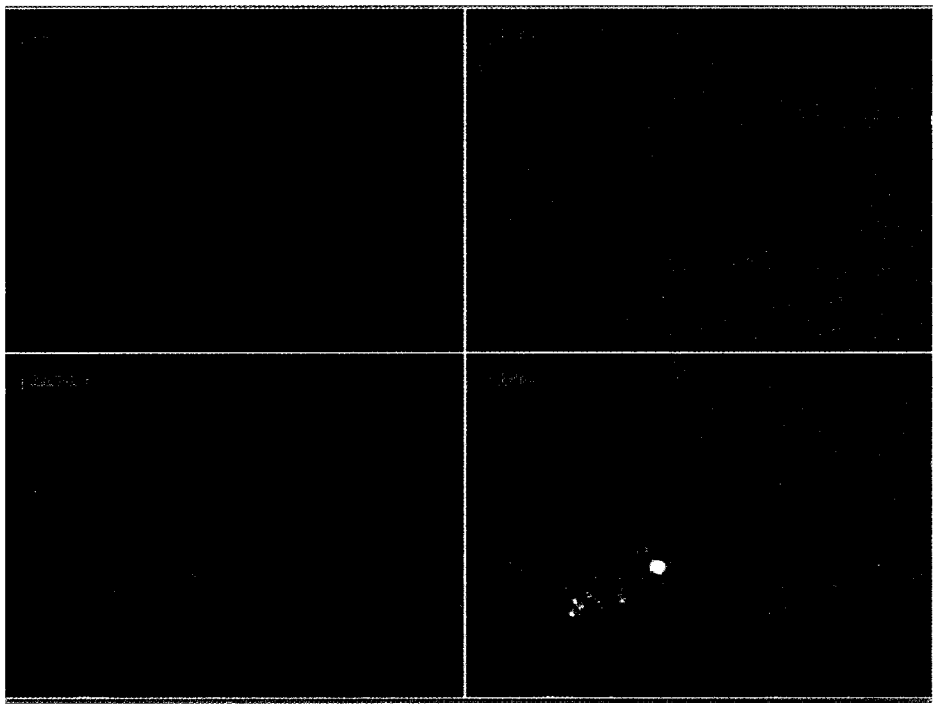

F

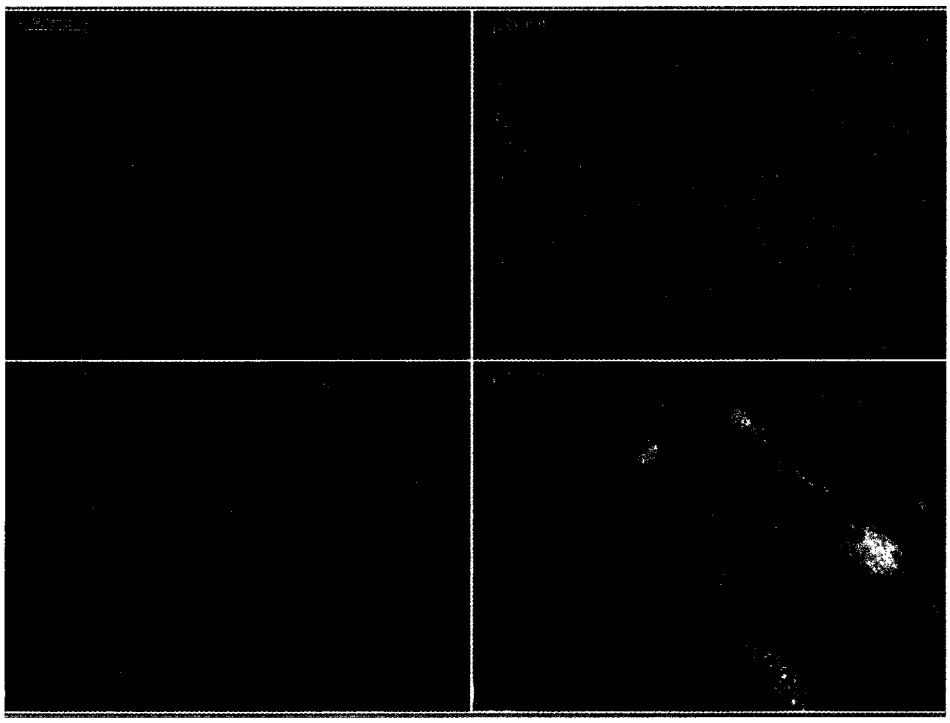

Chapter 4:

LITF interacts with chromatin

INTRODUCTION

4.1 LITF co-localization with LMNA and PML nuclear bodies

There are several lines of evidence suggesting that LITF may interact with chromatin. LITF is localized primarily to the nuclear envelope and as a punctate in close proximity of chromatin in the nucleus (Figure 1.5, 1.6). LITF co-localizes with Lamin A/C (LMNA) in the nuclear envelope and (Figure 1.5) with PML bodies of the nucleus in a punctate manner (Figure 1.6F). PML bodies are important nuclear substructures that have been implicated in both transcriptional activation and repression. They are present in almost every human cell type. The protein-based core of PML nuclear bodies are sites that are highly concentrated in sequestered transcription factors, sumoylated proteins and chromatin modifying enzymes. In addition, they are sites of post-translational modification of proteins. They are surrounded with chromatin, which provides their structure with stability (3, 62, 80). In addition, LITF was discovered through its interaction with LMNA. It has been demonstrated by several groups that lamins bind directly to chromatin and DNA, and are involved in tasks such as chromatin reorganization (18, 19, 24, 46, 60, 69). Based on these observations we propose that LITF interacts with chromatin. To test this hypothesis, chromatin immunoprecipitation assay (Cell Signaling) was performed on C2C12 cells using a specific LITF antibody. The aim of this chapter was to determine the putative LITF targets using ChIP assays and ChIP-on-chip experiments.

4.2 Results

4.2.1 Chromatin Immunoprecipitation (ChIP) assay confirm LITF interaction with chromatin

Based on the observations that LITF localizes with PML bodies in the nucleus and LMNA, it was speculated that LITF interacts with chromatin. To test whether LITF interacts with chromatin was addressed in the following experiments (Figure 4.1).

Formaldehyde cross-linked chromatin was obtained from undifferentiated C2C12 (myoblast) cells using the SimpleChIP Enzymatic IP Kit with Protein G magnetic beads from Cell Signaling (Figure 4.1) (n=4). Originally the EZ ChIP chromatin Immunoprecipitation kit from Upstate Cell Signaling Solutions was used. This kit allowed immunoprecipitation through use of protein G-conjugated agarose beads and centrifugation as opposed to Protein G magnetic beads supplied with the SimpleChIP IP kit (Cell Signaling). Magnetic beads were preferred on the basis of specificity and reduced background for protein-DNA complexes whereas compared to centrifugation based methods for resolving bound from free protein-DNA complexes.

The chromatin obtained was immunoprecipitated using a specific LITF antibody (C-LITF), in addition to a positive control (Histone H3) and negative control (normal rabbit IgG). Histone H3 is a core component of chromatin in the cell and is bound to most DNA sequences throughout the genome, including the RPL30 gene locus. LITF immunoprecipitated ChIP DNA was subjected to PCR application using DNA primers targeted to the ligated 5' and 3' linkers according to the Agilent method. The positive and negative controls were subjected to PCR using specific primers supplied within the kit to the mouse ribosomal protein L39 (RPL30) gene locus (a target of Histone H3 protein) to

validate that the ChIP experiment was performed successfully (n=4). A band of 159 bp was expected and seen for mouse RPL30 (Figure 4.1A). All samples from four independent ChIP assays were separated on a 2% agarose gel to verify whether a DNA smear of varying sizes is distinguished (Figure 4.1A). A band at appropriate size was seen for both the positive and negative controls indicating that the ChIP assay was successful. In addition, a DNA smear of 190-1000 bp was noticed for the LITF immunoprecipitated ChIP DNA indicating that LITF binds chromatin (Figure 4.1).

4.2.2 LITF enriches for genes that are important in commitment, development, differentiation, apoptosis and growth

To identify the putative targets of LITF and the type of enriched genes by LITF, ChIP sequencing and ChIP-on-chip experiments were performed. Purified LITF ChIP DNA was used to perform TOPO-TA cloning (Figure 4.1B). The LITF ChIP DNA was cloned into pCR2.1 TOPO vector and transformed into bacteria DH5-α cells. Samples were plated on ampicillin plates and incubated in a 37°C incubator for 16-20 hours. The next day approximately 100 colonies were picked and direct PCR and sequencing was performed using primers designed to pCR2.1 TOPO vector (Figure 4.1C). Bands of varying sizes were observed as expected from the DNA smear as seen in Figure 4.1A. Approximately 96 clones were picked and sequenced. Results of some of the putative LITF targets in addition to the BLAST (basic local alignment search tool) results of sequencing are shown in Figure 4.1E. A full list of the targets generated from ChIP sequencing is attached in the appendix (Table S2), showing the exact promoter regions. Analysis revealed that LITF ChIP enriches for chromatin that is in close proximity to genes that are primarily associated with commitment, differentiation, development, growth and apoptosis. These ontologies are similar to those

observed for the Lamin A/C gene (LMNA); however Lamin A/C was not identified as one of the LITF putative targets. Based on these observations, ChIP-on-chip microarray slides were designed to target genes with similar ontologies as those observed in Table S2. With the assistance of Dr. Alex Blais, it was determined that mouse chromosome 2 (182 Mbp) and mouse chromosome 11 (122 Mbp) have the greatest number of genes with ontologies similar to those enriched by LITF. In order to determine LITF chromatin targets, mouse chromosome 11 (1,690 genes) was chosen to be tiled out across Agilent ChIP-on-chip DNA microarrays because it is smaller and allows for more precise mapping. Also an additional 1,600 promoter regions (-5kbp to +2kbp around the transcriptional start sites) of mouse genes with similar ontologies were tiled out onto the same ChIP-on-chip DNA microarray (n=2). The LITF immunoprecipitated ChIP DNA and input (whole cell extract control) DNA were fluorescently labelled using Cy-3 and Cy-5 respectively and then hybridized onto ChIP-on-chip DNA microarrays. Slides were scanned using the Agilent scanner (Agilent) and data extracted using the Agilent Feature Extraction Software (Agilent). Targets were uploaded and determined using the mouse genome browser bioinformatics site at UCSC (http://genome.ucsc.edu) and BLAT (BLAST Like Alignment Tool) analysis performed. In order to account for any biological variation ChIP-on-chip was performed two times according to the Agilent Mammalian ChIP-on-chip protocol. The complete results from two independent biological replicates, of putative LITF targets are shown in appendix, Table S1.

Gene specific ChIP PCR was performed on a selected number of identified LITF targets including Myogenin, retinoic acid receptor alpha (RARα) and Six1/4. PCR was also performed on the positive H3 and negative IgG control and assessed along with other

samples on agarose gel. We observed an enrichment of the Myogenin, RARα and Six1/4 in LITF immunoprecipitated chromatin compared to input (whole cell extract control).

Analysis of the ontological enrichment, by DAVID Bioinformatics Resources 2008 (20, 31) of 45 putative LITF gene targets found on chromosome 11, revealed a significant enrichment of genes for multi-cellular organismal development ($p<0.000044$) and developmental process ($p<0.001$) as compared to all chromosome 11 encoded genes. Furthermore >50% of the LITF targeted genes identified have biological roles associated with development and differentiation (Table 4.1).

Figure 4.1 LITF interacts with chromatin. ChIP was performed using the SimpleChIP Enzymatic Chromatin IP kit with Protein G magnetic beads (Cell Signalling) (n=4). **A)** Chromatin was isolated from C2C12 myoblasts and immunoprecipitated (IP) with a specific LITF antibody. Positive (Histone H3) and negative (normal rabbit IgG) controls were run along with four independent C2C12 chromatin IP with LITF antibody on a 1% agarose gel. DNA size ladder is shown on the right of the gel. **B)** Chromatin IP DNA was subjected to PCR to add 5' and 3' linkers, cleaned using QIAquick PCR purification kit and TOPO-TA cloned into pCR-II.I TOPO vector and transformed into DH5-α cells. **C)** Several colonies (n=96) were picked and **D)** direct PCR was performed and product sizes visualized on 2% agarose gel (same DNA ladder as shown above) followed by sequencing to identify putative LITF targets. **E)** BLAT and molecular function analysis using DAVID 2008, revealed that LITF enriched for genes with ontologies associated with commitment, development, differentiation, apoptosis and growth. These ontologies are similar to those associated with the LMNA gene in which LITF interacts with. Note: LMNA was not one of the targets returned by ChIP-on-chip analysis.

A

Figure 4.1

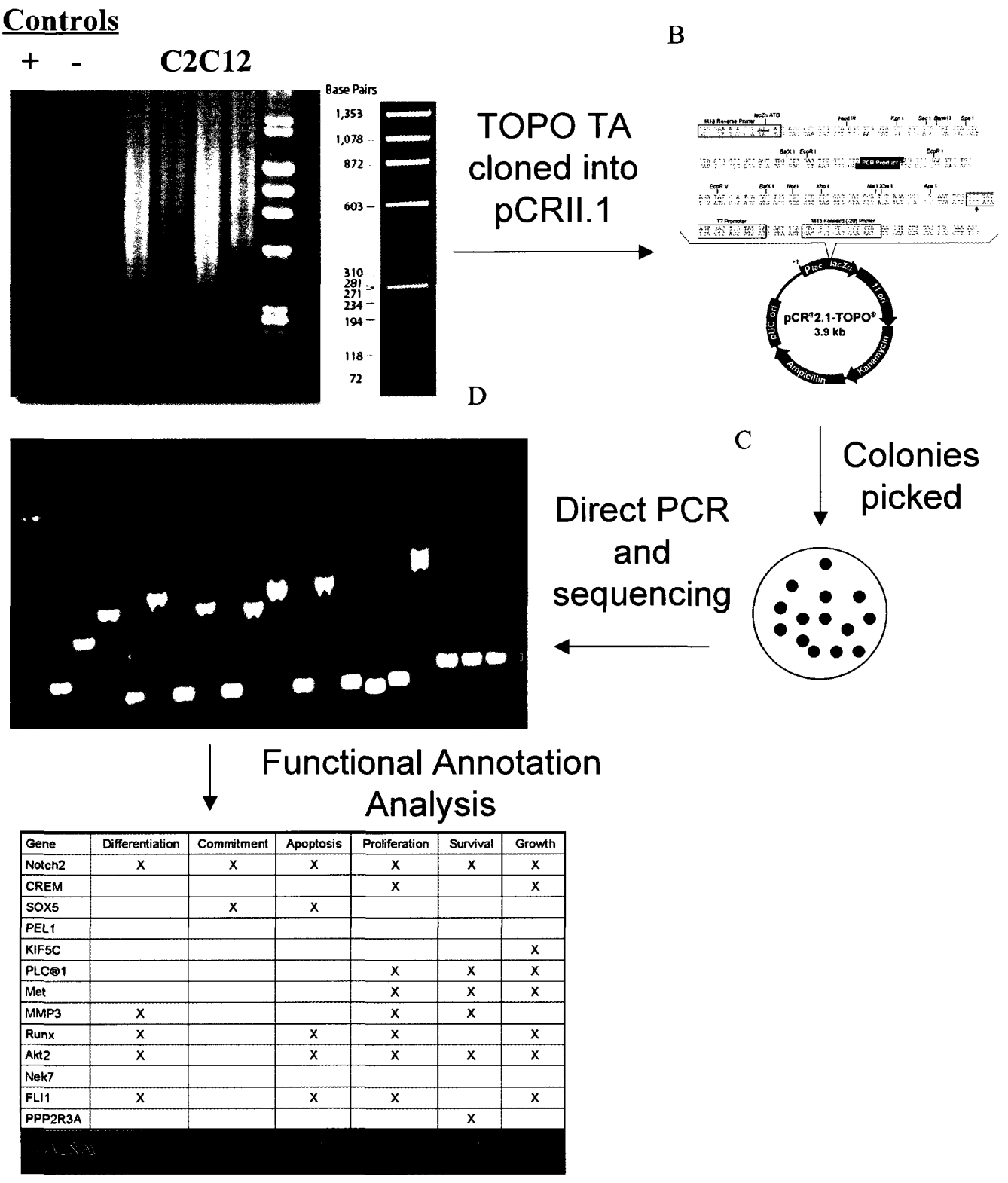

Gene	Differentiation	Commitment	Apoptosis	Proliferation	Survival	Growth
Notch2	X	X	X	X	X	X
CREM				X		X
SOX5		X	X			
PEL1						
KIF5C						X
PLC®1				X	X	X
Met				X	X	X
MMP3	X			X	X	
Runx	X		X	X		X
Akt2	X		X	X	X	X
Nek7						
FLI1	X		X	X		X
PPP2R3A					X	

Table 4.1. Biological process ontologies enriched by putative LITF gene targets assessed by DAVID bioinformatics (20, 31).

Gene Ontology Term (Biological Process)	**LITF Enriched Chr 11 genes**	**All Chr 11 genes**
	P-value	**P-value**
0007275~ multicellular organismal development	0.00004415	0.01820829
0032505 ~ developmental process	0.00099698	0.03170131
0009987 ~ cellular process	0.00146013	0.00000553
0016043~ cellular component organization and biogenesis	0.00175770	0.00000001
0048731~ system development	0.00243918	0.04057584
0006665 ~ sphingolipid metabolic process	0.00257593	ND
0048856 ~ anatomical structure development	0.00297968	0.02503862
0006886 ~ intracellular protein transport	0.00359201	0.00028535
0048513~ organ development	0.00386375	ND
0043407 ~ negative regulation of MAP kinase activity	0.00476669	0.03816350
0009888 ~ tissue development	0.00621520	ND
0006629 ~ lipid metabolic process	0.00952032	ND

4.2.3 LITF binds to DNA directly and is able to activate Transcription

To confirm the ChIP-on-chip studies, gene-specific ChIP PCR was performed on a selected number of LITF targets including Myogenin, Retinoic acid receptor alpha (RARα) and Sine oculis homeobox homolog 1/4 (Six1/4) (n=3). Positive control, Histone H3 and negative control normal rabbit IgG were also separated on agarose gel along with PCR of identified targets. An enrichment was observed with LITF immunoprecipitated DNA compared to Input control DNA (chromatin not immunoprecipitated with LITF antibody) (Figure 4.2A).

To further validate the ChIP-on-chip results I performed electrophoretic mobility shift assays (EMSA) on four sets of synthetic double stranded DNA (dsDNA) oligonucleotides: Six1, Six3, Six4 and RARα as determined by ChIP-on-chip experiments (Table 2.1) (n=3). In the presence of 2.0μg of C2C12 nuclear extract (NE) we observed a mobility shift for all the targets with the most significant shift observed with the Six3 target. To determine if LITF is part of the complex associated with the Six3 EMSA, a Gel-Super-Shift Assay was performed with a LITF-specific antibody. A strong super-shift of the Six3-associated complex was observed in the presence of LITF antibody (Figure 4.2B). This super-shift complex was disrupted by specific competition with unlabelled Six3 dsDNA (cold probe) as well as with a peptide neutralized LITF antibody (Figure 4.2B). This provides evidence that the mobility shift viewed in the presence of labelled Six3 probe is specifically due to LITF association with the DNA-protein complex.

To determine if the binding of LITF with specific DNA was direct, LITF was *in vitro* translated using the T7 eukaryotic cell-free, wheat germ extract transcription-coupled-translation system (Promega) (n=3). In this system LITF cloned in the pET100 vector was

incubated with T7 RNA polymerase forming a coupled transcription-translation, *in vitro,* to generate recombinant LITF. Biotin labelled specific DNA probes (Six1, Six3, Six4, RARα) were incubated with the *in vitro* translated LITF in the absence or presence of LITF-specific antibody for 20 minutes in appropriate binding conditions. Binding reactions were then separated on a 6% 0.5x TBE gel and visualized using the LightShift chemiluminescent EMSA kit from Pierce on X-ray films (Figure 4.2C). A direct interaction between LITF and specific DNA sequences was observed and is indicated by the asterisks in Figure 4.2C. In order for the interactions to be observed, LITF antibody had to be present within the reaction conditions. This data put forward the concept that stabilization of the amino and/or carboxy terminus of LITF is required. Furthermore, the amino and carboxy terminus of LITF could potentially be points of regulation for LITF binding to DNA.

A former honours student in Dr. Burgon's lab, Stanimira Krotneva performed co-transfection experiments with human embryonic kidney (HEK293) cells using a Gal4 promoter-luciferase reporter construct with a Gal4-DNA-binding-domain fused to LITF (GAL4-DBD-LITF) to assess if LITF is capable of transcribing a gene through a Gal4 promoter. The GAL4-DBD-LITF significantly ($p<0.01$) trans-activated the Gal4 promoter ~8 fold in HEK293 cells as assessed through luciferase expression using the Luminometer (Figure 4.2D). These experiments demonstrated that LITF contains both a DNA binding domain and a transcriptional activation domain, and therefore by definition LITF is a transcription factor.

Summary of findings

The results presented in Chapter 4 demonstrate through a chromatin immunoprecipitation (ChIP) assay that LITF interacts with chromatin. ChIP sequencing and ChIP-on-chip microarrays revealed several putative LITF targets. These targets play important roles in commitment, differentiation, development, growth and apoptosis. EMSA and co-transfection experiments revealed that LITF is able to bind DNA directly and activate transcription; hence LITF is a novel transcription factor. The exact DNA binding motif of LITF remains to be elucidated and is currently underway within our laboratory. In Chapter 5, the biological significance of LITF interaction with chromatin is investigated through generation and assessment of LITF stably down-regulated C2C12 cells.

Figure 4.2. LITF, a novel transcription factor. A) Gene-specific PCR. Gene-specific ChIP PCR was performed on LITF targets Myogenin, Retinoic acid receptor alpha (RARα) and Sine oculis homeobox homolog 1/4 (Six1/4) as identified by ChIP-on-chip studies. Controls, positive Histone H3 along with negative normal rabbit IgG are also shown. **B-C) Electrophoretic mobility shift assay (EMSA) on putative LITF targets (Retinoic acid receptor alpha (RARα), Six1, Six3, Six4).** Supershift assay using endogenous LITF (C2C12 nuclear extract) and biotin labelled Six3 probes. Astericks (*) represent shifts (n=3) **C)** Supershift assay using *in vitro* translated LITF (T7 wheat germ extract *in vitro* translation extraction system) and biotin labelled double stranded oligonucleotide DNA probes retinoic acid receptor alpha, six1, six3, six4 in the presence and absence of LITF antibody (n=3).**D) LITF activates gene transcription through a Gal4 promoter.** Co-transfection experiment was performed with human embryonic kidney cells (HEK293) using a Gal4 promoter-luciferase reporter construct and a Gal4-DNA-binding-domain fused to LITF (GAL4-DBD-LITF). GAL4-DBD-LITF transactivated the GAL4 promoter ~8 fold in HEK293 cells (n=3, $p<0.01$). Figure 4D was obtained with permission from Stanimira Krotneva (Former Honour student in Dr. Burgon's Laboratory, submitted).

Figure 4.2

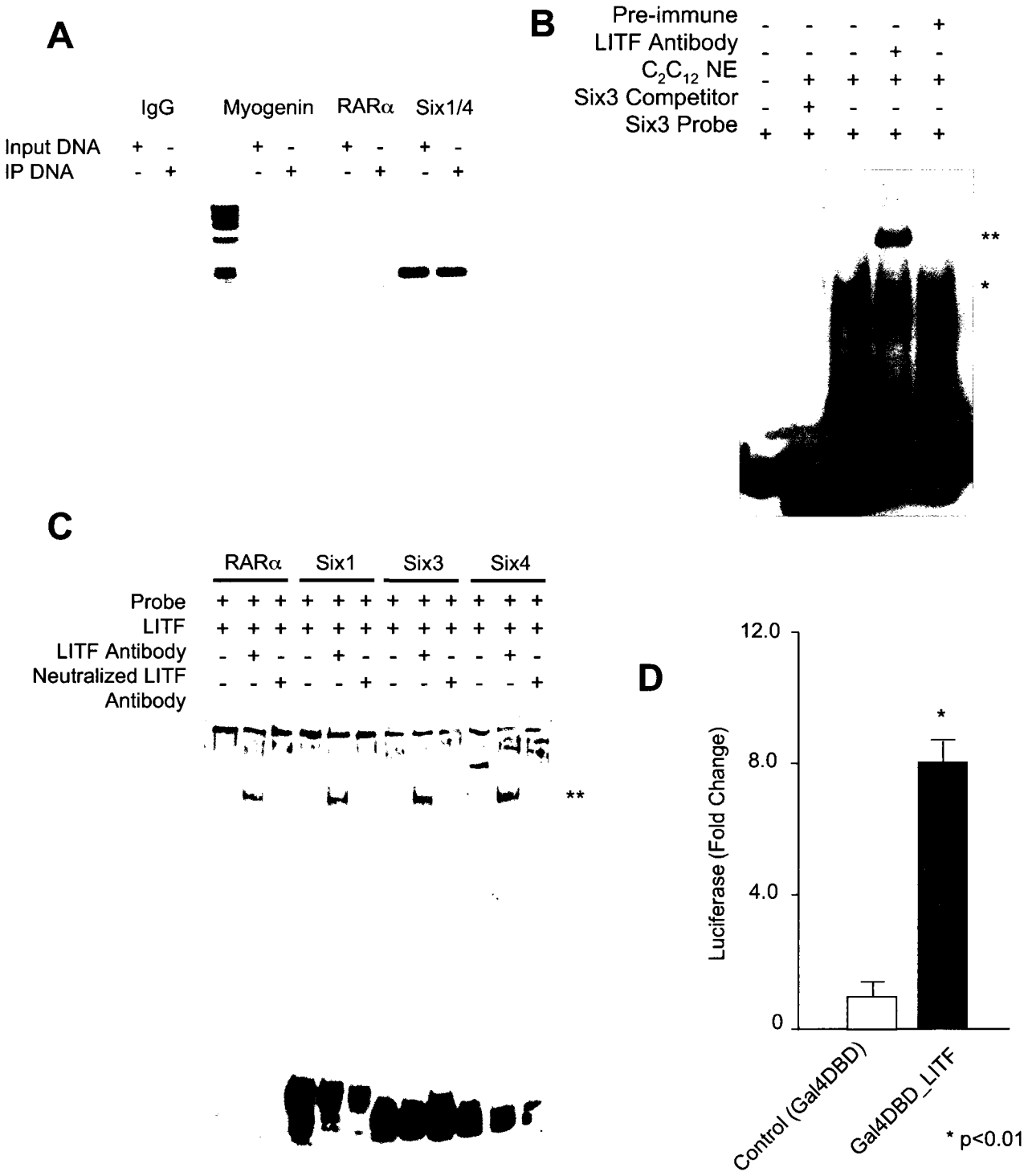
A
IgG
Myogenin
RARα
Six1/4
Input DNA + - + - + - + -
IP DNA - + - + - + - +
B
Pre-immune - - - - +
LITF Antibody - - - + -
C2C12 NE - + + + +
Six3 Competitor - + - - -
Six3 Probe + + + + +
**
*
C
RARα
Six1
Six3
Six4
Probe + + + + + + + + + + + +
LITF + + + + + + + + + + + +
LITF Antibody - + - - + - - + - - + -
Neutralized LITF Antibody - - + - - + - - + - - +
**
D
Luciferase (Fold Change)
12.0
8.0
4.0
0
*
Control (Gal4DBD)
Gal4DBD_LITF
* p<0.01

Chapter 5:

LITF is required for myotube formation

INTRODUCTION

5.1 shRNAmir technology to study stable LITF down-regulation

ChIP-on-chip studies revealed several putative LITF targets, as described in Chapter 4. However, the biological significance of LITF's interaction with chromatin remained unknown. To substantiate the ChIP-on-chip results, stable cell lines in which LITF expression was knock-downed were generated using shRNAmir mediated technology (OpenBiosystems). shRNAmir technology is designed to mimic natural microRNA (miRNA) primary transcript therefore allowing processing by the endogenous RNA interference (RNAi) processing machinery to achieve knockdown of target gene expression (OpenBiosystem). The aim of this chapter was to examine the effects and biological significance of shRNAmir-mediated down-regulation of LITF on myogenic differentiation through generation and characterization of LITF stably knockdown C2C12 cells.

MicroRNAs (miRNA) are small single stranded non-coding RNA molecules (21-23 nucleotides) encoded within the genome of plants and animals. MicroRNAs generally regulate gene expression within cells by binding to the 3'untranslated region (UTR) of specific messenger RNAs (mRNAs). miRNAs are first transcribed as primary transcripts or pri-miRNA by RNA Polymerase II and contain 5'cap and 3'poly(A) tail. The miRNA portion of the pri-miRNA forms a stem-loop or hairpin structure with signals for a dsRNA-specific nuclease cleavage. The pri-miRNA is then processed by a protein complex, the microprocessor complex consisting of dsRNA-specific ribonuclease Drosha and RNA-binding protein Pasha to a stem loop structure or hairpin (70-100nt) in the nucleus known as pre-miRNA. Pre-miRNAs are transported from the nucleus to the cytoplasm by exportin-5 (Exp5). The pre-miRNAs are then further processed in the cytoplasm to form mature

miRNAs by the endonuclease Dicer. Mature miRNA strand and Dicer form a complex known as the RNA-induced silencing complex (RISC) (12, 28, 68). The RISC complex controls the translation of targeted mRNAs (Figure 5.1A). miRNA processing is the endogenous machinery which is similar to the synthetically designed RNA interference (RNAi) (12, 28, 68). Several genome wide shRNAmir libraries have been designed. These libraries contain features that increase the efficiency and specificity of gene knockdown.

Three LITF-shRNAmir constructs were purchased from OpenBiosystems and tested for their efficacy to knockdown LITF expression. The design of these constructs is based on the endogenous mir-30 primary transcript. The mature microRNA sequence in mir-30 is replaced with gene-specific duplexes. Having the mir-30 loop sequence adds endogenous processing by Drosha which increases Dicer recognition and subsequent RISC processing and hence greater gene knockdown is achieved (Figure 5.1B).

Stable cell lines pGIPZ (empty vector), KD1 and KD2 were generated from the constructs pGIPZshRNAmir, LITFshRNAmir-1 and LITFshRNAmir-3 respectively. Stable cell lines were generated instead of transient transfections because stables allow greater opportunity to see an effect over time.

Furthermore, the effects of LITF knockdown on the expression of important myogenic transcription factors: Myogenin and MyoD were determined. As well as the effects of LITF down-regulation on members of the Six homeobox genes Six1 and Six4 (based on the ChIP studies). Stable cell lines were also assessed in their ability to express myosin heavy chain (MHC), a marker of differentiated myotubes or terminal differentiation. It was determined that LITF knockdown cell lines formed few or no myotubes. As a result, it was concluded that LITF is a myogenic factor and thus necessary for myotube formation.

Figure 5.1 A) shRNAmir processing and formation. shRNAmir mimic microRNAs that are endogenously present within cells. Primary shRNAmir is processed by dsRNA-specific ribonuclease Drosha to form precursor shRNAmir within the nucleus. Precursor shRNAmir is further processed in the cytoplasm to form mature shRNAmir by the endonuclease Dicer and is recruited onto the RNA-induced silencing complex (RISC). The RISC complex then controls the translation of target mRNA and results in repression of translational expression of target gene. **B) shRNAmir design based on mir-30.** The design of shRNAmir is based on the endogenous mir-30 primary transcript. The OpenBiosystems mir-30 hairpin design contains the miR-30 loop but the mir-30 microRNA sequence is replaced with gene duplexes. Figures are obtained from OpenBiosystems website (www.openbiosystems.com).

Figure 5.1

A

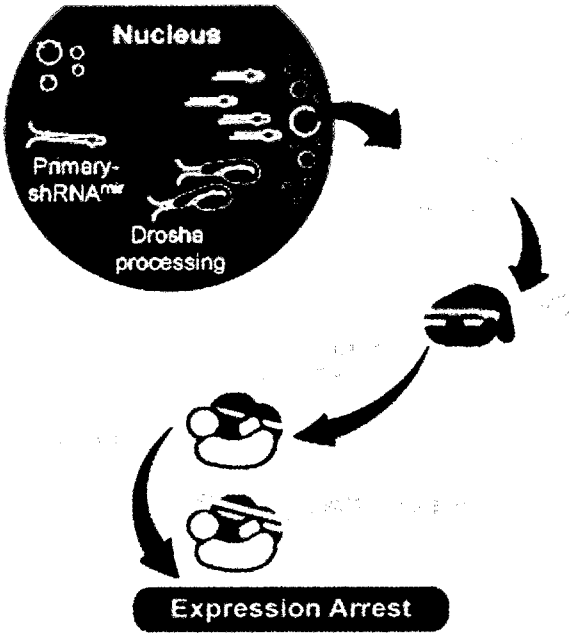

B

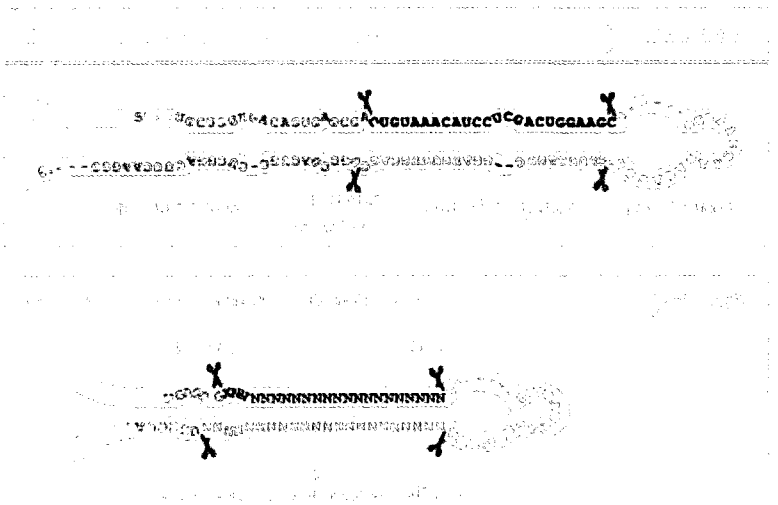

Obtained from: OpenBiosystems, http://www.openbiosystems.com

5.2 Results

5.2.1 LITFshRNAmir downregulate LITF expression

To assess the effect of LITF down-regulation in C2C12 cells on myogenic targets three shRNAmir that target the 3'UTR or exon 2 of mouse LITF were purchased from OpenBiosystems (Figure 5.2A). These shRNAmirs were designed relative to the structure of *mir30* and were cloned into the pGIPZ vector (Figure 5.2B). The pGIPZ vector allows for analysis of transfection efficiency using a turbo-GFP (green fluorescent protein) tag and generation of stable cell lines through puromycin selection. The three constructs: LITF-shRNAmir-1, LITF-shRNAmir-3, and LITF-shRNAmir-4 were transiently transfected into undifferentiated C2C12 cells using Arrest-In transfection reagent and protein lysates were isolated 48 hours after transfection, to assess the efficacy of constructs on downregulating LITF protein expression (n=3). LITF-shRNAmir-1 and LITF-shRNAmir-3 were the most successful at down regulating LITF expression (Figure 5.2C). In addition, transient down-regulation of LITF resulted in down-regulation of Myogenin protein expression as shown in Figure 5.2C. As a result, LITF-shRNAmir-1 and LITF-shRNAmir-3 were used to generate stable cell lines knockdown 1 (KD1) and knockdown 2 (KD2) through puromycin selection. Furthermore, a non-silencing GIPZ-lentiviral shRNAmir control stable cell line was generated. Cells were selected in puromycin for approximately four weeks until isolated colonies were seen and able to be selected for expansion. Stable cell lines were able to suppress LITF expression by greater than 95%. Stable cell lines were further genotyped and assessed for biological significance.

Figure 5.2 shRNAmir knockdown of LITF protein expression in C2C12 cells. A) Three shRNAmir constructs were designed and purchased from OpenBiosystems to exon 2 and 3'UTR of mouse LITF. ShRNAmir-1, -3, and -4 were used to transfect C2C12 myoblasts using Arrest-In transfection reagent. (n=3) **B)** shRNAmir constructs were cloned into the pGIPZ vector which allows for evaluation of transfection efficiency using turbo GFP and generation of stable cell lines through puromycin selection (1.5μg/mL). **C)** Protein lysates were isolated 48 hours after transfection and Western blot analysis performed (n=3) to analyze the expression of LITF, Myogenin and α-Tubulin.LITF-shRNAmir-1 and LITF-shRNAmir-3 demonstrated the greatest knockdown of LITF expression and were used to generate stable LITF knockdown C2C12 cell lines KD1 and KD2 respectively using puromycin selection. α-tubulin is shown as a loading control.

A

Mouse shRNAmir	Hairpin Sequence	Location on LITF
shRNAmir-1	TGCTGTTGACAGTGAGCGAGCCAACTACTTGCTAATTATA GTGAAGCCACAGATGTATAGTTTAGCAGTAGTTGGCCTGC TACTGCCTCGA	3'UTR
shRNAmir-3	TGCTGTTGACAGTGAGCGCGCCTATAATGCCTTCTATTAAT AGTGAAGCCACAGATGTATTAATAGAAGGCATTATAGGCT TGCCTACTGCCTCGGA	3'UTR
shRNAmir-4	TGCTGTTGACAGTGAGCGCCCAACTGATAAGAGTCCAGAA TAGTGAAGCCACAGATGTATTCTGGACTCTTATCAGTTGG TTGCCTACTGCCTCGGA	Exon 2

Color codes: sense loop antisense

B

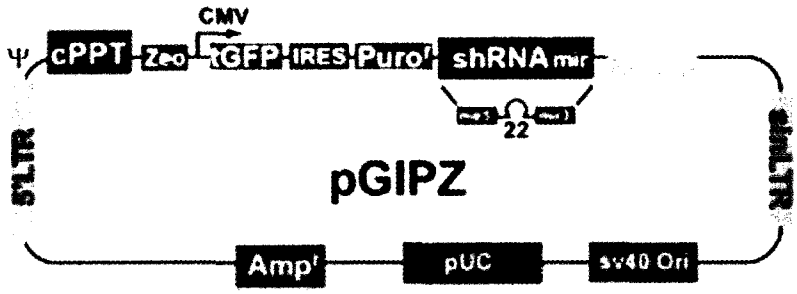

C

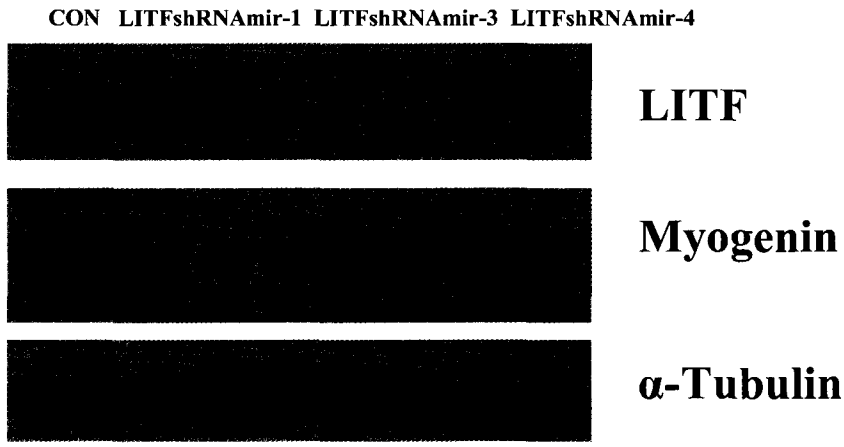

Figure 5.2

5.2.2 LITF is required for myotube formation during skeletal myogenesis in C2C12 cells

To verify the biological significance of LITF interaction with chromatin, LITF was specifically and stably knockdown in C2C12 cells using shRNAmir technology as described in section 5.2.1. Two independent LITF knockdown C2C12 stable cell lines KD1 and KD2 were generated and were able to suppress LITF protein expression to greater than 95%. In addition a non-silencing-GIPZ lentiviral shRNAmir stable control was generated. Morphologically these stably LITF knockdown C2C12 myoblasts appeared normal. Initiation of differentiation of normal C2C12 myoblasts led to the appearance of two additional splice forms of LITF (30 kDa and 45 kDa) by 6 hours with no observed change in the expression of the 25kDa LITF splice variant (Figure 5.3). Total LITF expression peaked at 30 hours post-differentiation and all three LITF forms persisted throughout differentiation of the C2C12 myotubes. LITF knockdown resulted in down-regulation of the myogenic transcription factors Myogenin and MyoD expression upon differentiation. Myogenin is a LITF target-based on ChIP-on-chip analysis. I was unable to assess the expression of MRF4 as there is no good antibody commercially available. Immunofluorescence staining for myosin heavy chain (red) revealed that compared to normal C2C12 cells and pGIPZ scrambled control, (Figure 5.4) LITF KD1 and KD2 cell lines formed no or very few myotubes after 24, 72 and 120 hours of differentiation in DMEM + 2% horse serum. This was also represented by the down-regulation of Myogenin and MyoD which are essential for proper myotube formation during skeletal myogenesis. The myotubes formed were morphologically different from normal C2C12 cell myotubes; they were smaller and flatter structures.

In addition the number of nuclei in myotubes was compared to the total of nuclei for normal C2C12 cells, KD1 and KD2 at 0, 24, 48 and 72 hours of differentiation (Figure 5.5). It was determined that the number of nuclei associated with myotubes was significantly ($p<0.05$) greater for normal C2C12 cells when compared to either KD1 or KD2 (Figure 5.5). Therefore, myotube formation appears to be inhibited or delayed in KD cell lines compared to normal C2C12 cells.

LITF ChIP-on-chip analysis identified several members of the *sine oculis* or the homeobox Six gene family (Six1, Six3, Six4) as potential LITF targets. The Six family of transcription factors, specifically Six1 and Six4, are essential for skeletal muscle development through their interaction with myogenic regulatory factors (MyoD, Myogenin, MRF4 and Myf5) (17, 25, 27, 33, 55, 72). LITF knockdown resulted in a decrease in Six1 and Six4 expression in the C2C12 undifferentiated myoblasts (Figure 5.3). In contrast, differentiation of the LITF knockdown lines resulted in an upregulation of Six1 and Six4 protein expression similar to the control cells. However, despite this upregulation of Six1 and Six4 expression during differentiation both MyoD and Myogenin expression were noticeably reduced and these cells did not have the ability to form normal myotubes. Therefore, this data indicates that LITF is necessary for skeletal myogenesis and thus supporting the hypothesis LITF is necessary for the progression of skeletal myogenesis and for proper myotube formation.

Analysis of LITF stable cell lines demonstrates that LITF is required for myogenesis to proceed and for myotube formation. Down-regulation of LITF results in a decrease in the expression of MyoD and Myogenin.

Summary of findings

Using shRNAmir technology, LITF expression was stably knockdown in C2C12 myoblasts. Analysis of differentiated LITF stable cell lines, KD1 and KD2 revealed a down-regulation in the expression of myogenic transcription factors Myogenin and MyoD. In addition the expression of developmentally important transcription factors Six1 and Six4, both putative targets of LITF as identified in the ChIP experiments (Chapter 4), were also affected. Immunofluorescent images revealed a lower myosin heavy chain (MHC) expression in knockdown cell lines compared to normal C2C12 cells. This lower expression corresponded to few or no myotubes being formed. Based on the down-regulation of the expression of Myogenin, MyoD and MHC it was concluded that maybe LITF is required for skeletal myogenesis and myotube formation.

Figure 5.3 Western blot analyses of LITF stably knockdown C2C12 cells. Western blot analysis of myogenic transcription factors (Myogenin , MyoD) and developmentally important transcription factors (Six1, Six4) protein expression in two stably knockdown LITF C2C12 cell lines (KD1 and KD2) 0, 24, 48, 72, 96 and 120 hours post-differentiation in DMEM + 2% horse serum (DM). Mouse monoclonal anti-α-tubulin is shown as a loading control. Myogenin and MyoD are downregulated in stably knockdown cell lines and Six1 and Six4 protein expression is altered upon LITF knockdown (n=3).

Figure 5.3

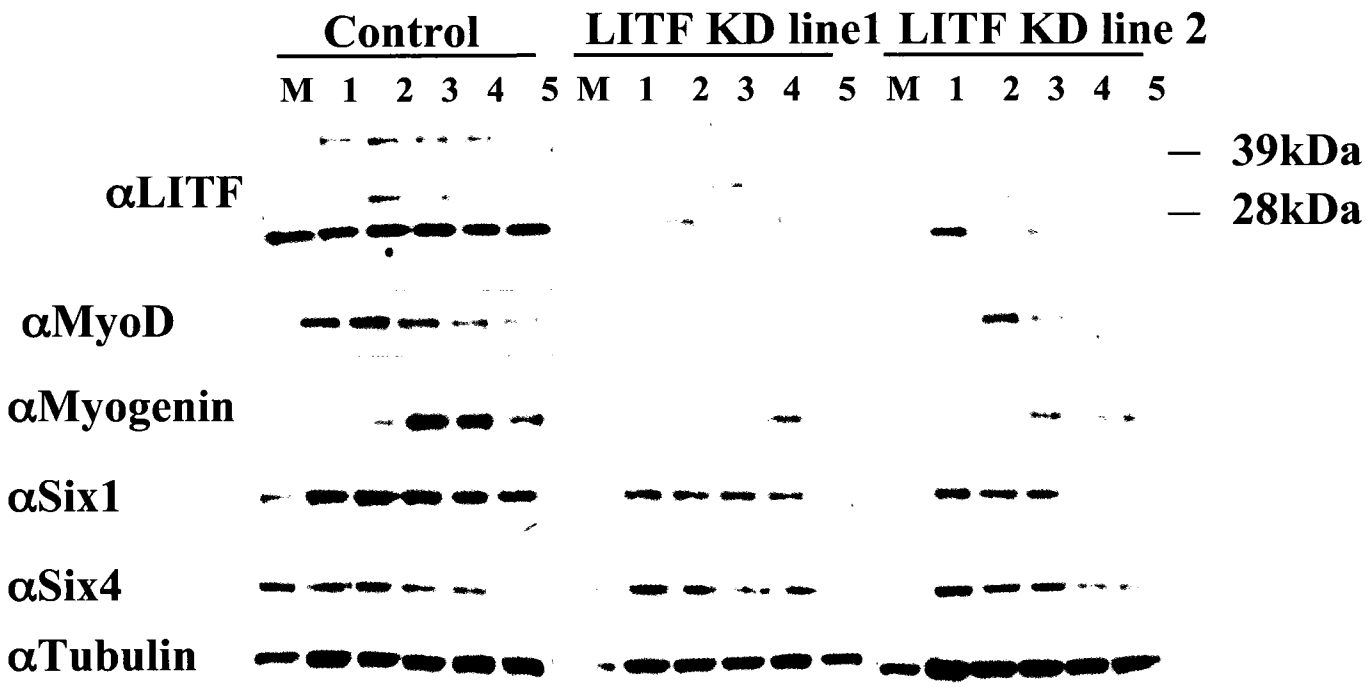
Control
LITF KD line1
LITF KD line 2
M 1 2 3 4 5 M 1 2 3 4 5 M 1 2 3 4 5
— 39kDa
— 28kDa
αLITF
αMyoD
αMyogenin
αSix1
αSix4
αTubulin

Figure 5.4 LITF is required for C2C12 (mouse myoblast) cell differentiation into myotubes. Normal C2C12 cells, pGIPZ scrambled controls and LITF stably knockdown C2C12 cells were grown on gelatin coated coverslips and differentiated for 24, 72, and 120 hours in DMEM + 2% horse serum (DM). Coverslips were fixed in methanol and incubated with primary antibody: Myosin Heavy Chain (MF20) 1:20 (red) and nuclei were stained with DAPI (blue). Few or no myotubes were observed in LITF stably knockdown cell lines (KD1 and KD2) compared to controls upon differentiation (n=3). Images shown are at an objective resolution of 10x.

Figure 5.4

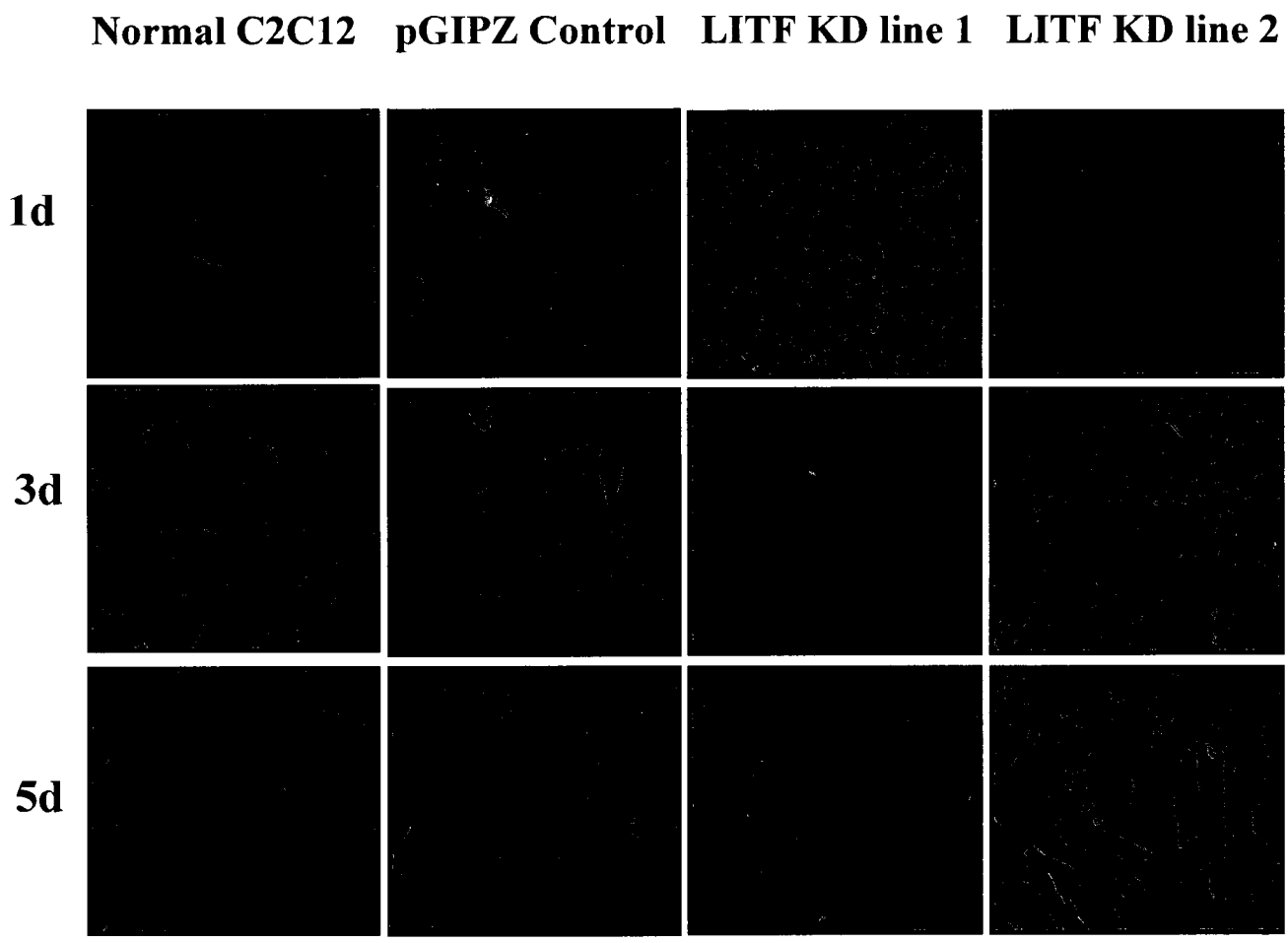
Normal C2C12
pGIPZ Control
LITF KD line 1
LITF KD line 2
1d
3d
5d

Figure 5.5 The number of total nuclei divided by the number of nuclei associated with myotubes for normal C2C12, KD1 and KD2 at 0, 24, 48 and 72hr of differentiation. All values are statistically significant ($p<0.05$) when normal C2C12 are compared to KD1 and KD2 at respective time point. (*) Represents statistical significance (n=3).

Figure 5.5

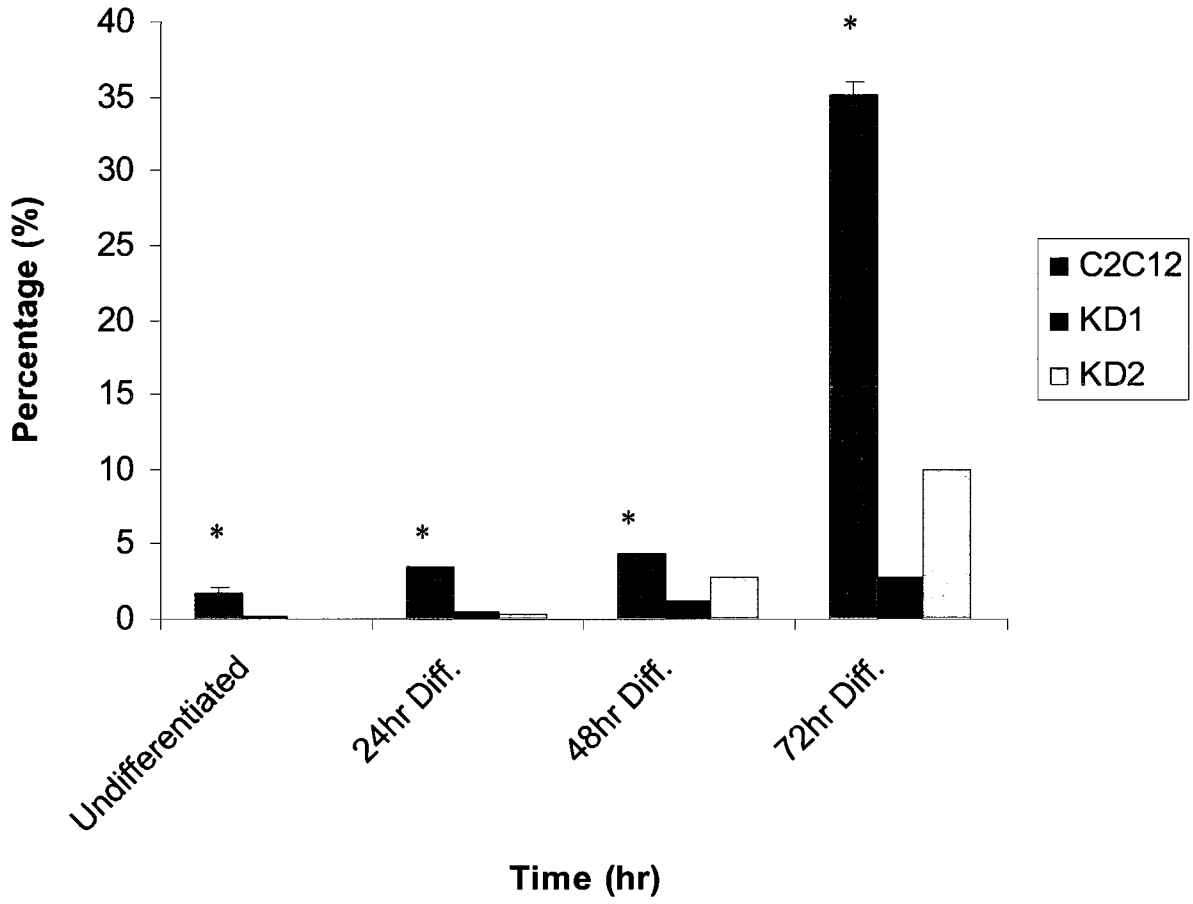
40
35
30
25
20
15
10
5
0
Percentage (%)
*
*
*
*
C2C12
KD1
KD2
Undifferentiated
24hr Diff.
48hr Diff.
72hr Diff.
Time (hr)

Chapter 6:

General Discussion and Conclusions

GENERAL DISCUSSION

In this thesis the function of a novel unique single copy gene, A-type lamin interacting transcription factor (LITF) was determined using several molecular and cellular biology techniques. LITF is the first reported (that we are aware of) example of a unique single copy vertebrate gene that is conserved only in amniotes. Bioinformatics analysis reveals that LITF does not have a common ancestor unlike most other genes. Most genes during evolution undergo duplication and divergence from a common ancestor; this is not observed with LITF. The most ancient species in which LITF is detected in is the chicken which had a common ancestor with Homo sapiens ~300 million years ago. One key fact that is known is that LITF is a Lamin A/C interacting protein and lamins have been shown to be important in a wide range of nuclear processes including transcription and gene expression (18-19, 24, 26, 60, 69). Mutations in the Lamin A/C gene lead to the development of a spectrum of human diseases collectively termed laminopathies. These mutations result in a heterogeneous group of disorders that affects specific combinations of tissues, including heart, skeletal muscle, tendons, neurons, adipocytes and bones (60). The molecular mechanisms that relate mutations in LMNA with different human diseases are poorly understood but might arise from mis-regulation of lamin-associated tissue-specific genes (13). In addition, previous studies have demonstrated that A-type lamins are markers of stem cell differentiation (14, 59) and loss of A-type lamins result in age related diseases such as progeria in both mice and humans (8, 43, 45, 71, 82). Our studies suggest that LITF may be a molecular link between the Lamin A/C gene and gene expression. This connection alone may account for the role Lamin A/C plays in cellular differentiation, aging and disease.

The presence of several missense mutations within the rod-1 domain of the LMNA gene leading to diseases of the muscle including Emery-Dreifuss muscular dystrophy (EDMD) and dilated cardiomyopathy with conduction defects (DCM-CD) suggested a possible role of LITF in muscle development. As a result, the C2C12 mouse myoblast cell line was used to elucidate the function of LITF during the multi-step coordinated process of skeletal myogenesis. ***The overall aim of this thesis was to determine the function of LITF and to test the hypothesis that LITF is necessary for skeletal myogenesis and proper myotube formation.***

Chromatin Immunoprecipitation (ChIP) assays suggested that LITF interacts with chromatin and ChIP sequencing and ChIP-on-chip analysis revealed several putative LITF targets. These putative LITF enriched targets shared ontologies that are similar to those enriched by the Lamin A/C gene including differentiation, commitment, apoptosis, survival and growth. There is increasing evidence that Lamin A/C has a critical role in stem cell regulation, differentiation and cellular aging. Furthermore, undifferentiated stem cells of both human and mouse origin lack Lamin A/C expression, whereas differentiated cells express Lamin A/C (94). Our data suggest that perhaps the interaction between LITF and Lamin A/C may be the molecular link that facilitates Lamin A/C role in regulating cell differentiation and ageing. In the hearts of the previously published LMNA H222P mutant mouse model of autosomal dominant Emery-Dreifuss muscular dystrophy (95) a significant reduction in LITF expression was observed (wildtype versus homozygous mutant $p=0.0035$ and wildtype versus heterozygous mutant $p=0.0399$, NCBI GEO profile GDS2746 record). Furthermore, dominant mutations in the LMNA gene cause Hutchinson-Gilford progeria syndrome a developmental disorder that affects many of the same mesodermal and mesenchymal cell

lineages in which LITF expression is evident. Analysis of expression profiles of mouse LITF (2310046A06Rik) demonstrated a significant ($p = 0.044$) increase in LITF expression in mouse hearts from miRNA-1-2 knockout mutants at postnatal day 10 compared to wild type postnatal day 10 controls (NCBI, Gene expression omnibus (GEO), record GDS5610, 2614) (Figure 6.1). As well an increase in LMNA expression was seen in miRNA-1-2 knockout mice (NCBI, Gene expression omnibus (GEO), record GDS2614/1457670). miRNA-1-2 shows cardiac and skeletal muscle specific expression and encodes mir-1 (61). In addition mir-1-2 is able to promote muscle cell differentiation, inhibits cell proliferation and controls the thickness of the ventricular wall. miRNA-1-2 is under the control of the myoblast determination protein-1, MyoD (76, 87). The expression of miRNA-1-2 in cardiac muscle requires the presence of the myogenic transcription factor SRF (serum response factor) (87). Mir-1-2 deficient mice demonstrate an increase in the number of proliferating cardiomyocytes and electrophysiological defects (92). Expression profile analysis of human LITF (c6orf142) demonstrated a decrease in LITF expression in Duchenne Muscular Dystrophy (DMD) patient's skeletal muscle samples compared to normal human skeletal muscle samples (NCBI, GEO profiles, record GDS610) (Figure 6.2). Therefore LITF reduction may be involved in the cascade of reactions that leads to the development of diseases of the muscle. The above findings suggest that LITF may be the molecular link that facilitates the pathogenesis of LMNA associated diseases; either through changes that lead to dys-regulation of tissue-specific genes or cell-type specific gene expression affecting adult stem cell differentiation. Together the above studies suggest a role for LITF in the development of muscle diseases and a possible link in the LMNA pathway in the development of laminopathies (Figure 6.3).

Employment of quantitative real-time PCR (qPCR), semi-quantitative reverse transcriptase PCR and Western blot analysis methods revealed fluctuations in both LITF mRNA and protein expressions with similar trends in RNA and protein. These changes in LITF expression in the C2C12 mouse cell line suggested that perhaps LITF's expression is regulated either by other myogenic factors or through positive-feedback loops. Post-translational modifications such as ubiquitination, sumoylation or phosphorylation may also play important roles in the regulation of LITF function. Analysis using the ExPASy (Expert Protein Analysis System) Proteomics Server a putative sumoylation site with the consensus sequence ΨKXE (where Ψ is any hydrophobic residue, K= lysine, X= any amino acid and E = glutamic acid) is predicted within a conserved LITF domain (exon 3). This suggests that LITF may be sumoylated like A-type lamins and that this sumoylation can be important in many processes such as LITF localization to the nuclear envelope and with Lamin A/C; nuclear-cytosolic transport since LITF is present within the nucleus and cytosol; and transcriptional regulation as demonstrated through ChIP-on-chip studies, electrophoresis mobility assays and co-transactivation experiments.

Insight into the LITF binding motif will be important in determining exactly which DNA sequences are important in LITF function. Comparison to other transcription factors reveals that there is no transcription factor similar to LITF. LITF is unique in structure at both the level of nucleic acid and protein. This is very important as LITF is the first reported transcription factor/gene regulator like itself. These concepts require further investigation.

The generation of two independent LITF stably knockdown C2C12 cell lines using shRNAmir technology implicates a possible important role for LITF during the process of

skeletal myogenesis and for proper myotube formation. Using Western blot analysis the expression of ChIP-on-chip revealed LITF targets Six1, Six4 and myogenic transcription factors Myogenin and MyoD was assessed in differentiated stable cell lines knockdown (KD1 and KD2). Compared to controls, LITF knockdown resulted in down-regulation of myogenic transcription factors Myogenin and MyoD (Figure 5.3). MyoD is an important factor which commits myoblasts to a myogenic lineage. Myogenin acts downstream of MyoD and is needed for the formation of myotubes. Therefore, this data suggests that in the hierarchy of skeletal myogenesis signaling pathway, LITF is acting upstream of MyoD activation. This concept requires further investigation. In addition, immunofluorescence microscopy staining of the differentiated knockdown cell lines for myosin heavy chain revealed a lower myosin heavy chain expression and thus fewer or no myotube formation. This result is in support of the protein analysis which reveals that when LITF expression is down-regulated a decrease in the expression of MyoD and myogenin was observed. A low myogenin expression corresponds to lower myotube formation or myosin heavy chain expression. However, transcription factors upstream of LITF were not assessed such as β-Catenins or those involved in Wnt/Shh (sonic-hedgehog) signaling pathways. In addition, rescue experiments in which LITF is transfected in the two knockdown cell lines is important to be able to confirm our findings that LITF is needed for myotube formation. Myf5 and Mrf4 expression was not assessed at this time due to the lack of validated antibodies to Myf5 and Mrf4. Therefore, further studies need to be performed to determine upstream and downstream effectors of LITF and to confirm the potential role of LITF as a transcription factor/regulator of skeletal myogenesis.

In addition, LITF knockdown also affected the expression of developmentally important transcription factors of the *sine oculis* (Six) gene family. In the myoblasts of both knockdown cell lines Six1 and Six4 expression was low and upon induction of differentiation this expression was rescued or increased. The Six gene family which contain six members in vertebrates (Six1, Six2, Six3, Six4, Six5 and Six6) are homeobox proteins that also play essential roles in development and myogenesis. The Six gene family is characterized by the presence of the Six domain and Six-type homeodomain in the encoded proteins, which confer specific DNA binding activity and function as transcription factors (55). Originally the Six gene family was identified in *Drosophila*, where it belongs to a network of genes that drive eye development. In mammals, Six5, Six4 and Six1 genes are co-expressed during mouse myogenesis. Six1 is expressed at high levels in adult skeletal muscle. Six1 and Six4 are required for the expression of myogenic transcription factors Pax3 and MRF during myogenesis in the mouse embryo (17, 25, 27, 33, 35, 55, 72). In addition, Six proteins regulate the activation of Myf5 expression in embryonic mouse limbs (25). Single Six1 knockout (KO) neonates do not survive and portray several organ developmental defects including kidney, thymus and parathyroid glands. With respect to muscle, $Six1^{-/-}$ fetuses have a selective loss of muscles including diaphragm, proximal and distal forelimb muscles and abdominal muscles (35). Six4 and Six5 single KO mice have no developmental defects (27). Within the myotome, absence of Six1 and Six4 impairs the expression of the myogenic regulatory factors Myogenin and Myod1 and MRF4 expression becomes undetectable (33, 35).

There are still several questions to be answered as to the exact function of LITF. One key fact is its implications in diseases such as laminopathies and age-related diseases. LITF

being an A-type lamin interacting transcription factor can be involved in signaling cascades that are important in the development and progression of these diseases and must be further examined. A conditional LITF knockout mouse model in which exon 1 and 5' untranslated region (UTR) and region proximal of 5' UTR has been knocked out is currently under investigation. This mouse model will provide further insight into the importance of LITF in an *in vivo* model and will be beneficial for assessment of laminopathies associated with LITF-Lamin A/C interaction.

Thus far, based on the data presented, it is concluded that LITF may be a novel transcription factor/regulator that is necessary for skeletal myogenesis and proper myotube formation.

Conclusions:

We were able to demonstrate using ChIP assay that LITF interacts with chromatin. ChIP-on-chip experiments were performed and revealed several putative LITF targets with important roles in muscle development, commitment and differentiation. Electrophoretic mobility shift assays (EMSA) on labelled probes as identified from ChIP-on-chip and co-transactivation experiments demonstrated that LITF is able to bind DNA directly and can activate gene transcription. Hence we demonstrated for the first time that LITF may be a novel transcription factor/gene regulator.

To assess the biological significance of LITF down-regulation LITF stable cell lines were generated using shRNAmir technology. Differentiated stable LITF suppressed cell lines had a decrease in the expression of the myogenic transcription factors Myogenin and MyoD. As well a lower myosin heavy chain (MHC) expression was present in differentiated LITF

stable knock-down cell lines. MHC is a marker of terminal differentiation and thus myotube formation. Consequently, the stable cell lines formed few or no myotubes upon differentiation. The myotubes formed were morphologically different from those of normal C2C12 cells. Additionally, as described above knockout of miRNA-1-2 increases both LITF and LMNA expression. miRNA-1-2 is heart and muscle specific and has several putative targets including targets that are important factors in the myogenic pathways: Pax3, Wnt and Mef2c. Therefore, further experiments are needed to elucidate the link between LITF and laminopathies as well as a possible role of miRNA-1-2.

Overall, all the studies performed establish that LITF may be a novel transcription factor/regulator that is required for skeletal myogenesis. There are many gaps in our knowledge specifically LITF's role in pathways leading to muscle differentiation and development of muscle associated diseases as seen in laminopathies including EDMD. Thus further studies are needed to elucidate these pathways and to further define the biological role of LITF.

Figure 6.1 Expression profile analysis of mouse LITF (2310046A06Rik) (TOP) and LMNA (BOTTOM) expression in hearts from mouse miRNA-1-2 knockout mutants at post-natal day 10 compared to normal wild-type post-natal 10 day hearts. Obtained from NCBI, GEO profiles, GEO records GDS2614/1453059_at/2310046A06Rik and GDS2614/1457670_s_at/Lmna).

Figure 6.1

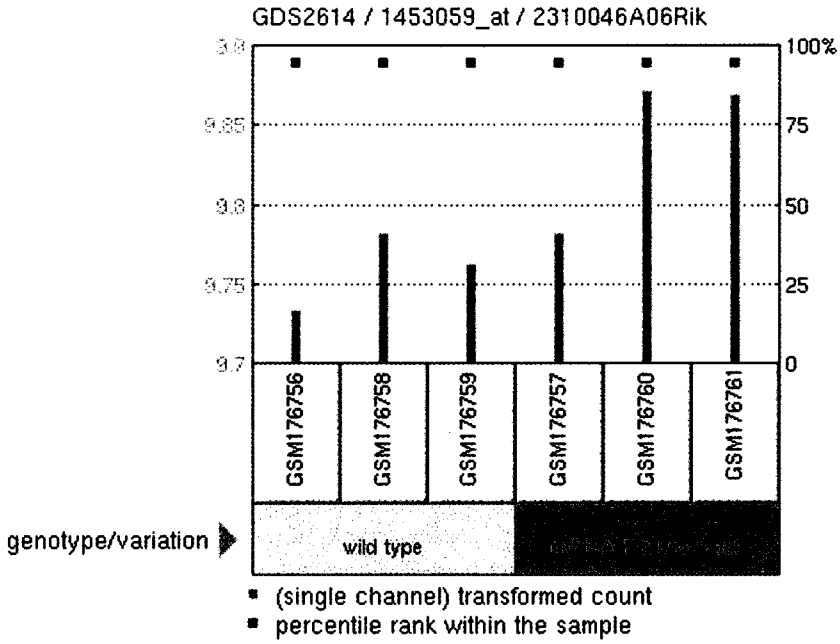

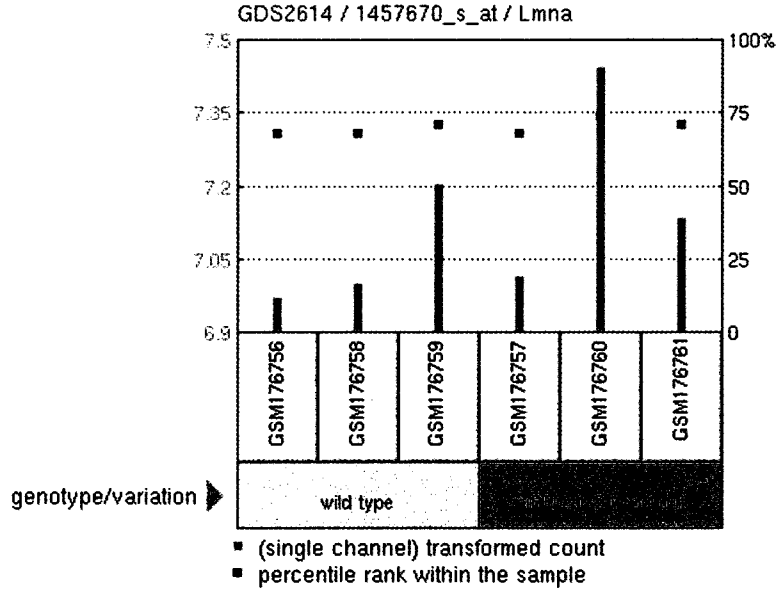

Obtained from: NCBI, GEO profiles, GEO records: GDS2614/1453059_at/2310046A0Rik and GDS2614/1457670_s_at/Lmna

Figure 6.2. Expression profile analysis of human LITF (c6orf142) expression in individuals with Duchenne muscular dystrophy (DMD) compared to normal state (11 samples). Obtained from NCBI, GEO Profile, record: GDS610/54910_at/C6orf142.

Figure 6.2

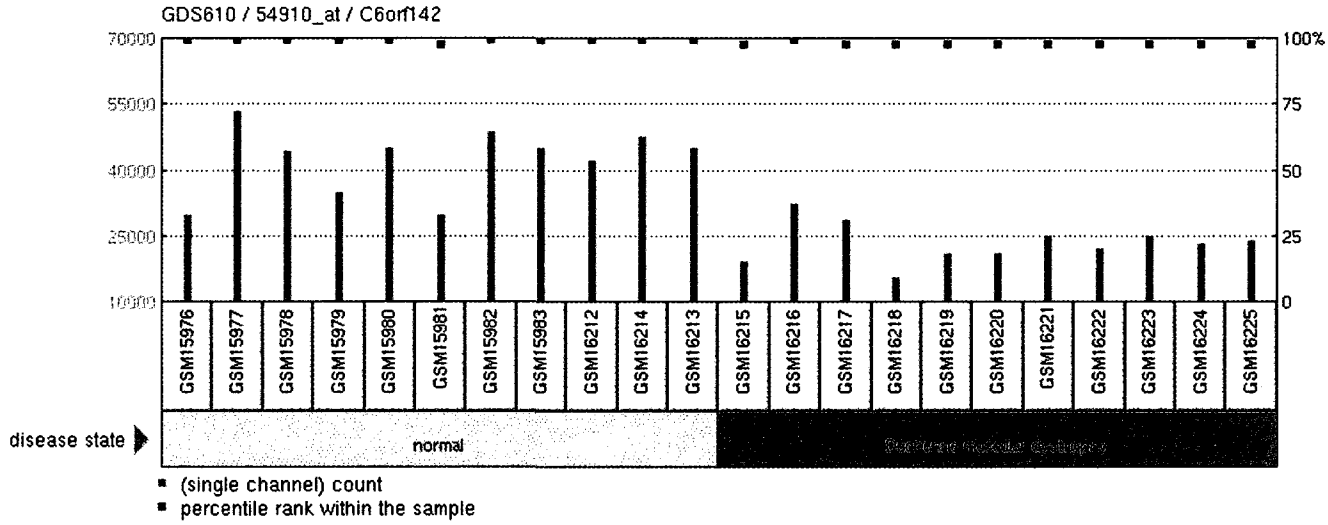

Obtained from: NCBI, GEO profiles, GEO Record: GDS610/54910_at/C6orf142

Figure 6.3 Schematic diagram of LITF's role in skeletal myogenesis and putative targets.

Figure 6.3

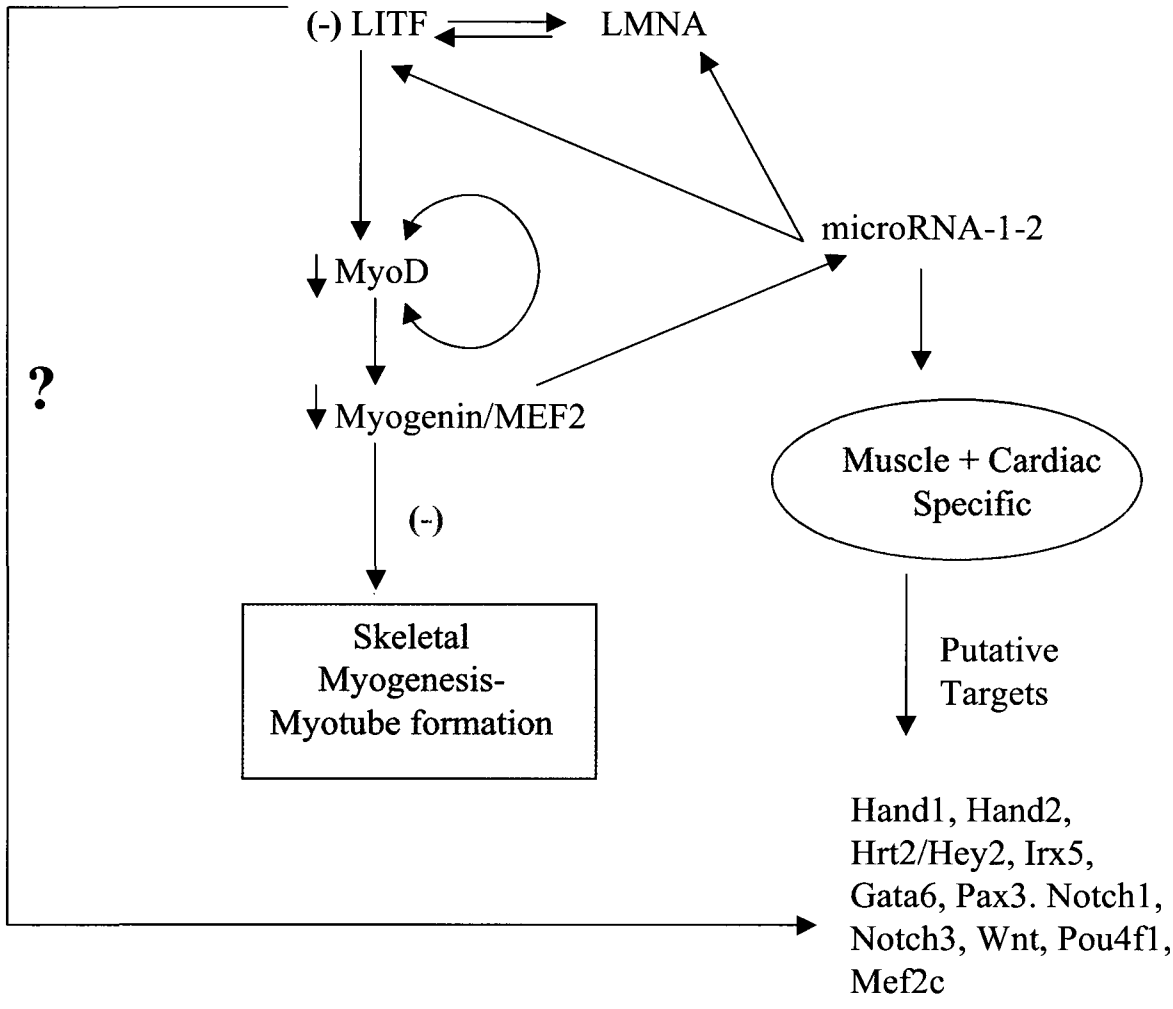
(-) LITF
LMNA
microRNA-1-2
MyoD
?
Myogenin/MEF2
Muscle + Cardiac Specific
(-)
Skeletal Myogenesis- Myotube formation
Putative Targets
Hand1, Hand2, Hrt2/Hey2, Irx5, Gata6, Pax3. Notch1, Notch3, Wnt, Pou4f1, Mef2c

APPENDIX

Table S1. Pooled replicated independent experiments of putative LITF targets identified by ChIP-on-chip analysis.

#Sequence Identification	Chromosome	Start	End	Gene Name (refseq_id)
1	chr11	100630562	100631801	Ghdc (NM_031871); Stat5b (NM_011489); Hcrt (NM_010410)
2	chr12	87699569	87701282	1700020O03Rik (NM_027405); Esrrb (NM_011934)
3	chr4	94718170	94720094	Jun (NM_010591)
4	chr11	103792159	103792691	Nsf (NM_008740); Arf2 (NM_007477)
5	chr7	19679683	19680704	Six5 (NM_011383); Dmpk (NM_032418); Fbxo46 (NM_175530)
6	chr17	74298854	74299437	Xdh (NM_011723); Srd5a2 (NM_053188)
7	chr1	136186541	136187377	Myog (NM_031189); Tmem183a (NM_001042485); Adora1 (NM_001039510)
8	chr19	5424222	5425145	Drap1 (NM_024176); Sart1 (NM_016882); AI837181 (NM_134149)
9	chr11	98448048	98448687	Ormdl3 (NM_025661); Zpbp2 (NM_199419); Gsdm3 (NM_001007461)
10	chr11	102211161	102212432	Slc4a1 (NM_011403); Ubtf (NM_011551); Rundc3a (NM_016759)
11	chr12	74146686	74147395	Six1 (NM_009189); Six4 (NM_011382)
12	chr11	51911086	51912012	Cdkl3 (NM_153785); Ppp2ca (NM_019411)
13	chr11	97440016	97440554	E130012A19Rik (NM_175332); P140 (NM_018873)
14	chr6	133984873	133986247	Etv6 (NM_007961)
15	chr13	29043739	29044507	Sox4 (NM_009238)
16	chr8	74998169	74999364	Cherp (NM_138585); 1700030K09Rik (NM_028170); Slc35e1 (NM_177766)
17	chr10	77531835	77532953	Icosl (NM_015790); Dnmt3l (NM_019448); D10Jhu81e (NM_138601)
18	chr11	99370875	99371428	Krt39 (NM_213730); Krt23 (NM_033373)
19	chr11	119405479	119406288	Nptx1 (NM_008730);

				A730011L01Rik (NM_177394); 4932417H02Rik (NM_028898)
20	chr15	77671713	77672494	Myh9 (NM_022410); Txn2 (NM_019913)
21	chr18	64499119	64499702	St8sia3 (NM_009182); Onecut2 (NM_194268)
22	chr11	71843935	71844719	Aipl1 (NM_053245); 6720460F02Rik (NM_144526)
23	chr11	63525177	63525778	---
24	chr13	83641997	83642986	Mef2c (NM_025282)
25	chr18	11998769	11999295	Cables1 (NM_022021); Rbbp8 (NM_001081223)
26	chr11	116155777	116156708	Exoc7 (NM_016857); Galr2 (NM_010254); Foxj1 (NM_008240)
27	chr13	31898394	31900508	Foxc1 (NM_008592); Gmds (NM_146041)
28	chr14	63863727	63864246	Gata4 (NM_008092); Neil2 (NM_201610)
29	chr2	56966823	56969069	Nr4a2 (NM_013613)
30	chr12	57796678	57798624	Pax9 (NM_011041); Slc25a21 (NM_172577); Nkx2-9 (NM_008701)
31	chr11	74361444	74361993	Garnl4 (NM_001015046); E130309D14Rik (NM_001013784)
32	chr11	117127202	117127890	Sept9 (NM_017380)
33	chr4	40800300	40801433	B4galt1 (NM_022305); Smu1 (NM_021535); Spink4 (NM_011463)
34	chrX	83437391	83438048	Nr0b1 (NM_007430); CN716893 (NM_001033492);
35	chrX	49966819	49967783	Gpc3 (NM_016697)
36	chr15	74785771	74786586	Ly6e (NM_008529); Ly6i (NM_020498); 2010109I03Rik (NM_025929)
37	chr8	28338228	28339098	Adrb3 (NM_013462); Got1l1 (NM_029674); Eif4ebp1 (NM_007918)
38	chr14	73724457	73725035	P2ry5 (NM_175116); Itm2b (NM_008410)
39	chr19	5490409	5491450	Cfl1 (NM_007687); B930037P14Rik (NM_001024560); Mus81 (NM_027877)
40	chr10	86955436	86955989	Ascl1 (NM_008553); Pah (NM_008777)
41	chr11	68504683	68506247	Myh10 (NM_175260); Ccdc42 (NM_177779)
42	chr12	28025952	28027255	Sox11 (NM_009234)
43	chr4	99322713	99324046	Foxd3 (NM_010425); Alg6 (NM_001081264)

44	chr7	146766745	146767789	Nkx6-2 (NM_183248); Inpp5a (NM_183144)
45	chr9	31720468	31721092	Barx2 (NM_013800)
46	chr15	101754616	101755305	Krt4 (NM_008475); Krt79 (NM_146063); Krt76 (NM_001033177)
47	chr1	93697504	93699849	Twist2 (NM_007855)
48	chr18	9957761	9958372	Colec12 (NM_130449); Thoc1 (NM_153552)
49	chr6	128347966	128348494	4933413G19Rik (NM_027697); Nrip2 (NM_021717)
50	chr5	124022660	124023186	Vps33a (NM_029929); CLITF1 (NM_019765); Diablo (NM_023232)
51	chr5	42155140	42155663	Nkx3-2 (NM_007524); A230054D04Rik (NM_001081422); Rab28 (NM_027295)
52	chr2	104967444	104968001	Wt1 (NM_144783); 0610012H03Rik (NM_028747)
53	chr11	93816692	93817462	Nme1 (NM_008704); Nme2 (NM_001077529)
54	chr11	96896561	96898285	Lrrc46 (NM_027026); Scrn2 (NM_146027); Mrpl10 (NM_026154)
55	chr11	115719698	115720727	Llgl2 (NM_145438); Recql5 (NM_130454)
56	chr11	19727743	19728296	Spred2 (NM_033523)
57	chr13	60278102	60279401	Gas1 (NM_008086)
58	chr11	95479950	95480528	Ngfr (NM_033217); Phb (NM_008831)
59	chr12	8506083	8507206	Rhob (NM_007483); Slc7a15 (NM_177802)
60	chr11	95040709	95041283	Dlx4 (NM_007867); Tac4 (NM_053093)
61	chr11	120675056	120676177	Fasn (NM_007988); Ccdc57 (NM_027745); Dus11 (NM_026824);
62	chr10	87922177	87922771	Sycp3 (NM_011517); Gnptab (NM_001004164); Chpt1 (NM_144807)
63	chr17	74927855	74928595	Birc6 (NM_007566); Yipf4 (NM_026417)
64	chr15	37162017	37162801	Grhl2 (NM_026496)
65	chr11	117643094	117643805	Tmc6 (NM_181321); Tmc8 (NM_181856)
66	chr15	38230634	38232322	Klf10 (NM_013692)
67	chr11	70265548	70266868	Med11 (NM_025397); Arrb2 (NM_145429); Cxcl16 (NM_023158)
68	chr17	86020825	86021335	Six3 (NM_011381); Six2

				(NM_011380)
69	chr18	67800598	67801272	Cep76 (NM_001081073); Spire1 (NM_194355); Psmg2 (NM_134138)
70	chr11	87392045	87392751	Tex14 (NM_031386); Sept4 (NM_011129)
71	chr3	81948799	81950480	Gucy1a3 (NM_021896)
72	chr1	120949506	120950599	Gli2 (NM_001081125)
73	chr11	115825936	115826456	Sap30bp (NM_020483); Recql5 (NM_130454); Itgb4 (NM_001005608)
74	chr12	86809880	86810448	Tmed10 (NM_026775); Fos (NM_010234)
75	chr2	179959087	179960141	Lama5 (NM_001081171); Adrm1 (NM_019822); Rps21 (NM_025587)
76	chr10	76576174	76577066	Col18a1 (NM_009929); Col18a1 (NM_001109991)
77	chr6	52208927	52210108	Hoxa13 (NM_008264); Hoxa11 (NM_010450); Evx1 (NM_007966)
78	chr9	62993518	62994021	Lbxcor1 (NM_172446); Map2k5 (NM_011840)
79	chr2	115889119	115889844	Meis2 (NM_010825)
80	chr5	34529892	34530646	Mxd4 (NM_010753); Zfyve28 (NM_001015039); BC023882 (NM_146159)
81	chr7	151767875	151768526	Fadd (NM_010175); Tmem16a (NM_178642)
82	chr1	59819791	59820862	Nol5 (NM_018868); Bmpr2 (NM_007561)
83	chr17	25707253	25708776	Sox8 (NM_011447); Tmem112 (NM_029624)
84	chr11	4940358	4942017	Ap1b1 (NM_007454); Nefh (NM_010904); Rasl10a (NM_145216)
85	chr11	115674223	115675252	Caskin2 (NM_080643); 2310067B10Rik (NM_028014); Tsen54 (NM_029557)
86	chr7	144510580	144511119	Ebf3 (NM_010096)
87	chr19	7016327	7016862	Bad (NM_007522); Plcb3 (NM_008874); Gpr137 (NM_207220)
88	chr4	120339211	120340424	Cited4 (NM_019563); Kcnq4 (NM_001081142); Ctps (NM_016748)
89	chr11	98608474	98609336	Thra (NM_178060); Nr1d1 (NM_145434); Med24 (NM_011869)
90	chr4	126412930	126413573	Tcfap2e (NM_198960); Psmb2 (NM_011970); Ncdn (NM_011986)
91	chr7	150644921	150647194	Cdkn1c (NM_009876); Kcnq1

				(NM_008434); Slc22a18 (NM_008767)
92	chr5	123093716	123094444	P2rx7 (NM_001038887); P2rx7 (NM_011027); P2rx7(NM_001038839): P2rx7 (NM_001038845); Ift81 (NM_009879); P2rx4 (NM_011026)
93	chr11	117151838	117152346	Sept9 (NM_017380)
94	chr6	54922105	54922934	A030007L17Rik (NM_026637); Nod1 (NM_172729)
95	chr11	106916663	106917182	Bptf (NM_176850); Kpna2 (NM_010655)
96	chr3	108217649	108218310	Celsr2 (NM_001004177); Celsr2 (NM_017392); Psrc1 (NM_019976); Sars (NM_011319)
97	chr10	126723023	126723537	Mbd6 (NM_033072); Dctn2 (NM_027151); Ddit3 (NM_007837)
98	chr11	58773501	58775801	Hist3h2a (NM_178218); Trim17 (NM_031172)
99	chr11	100831429	100831962	Ptrf (NM_008986); Stat3 (NM_011486); Atp6v0a1 (NM_016920)
100	chr11	68605382	68606822	Myh10 (NM_175260); Ndel1 (NM_023668)
101	chr7	147129648	147130200	Utf1 (NM_009482); Kndc1 (NM_177261); 6430531B16Rik (NM_001033465)
102	chr15	102552835	102553425	Calcoco1 (NM_026192)
103	chr9	58883036	58883646	Neo1 (NM_001042752); Neo1 (NM_008684)
104	chr11	118268930	118269765	Cant1 (NM_001025617); Cant1 (NM_001025618); Cant1 (NM_029502); Lgals3bp (NM_011150); C1qtnf1 (NM_019959)
105	chr2	25402131	25402797	Traf2 (NM_009422); Edf1 (NM_021519)
106	chr6	66986606	66987224	Gadd45a (NM_007836); Gng12 (NM_025278)
107	chr11	60521418	60523920	Llgl1 (NM_008502); Flii (NM_022009)
108	chr3	109143159	109143979	Vav3 (NM_020505)
109	chr13	100669858	100670438	Cartpt (NM_001081493); Cartpt (NM_013732); Mccc2 (NM_030026)
110	chr4	124330281	124330780	Pou3f1 (NM_011141)
111	chr11	100940818	100941389	Hsd17b1 (NM_010475); Naglu (NM_013792); Coasy (NM_027896)
112	chr16	91225808	91226939	Olig2 (NM_016967); Olig1 (NM_016968)

113	chr11	120672947	120673639	Fasn (NM_007988); Ccdc57 (NM_027745); Dus11 (NM_026824)
114	chr11	115179551	115180565	Otop2 (NM_172801); Ush1g (NM_176847); Fads6 (NM_178035); Otop3 (NM_027132)
115	chr11	96133010	96133623	Hoxb9 (NM_008270); Hoxb13 (NM_008267); Hoxb8 (NM_010461)
116	chr14	56443355	56445575	Nfatc4 (NM_023699); Cbln3 (NM_019820); Ripk3 (NM_019955)
117	chr11	95047034	95047892	Dlx4 (NM_007867); Tac4 (NM_053093)
118	chr11	119099564	119100144	Ccdc40 (NM_175430); Tbc1d16 (NM_172443); Gaa (NM_008064)
119	chr8	109127090	109128309	Cdh1 (NM_009864); Cdh3 (NM_001037809); Tmco7 (NM_173037)
120	chr11	120145451	120146020	Bahcc1 (NM_198423); Actg1 (NM_009609)
121	chr3	52071980	52072824	Foxo1 (NM_019739)
122	chr10	80894130	80894639	Ncln (NM_134009); Nfic (NM_008688)
123	chr12	105711659	105712812	Gsc (NM_010351)
124	chr11	102102458	102103002	Hdac5 (NM_010412); BC030867 (NM_153544)
125	chr9	56920383	56921470	Sin3a (NM_001110351); Ptpn9 (NM_019651); Sin3a (NM_001110350)
126	chr8	94880016	94881431	Irx5 (NM_018826)
127	chr15	76303887	76305767	Scx (NM_198885); Hsf1 (NM_008296)
128	chr3	57378168	57379615	Wwtr1 (NM_133784); Commd2 (NM_175095)
129	chrX	103222340	103222844	Cox7b (NM_025379); Atp7a (NM_001109757)
130	chr14	118634852	118636066	Sox21 (NM_145464)
131	chr13	94269153	94270030	Jmy (NM_021310); Homer1 (NM_152134)
132	chr11	75027252	75027826	Rtn4rl1 (NM_177708); Rpa1 (NM_026653); Dph1 (NM_144491)
133	chr11	118934267	118934799	Cbx4 (NM_007625); Cbx8 (NM_013926)

Table S2. ChIP sequencing BLAT results.

Gene	Genomic Location	
RIKEN cDNA 1110008L16 gene (Bone marrow macrophage cDNA	chr12:56,455,789-56,455,808	Intron 4
kinesin family member 5C (Kif5c)	chr2:49,588,950-49,589,278	Intron 15
13 repetative sequences Chr 5		
	chr1:57,755,651-57,756,022	
pellino 1	chr11:21,013,553-21,013,968	5' 20kbp
	repetative	
6720457D02Rik regulation of transcription, DNA-dependent	chr13:62,621,408-62,621,676	Exon 2
1810074P20Rik	chr4:25,176,525-25,177,086	3' UTR
St7	chr6:17,783,002-17,783,528	
	Repetative	
	repetative	X=chrom
zinc-finger protein FOG-2 (Fog-2) mRNA	chr15:40,656,558-40,656,809	intron
	chr15:13,990,983-13,991,284	
D15Ertd621e	chr15:58,292,100-58,292,374	3' UTR
ARSJ_MOUSE	chr3:126,162,878-126,163,242	20k 3'
ubiquitin specific peptidase 29(USP29)	chr7:6,851,693-6,852,252	Intron
AK085274 or ST3 beta-galactoside alpha-2,3-sialyltransferase	chr15:66,875,572-66,875,744	50k 3'
repetative	many chromosomes	
Crem cAMP responsive element modulator	chr18:3,324,229-3,324,635	Intron 1
Mus musculus phospholipase C beta-1 (Plcb1)	chr2:134,597,227-134,597,767	15k 5'
2810022L02Rik	chr1:57,755,638-57,756,187	60k 5'
AK077166	chr8:90,610,811-90,611,140	intron 2
Tmem188		25k 5'
Grxcr1 glutaredoxin cysteine-rich 1 protein	chr5:68,647,312-68,647,853	100k 3'
met proto-oncogene	chr6:17,430,097-17,430,633	5' UTR
glutaredoxin cysteine-rich 1 protein	chr5:68,647,314-68,647,856	90k 3'
glutaredoxin cysteine-rich 1 protein		90k 3'
steroid 5 alpha-reductase 2-like 2	chr5:83,784,034-83,784,570	5'UTR
mSox5L	chr6:144,402,815-144,403,278	intron 3 or 200k 5' Sox
membrane-type-3 matrix metalloproteinase	chr4:18,683,430-18,683,964	500k 3'
		500k 5'
runt related transcription factor 1	chr16:92,937,557-92,937,948	100k 5'
runt related transcription factor 2		100k 5'
deleted in colorectal carcinoma	chr18:71,272,607-71,273,116	125k 3'
Prdm16 transcription factor MEL1	chr4:153,999,360-153,999,801	5' UTR
AK165802 - AK033426	chr11:65,994,779-65,995,319	3' UTR
Akt2 thymoma viral proto-oncogene 2	chr7:28,380,282-28,380,732	5' UTR
ATPase, H+ transporting, lysosomal V1 subunit	chr1:140,186,569-140,187,012	0.5k 3'
Nek7 NIMA (never in mitosis gene a)-related expressed	chr1:140,370,034-140,370,607	120k 3'
Fli1 Friend leukemia integration 1	chr9:32,376,445-32,376,645	25k 5'
ADP-ribosylation factor-like 15	chr13:114,597,923-114,598,175	Intron 1
3222402P14Rik similar to serine/threonine protein phosphatase 2A	chr9:101,162,827-101,163,069	12k 5'
	chr15:24,135,651-24,136,171	
cytochrome P450, family 1, subfamily a,	chr9:57,534,630-57,535,036	0.7k 5'
repetative over several chromasomes		
arginine vasopressin receptor 1A		60k 3'
trichohyalin-like 1	chr3:93,298,512-93,299,020	25k 3'
S100 calcium binding protein A11 (calizzarin)		25k 5'
zinc finger protein 800 (Zfp800)	chr6:28,195,241-28,195,668	Intron 4
Notch2	chr3:97,813,669-97,814,251	3k 5'
ATPase, aminophospholipid transporter-like (Atp8a2)	chr14:60,346,464-60,346,588	Intron
NIMA (never in mitosis gene a)-related expressed (Nek7)	chr1:140,370,034-140,370,607	10k 3'

Figure S1. LITF antibody neutralization. Left panel normal C2C12 cells stained with LITF antibody, LITF: green, DAPI: blue. Right panel normal C2C12 cells stained with neutralized LITF antibody (1:5000).

Figure S1

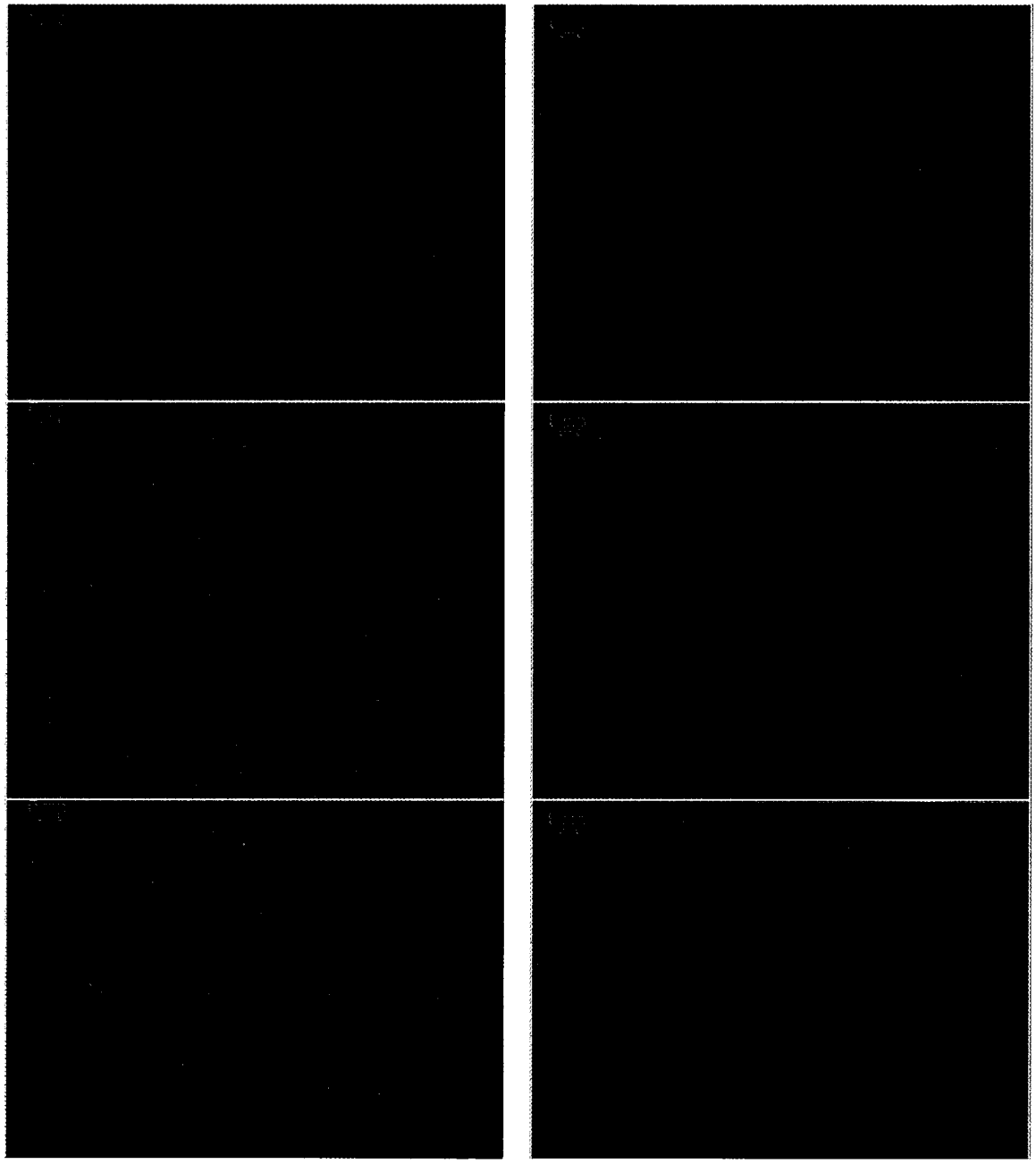

REFERENCES

1. Arimura T, *et al.* (2005) Mouse model carrying H222P-Lmna mutation develops muscular dystrophy and dilated cardiomyopathy similar to human striated muscle laminopathies. *Hum. Mol. Genet.* 14(1):155-169.
2. Blau HM, Chiu CP, & Webster C (1983) Cytoplasmic activation of human nuclear genes in stable heterocaryons. *Cell* 32(4):1171-1180.
3. Boisvert FM, Hendzel MJ, & Bazett-Jones DP (2000) Promyelocytic leukemia (PML) nuclear bodies are protein structures that do not accumulate RNA. *Journal of Cell Biology* 148(2):283-292.
4. Bridger JM, Foeger N, Kill IR, & Herrmann H (2007) The nuclear lamina. *FEBS Journal* 274(6):1354-1361.
5. Broers JL, Hutchison CJ, & Ramaekers FC (2004) Laminopathies. *The Journal of Pathology* 204(4):478-488.
6. Broers JLV, *et al.* (2005) Both lamin A and lamin C mutations cause lamina instability as well as loss of internal nuclear lamin organization. *Experimental Cell Research* 304(2):582-592.
7. Broers JLV, *et al.* (2004) Decreased mechanical stiffness in LMNA-/- cells is caused by defective nucleo-cytoskeletal integrity: implications for the development of laminopathies. *Hum. Mol. Genet.* 13(21):2567-2580.
8. Broers JLV, Ramaekers FCS, Bonne G, Yaou RB, & Hutchison CJ (2006) Nuclear lamins: laminopathies and their role in premature ageing. *Physiological Reviews* 86(3):967(942).
9. Buckingham M (2006) Myogenic progenitor cells and skeletal myogenesis in vertebrates. *Current Opinion in Genetics & Development* 16(5):525-532.
10. Burke B & Stewart CL (2006) The Laminopathies: The Functional Architecture of the Nucleus and Its Contribution to Disease*. *Annual Review of Genomics and Human Genetics* 7(1):369-405.
11. Capell BC & Collins FS (2006) Human laminopathies: Nuclei gone genetically awry. *Nature Reviews Genetics* 7(12):940-952.
12. Chua JH, Armugam A, & Jeyaseelan K (2009) MicroRNAs: Biogenesis, function and applications. *Current Opinion in Molecular Therapeutics* 11(2):189-199.
13. Cohen TV, Hernandez L, & Stewart CL (2008) Functions of the nuclear envelope and lamina in development and disease. *Biochemical Society Transactions* 036(6):1329-1334.
14. Constantinescu D, Gray HL, Sammak PJ, Schatten GP, & Csoka AB (2006) Lamin A/C Expression Is a Marker of Mouse and Human Embryonic Stem Cell Differentiation. *Stem Cells* 24(1):177-185.
15. Dahl, *et al.* (2008) Nuclear Shape, Mechanics, and Mechanotransduction. [Review]. *Circulation Research June* 102(11):1307-1318.
16. Dang C, *et al.* (2007) The Allen Brain Atlas: Delivering neuroscience to the Web on a genome wide scale. pp 17-26.
17. de Cordoba SR, Gallardo ME, Lopez-Rios J, & Bovolenta P (2001) The Human SIX Family of Homeobox Genes. *Current Genomics* 2(3):231.
18. Dechat T, Adam SA, & Goldman RD (2009) Nuclear lamins and chromatin: When structure meets function. *Advances in Enzyme Regulation* 49(1):157-166.

19. Dechat T, *et al.* (2008) Nuclear lamins: major factors in the structural organization and function of the nucleus and chromatin. *Genes & Development* 22(7):832-853.
20. Dennis Jr G, *et al.* (2003) DAVID: Database for Annotation, Visualization, and Integrated Discovery. *Genome biology* 4(5).
21. Dodou E, Xu S-M, & Black BL (2003) mef2c is activated directly by myogenic basic helix-loop-helix proteins during skeletal muscle development in vivo. *Mechanisms of Development* 120(9):1021-1032.
22. Favreau C, Higuet D, Courvalin J-C, & Buendia B (2004) Expression of a Mutant Lamin A That Causes Emery-Dreifuss Muscular Dystrophy Inhibits In Vitro Differentiation of C2C12 Myoblasts. *Mol. Cell. Biol.* 24(4):1481-1492.
23. Frock RL, *et al.* (2006) Lamin A/C and emerin are critical for skeletal muscle satellite cell differentiation. *Genes & Development* 20(4):486-500.
24. Galiová G, Bártová E, Raska I, Krejcí J, & Kozubek S (2008) Chromatin changes induced by lamin A/C deficiency and the histone deacetylase inhibitor trichostatin A. *European Journal of Cell Biology* 87(5):291-303.
25. Giordani J, *et al.* (2007) Six proteins regulate the activation of Myf5 expression in embryonic mouse limbs. *Proceedings of the National Academy of Sciences* 104(27):11310-11315.
26. Goldman RD, Gruenbaum Y, Moir RD, Shumaker DK, & Spann TP (2002) Nuclear lamins: Building blocks of nuclear architecture. *Genes and Development* 16(5):533-547.
27. Grifone R, *et al.* (2005) Six1 and Six4 homeoproteins are required for Pax3 and Mrf expression during myogenesis in the mouse embryo. *Development* 132(9):2235-2249.
28. Grimm D (2009) Small silencing RNAs: State-of-the-art. *Advanced Drug Delivery Reviews* 61(9):672-703.
29. Hegele RA, *et al.* (2006) Sequencing of the reannotated LMNB2 gene reveals novel mutations in patients with acquired partial lipodystrophy. *American Journal of Human Genetics* 79(2):383-389.
30. Houben F, *et al.* (2009) Disturbed nuclear orientation and cellular migration in A-type lamin deficient cells. *Biochimica et Biophysica Acta (BBA) - Molecular Cell Research* 1793(2):312-324.
31. Huang DW, Sherman BT, & Lempicki RA (2009) Systematic and integrative analysis of large gene lists using DAVID bioinformatics resources. *Nature Protocols* 4(1):44-57.
32. Jacob KN & Garg A (2006) Laminopathies: Multisystem dystrophy syndromes. *Molecular Genetics and Metabolism* 87(4):289-302.
33. Kawakami K, Ohto H, Takizawa T, & Saito T (1996) Identification and expression of six family genes in mouse retina. *FEBS Letters* 393(2-3):259-263.
34. Kiełbówna L & Merkel M (1997) Control of myogenic differentiation skeletal muscle by MyoD family proteins. *Acta Biologica Cracoviensia Series Zoologia* 39(SUPPL. 1):24.
35. Laclef C, *et al.* (2003) Altered myogenesis in Six1-deficient mice. *Development* 130(10):2239-2252.
36. Lee DC, Welton KL, Smith ED, & Kennedy BK (2009) A-type nuclear lamins act as transcriptional repressors when targeted to promoters. *Experimental Cell Research* 315(6):996-1007.

37. Lein ES, *et al.* (2007) Genome-wide atlas of gene expression in the adult mouse brain. *Nature* 445(7124):168-176.
38. Lluís F, Perdiguero E, Nebreda AR, & Muñoz-Cánoves P (2006) Regulation of skeletal muscle gene expression by p38 MAP kinases. *Trends in Cell Biology* 16(1):36-44.
39. Ludolph D & Konieczny S (1995) Transcription factor families: muscling in on the myogenic program. *FASEB J.* 9(15):1595-1604.
40. Maioli MA, *et al.* (2007) A novel mutation in the central rod domain of lamin A/C producing a phenotype resembling the Emery-Dreifuss muscular dystrophy phenotype. *Muscle & Nerve* 36(6):828-832.
41. Maraldi NM, *et al.* (2006) Laminopathies: A chromatin affair. *Advances in Enzyme Regulation* 46(1):33-49.
42. Maraldi NM, Lattanzi G, Marmiroli S, Squarzoni S, & Manzoli FA (2004) New roles for lamins, nuclear envelope proteins and actin in the nucleus. *Advances in Enzyme Regulation* 44(1):155-172.
43. Maraldi NM, *et al.* (2007) The nuclear envelope, human genetic diseases and ageing. *European journal of histochemistry : EJH* 51 Suppl 1:117-124.
44. Maraldi NM, *et al.* (2005) Laminopathies: Involvement of structural nuclear proteins in the pathogenesis of an increasing number of human diseases. *Journal of Cellular Physiology* 203(2):319-327.
45. Mattout A, Dechat T, Adam SA, Goldman RD, & Gruenbaum Y (2006) Nuclear lamins, diseases and aging. *Current Opinion in Cell Biology* 18(3):335-341.
46. Mattout-Drubezki A & Gruenbaum Y (2003) Dynamic interactions of nuclear lamina proteins with chromatin and transcriptional machinery. *Cellular and Molecular Life Sciences* 60(10):2053-2063.
47. Mejat A, *et al.* (2009) Lamin A/C-mediated neuromuscular junction defects in Emery-Dreifuss muscular dystrophy. *J. Cell Biol.* 184(1):31-44.
48. Mercuri E, *et al.* (2005) Extreme variability of skeletal and cardiac muscle involvement in patients with mutations in exon 11 of the lamin A/C gene. *Muscle & Nerve* 31(5):602-609.
49. Mittelbronn M, Sullivan T, Stewart CL, & Bornemann A (2008) Myonuclear Degeneration in LMNA$^{-/-}$ Null Mice. *Brain Pathology* 18(3):338-343.
50. Motsch I, *et al.* (2005) Lamins A and C are differentially dysfunctional in autosomal dominant Emery-Dreifuss muscular dystrophy. *European Journal of Cell Biology* 84(9):765-781.
51. Mounkes L, Kozlov S, Burke B, & Stewart CL (2003) The laminopathies: nuclear structure meets disease. *Current Opinion in Genetics & Development* 13(3):223-230.
52. Mounkes LC & Stewart CL (2004) Aging and nuclear organization: lamins and progeria. *Current Opinion in Cell Biology* 16(3):322-327.
53. Naidu P, Ludolph D, To R, Hinterberger T, & Konieczny S (1995) Myogenin and MEF2 function synergistically to activate the MRF4 promoter during myogenesis. *Mol. Cell. Biol.* 15(5):2707-2718.
54. Noda T, Fujino T, Mie M, & Kobatake E (2009) Transduction of MyoD protein into myoblasts induces myogenic differentiation without addition of protein transduction domain. *Biochemical and Biophysical Research Communications* 382(2):473-477.
55. Ozaki H, *et al.* (2001) Six4, a Putative myogenin Gene Regulator, Is Not Essential for

Mouse Embryonal Development. *Mol. Cell. Biol.* 21(10):3343-3350.
56. Padiath QS, *et al.* (2006) Lamin B1 duplications cause autosomal dominant leukodystrophy. *Nat Genet* 38(10):1114-1123.
57. Parker MH, Seale P, & Rudnicki MA (2003) Looking back to the embryo: defining transcriptional networks in adult myogenesis. *Nature Reviews Genetics* 4(7):497.
58. Parnaik VK & Manju K (2006) Laminopathies: Multiple disorders arising from defects in nuclear architecture. *Journal of Biosciences* 31(3):405-421.
59. Pekovic V & Hutchison CJ (2008) Adult stem cell maintenance and tissue regeneration in the ageing context: the role for A-type lamins as intrinsic modulators of ageing in adult stem cells and their niches. *Journal of Anatomy* 213(1):5-25.
60. Prokocimer M, *et al.* (2009) Nuclear lamins: Key regulators of nuclear structure and activities. *Journal of Cellular and Molecular Medicine* 13(6):1059-1085.
61. Rao PK, Kumar RM, Farkhondeh M, Baskerville S, & Lodish HF (2006) Myogenic factors that regulate expression of muscle-specific microRNAs. *Proceedings of the National Academy of Sciences* 103(23):8721-8726.
62. Reineke EL & Kao HY (2009) Targeting promyelocytic leukemia protein: a means to regulating PML nuclear bodies. *International journal of biological sciences* 5(4):366-376.
63. Rusiñol AE & Sinensky MS (2006) Farnesylated lamins, progeroid syndromes and farnesyl transferase inhibitors. *Journal of Cell Science* 119(16):3265-3272.
64. Salmon M, Owens GK, & Zehner ZE (2009) Over-expression of the transcription factor, ZBP-89, leads to enhancement of the C2C12 myogenic program. *Biochimica et Biophysica Acta - Molecular Cell Research* 1793(7):1144-1155.
65. Sartorelli V & Caretti G (2005) Mechanisms underlying the transcriptional regulation of skeletal myogenesis. *Current Opinion in Genetics and Development* 15(5 SPEC. ISS.):528-535.
66. Sassoon DA (1993) Myogenic Regulatory Factors: Dissecting Their Role and Regulation during Vertebrate Embryogenesis. *Developmental Biology* 156(1):11-23.
67. Schirmer EC & Foisner R (2007) Proteins that associate with lamins: Many faces, many functions. *Experimental Cell Research* 313(10):2167-2179.
68. Shi Y & Jin Y (2009) MicroRNA in cell differentiation and development. *Science in China Series C: Life Sciences* 52(3):205-211.
69. Shimi T, *et al.* (2008) The A- and B-type nuclear lamin networks: microdomains involved in chromatin organization and transcription. *Genes & Development* 22(24):3409-3421.
70. Shumaker DK, Kuczmarski ER, & Goldman RD (2003) The nucleoskeleton: lamins and actin are major players in essential nuclear functions. *Current Opinion in Cell Biology* 15(3):358-366.
71. Smith ED, Kudlow BA, Frock RL, & Kennedy BK (2005) A-type nuclear lamins, progerias and other degenerative disorders. *Mechanisms of Ageing and Development* 126(4):447-460.
72. Spitz F, *et al.* (1998) Expression of myogenin during embryogenesis is controlled by Six/sine oculis homeoproteins through a conserved MEF3 binding site. *Proceedings of the National Academy of Sciences of the United States of America* 95(24):14220-14225.
73. Stewart CL, Kozlov S, Fong LG, & Young SG (2007) Mouse models of the

laminopathies. *Experimental Cell Research* 313(10):2144-2156.
74. Stierle V, *et al.* (2003) The Carboxyl-Terminal Region Common to Lamins A and C Contains a DNA Binding Domain†. *Biochemistry* 42(17):4819-4828.
75. Stuurman N, Heins S, & Aebi U (1998) Nuclear lamins: Their structure, assembly, and interactions. *Journal of Structural Biology* 122(1-2):42-66.
76. Sweetman D, *et al.* (2008) Specific requirements of MRFs for the expression of muscle specific microRNAs, miR-1, miR-206 and miR-133. *Developmental Biology* 321(2):491-499.
77. Sylvius N, *et al.* (2008) Specific contribution of lamin A and lamin C in the development of laminopathies. *Experimental Cell Research* 314(13):2362-2375.
78. Sylvius N & Tesson F (2006) Lamin A/C and cardiac diseases. [Miscellaneous Article]. *Current Opinion in Cardiology May* 21(3):159-165.
79. TOMCZAK KK, *et al.* (2004) Expression profiling and identification of novel genes involved in myogenic differentiation. *FASEB J.* 18(2):403-405.
80. Torok D, Ching RW, & Bazett-Jones DP (2009) PML nuclear bodies as sites of epigenetic regulation. *Frontiers in bioscience : a journal and virtual library* 14:1325-1336.
81. Vergnes L, Péterfy M, Bergo MO, Young SG, & Reue K (2004) Lamin B1 is required for mouse development and nuclear integrity. *Proceedings of the National Academy of Sciences of the United States of America* 101(28):10428-10433.
82. Vlcek S & Foisner R (2007) Lamins and lamin-associated proteins in aging and disease. *Current Opinion in Cell Biology* 19(3):298-304.
83. Vlcek S & Foisner R (2007) A-type lamin networks in light of laminopathic diseases. *Biochimica et Biophysica Acta (BBA) - Molecular Cell Research* 1773(5):661-674.
84. Vytopil M, *et al.* (2003) Mutation analysis of the lamin A/C gene (LMNA) among patients with different cardiomuscular phenotypes. *J Med Genet* 40(12):e132-.
85. Wheeler MA & Ellis JA (2008) Molecular signatures of Emery–Dreifuss muscular dystrophy. *Biochemical Society Transactions* 036(6):1354-1358.
86. Wiesel N, *et al.* (2008) Laminopathic mutations interfere with the assembly, localization, and dynamics of nuclear lamins. *Proceedings of the National Academy of Sciences* 105(1):180-185.
87. Williams AH, Liu N, van Rooij E, & Olson EN (2009) MicroRNA control of muscle development and disease. *Current Opinion in Cell Biology* 21(3):461-469.
88. Worman HJ & Bonne G (2007) "Laminopathies": A wide spectrum of human diseases. *Experimental Cell Research* 313(10):2121-2133.
89. Worman HJ & Courvalin J-C (2004) How do mutations in lamins A and C cause disease? *Journal of Clinical Investigation* 113(3):349-351.
90. Yaffe D & Saxel O (1977) Serial passaging and differentiation of myogenic cells isolated from dystrophic mouse muscle. *Nature* 270(5639):725-727.
91. Zhao R, Bodnar MS, & Spector DL (2009) Nuclear neighborhoods and gene expression. *Current Opinion in Genetics & Development* 19(2):172-179.
92. Zhao Y, *et al.* (2007) Dysregulation of Cardiogenesis, Cardiac Conduction, and Cell Cycle in Mice Lacking miRNA-1-2. *Cell* 129(2):303-317.
93. ZhangYQ,SargeKD (2008).SumoylationregulateslaminAfunctionandislostinlam mutantsassociatedwithfamilialcardiomyopathies. *JCellBiol*182:35–39.

References added after revision:

94. Meshorer, E., & Misteli T. (2006) Chromatin in pluripotent embryonic stem cells and differentiation. *Nat. Rev. Mol. Cell. Biol.* 7, 540-6 (2006).

95. Muchir A., et al. (2007) Activation of MAPK pathways links LMNA mutations to cardiomyopathy in Emery-Dreifuss muscular dystrophy. *J Clin Invest.* 117, 1282-93

CURRICULUM VITAE

ELMIRA AHMADY
Molecular Signalling and Cardiovascular Endocrinology Research Group
University of Ottawa Heart Institute
40 Ruskin Street
Ottawa, Ontario, K1Y 4W7
613-798-5555 ext. 14274
eahmady@ottawaheart.ca

Education

M.Sc., Biochemistry, *University of Ottawa,* University of Ottawa Heart Institute, Ottawa, 2007 – Present (Candidate)

Honours Bachelor of Science Program, *University of Ottawa,* Ottawa, 2003 – 2007
Honours Biopharmaceutical Sciences, Genomics Option

Ontario Secondary School Diploma, *Hillcrest High School,* Ottawa, 1999 – 2003

Papers Published

Ahmady, E., Deeke, S.A., Rabaa, S., Kouri, L., Krotneva, S., Kenney, L., Blais, A., Stewart, A.F.R.and Burgon, P.G. (2009). LITF (C6orf142), a A-type lamin interacting transcriptional factor of vertebrates. *PNAS **(under review)**.*

Patents

United States Patent Application 20090100534
Title: MUSCLE LAMIN A/C INTERACTING PROTEIN, GENE ENCODING SAME, AND USES THEREFOR Inventor(s): BURGON, Patrick G. & Ahmady, Elmira

Awards

University of Ottawa Graduate Studies Admission Scholarship, for achieving cGPA of 8.0 or higher in undergraduate courses, 2007-2009
University of Ottawa Heart Institute Ontario Graduate Scholarship in Science and Technology, for academic achievement, 2007-2009
University of Ottawa Dean's Honour List, for academic achievement 2006-2007
Queen Elizabeth II Aiming for the top Scholarship, for academic achievement, 2003-2007
University of Ottawa Biopharmaceutical Science Director Scholarship, for recognition of excellence, 2004-2005
University of Ottawa Dean's Honour List and Renewed Admission Scholarship, for academic achievement, 2003-2004
University of Ottawa Undergraduate Admission Scholarship, for academic average of greater than 95% in High School courses, 2003

Extracurricular Activities

Vice president of social activities of the Biochemistry, Microbiology, Immunology Graduate Student Association, University of Ottawa, Ottawa, Ontario, 2007-2009

University of Ottawa Kiwanis Circle K club, University of Ottawa, Ottawa, Ontario, 2006-present.

Tournament Director/Vice-President for Bioethics Debating Society, University of Ottawa, Ottawa, Ontario, 2004-2007.

President of the Hillcrest High School Athletic Association, Hillcrest High School, Ottawa, Ontario, 2002-2003.

RESEARCH EXPERIENCE

***Summer Research Student,* University of Ottawa Heart Institute**
Ottawa, Ontario, May-August 2007

- Performed cloning, practiced cell culture techniques, designed primer for PCR and performed Western Blot analysis
- Ordered laboratory reagents
- Attended weekly meeting and prepared presentations
- Attended weekly journal clubs

***Honours Research Student,* University of Ottawa**
Ottawa, Ontario, May-April 2007

- Investigated the Effects of acute temperature change on catecholamine secretion in rainbow trout, *Oncorhynchus mykiss*
- Performed dorsal aorta cannulation surgeries, *in situ* saline perfusions, HPLC analysis, blood sampling, dissections
- Interpretation of data and statistical analysis
- Prepared thesis and poster presentation for the University of Ottawa, faculty of Science, department of Biology

Abstracts and Conferences Attended

Ahmady, E., Deeke, S.A., Rabaa, S., Kouri, L., Krotneva, S., Kenney, L., Stewart, A.F.R., Blais, A., and Burgon, P.G. A novel Lamin A/C Interacting Protein (LITF) that binds DNA regulatory regions of muscle developmental and cell cycle genes.Making Muscle in the Embryo and Adult Meeting, New York, NY, June 2009.

Burgon, P.G., Vulesevic, B., Kenney, L., Gheorghe, R., **Ahmady, E.** Identification and characterization of a novel myocardial Lamin A/C interacting protein (LITF). Canadian Cardiovascular Congress, Toronto, Ontario, October 2008.

Ahmady E., and Burgon, P.G. Identification and characterization of a novel Muscle Lamin A/C (LMNA) Interacting Protein (LITF): A regulator of Pax7.Experimental Biology Conference, San Diego, California, April 2008.